UNIVERSITY OF LONDON THESIS

Degree PhD Year 2006 Name of Author D'ARCY, Kevin

A Study of the Inter-Bouton Exchange of Synaptic Vesicles at Central Synapses

Kevin D'Arcy

March, 2006

Thesis presented in partial fulfilment of the degree of
Doctor of Philosophy at the University of London

MRC Laboratory for Molecular Cell Biology, UCL, London
Department of Pharmacology, University College London

ProQuest LLC
789 East Eisenhower Parkway
P.O. Box 1346
Ann Arbor, MI 48106-1346

Acknowledgements

I am most grateful to the Medical Research Council and the LMCB Graduate Program in particular, for creating a great situation in which to study and learn. I wish to thank my supervisor, Yuki Goda, for giving me the chance to work in her lab and for all the help in providing me with the environment and the opportunities in which to pursue my graduate studies.

During my Ph.D. I have been lucky enough to work with Kevin Staras. As well as teaching me a great deal, he has been a good friend whose company, advice and on rare occasions wit I have enjoyed over the past years. I have appreciated massively my many discussions with Tiago Branco about neuroscience and life in general either at the bench, the bar or the running track. A better compatriot on the road through to a Ph.D. could not have been imagined. I would like to thank Christian Dillon, a one time instituition in the Goda lab for his sage words, tips on molecular biology and great curries at ridiculus times of the night. Thanks also to Lucy Collinson for her good sense of humor, great skill and patience in teaching me the ins and outs of electron microscopy.

I am eternally grateful to my parents for their love and support. I would also like to thank my friends in Goodenough College, my home for the majority my Ph.D. It has taken a crazy place to keep me sane.

Abstract

Neurotransmitter release at central synapses is sustained by the synaptic vesicle cycle. It has been assumed that vesicle replenishment operates autonomously at individual presynaptic terminals. In this study the classical model of a compartmentalized synaptic vesicle cycle was tested by using a novel combination of FRAP (fluorescence recovery after photobleaching) and CLEM (correlative light and electron microscopy) in cultured hippocampal neurons. The stability of vesicle clusters labelled with fluorescent styryl dye at individual synapses were assessed by photobleaching using a confocal laser microscope and monitoring fluorescence recovery over time. The observed fluorescence recovery which was abolished by inhibitors of vesicular transport, suggested that synaptic vesicles recycled at sites outside the bleach region were transported along axons into bleached synapses. These newly-imported vesicles could undergo exocytosis upon stimulation, demonstrating that they formed part of the functional recycling pool. The spatial organization of imported vesicles in presynaptic boutons was examined using CLEM and FM dye photoconversion techniques. Imported vesicles were distributed throughout the native vesicle cluster, indicating that they become morphologically integrated into the synapse. The ability of imported vesicles to mix well with native vesicles highlights the dynamic nature of vesicle clusters at resting synapses. The departure of fluorescent packets from boutons into axons was observed by time-lapse microscopy. Ultrastructural analysis confirmed the mature state of donor synapses and showed these mobile packets to be loose aggregates of synaptic vesicles. Mobile vesicle clusters were comprised of vesicles from both the recycling and resting pools of the synapse, thus demonstrating no preference for mobility of any one vesicle population.

Table of Contents

Chapter 1 | Introduction **11**

1.1 Synapse Structure **12**

1.1.1 The presynaptic compartment 12

Ultrastructural detail 12

Molecular components 17

1.1.2 Synaptic cleft and synapse adhesion 21

1.2 The Synaptic Vesicle Cycle **24**

1.2.1 Exocytosis and neurotransmitter release 24

1.2.2 Vesicle cluster organization 27

1.2.3 Endocytosis and synapse maintenance 29

Monitoring vesicle release and reuptake 29

Modes of recycling 31

Modulation of vesicle pool organization 36

1.3 Transport of Synaptic Components **37**

1.3.1 Axonal transport 37

Fast axonal transport 37

Slow axonal transport 40

1.3.2 Synaptic vesicle movements 41

Sorting synaptic components 41

Vesicle formation 42

Localizing synaptic vesicles 43

Movement of synaptic packets 45

Maintaining vesicle clusters 46

Intra-bouton vesicle movements 47

Concluding comments 48

Aims **49**

Chapter 2 | Materials and Methods 50

Materials **50**

2.1 Chemicals/Reagents/Products 50

2.2 Buffers and Solutions 51

Methods **53**

2.3 Dissociated Hippocampal Cell Culture 53

2.3.1 Growth and maintenance of hippocampal neurons 53

Preparation of coverslips 53

Preparing astrocyte feeder layer 53

Dissection and plating of hippocampal neurons 53

Maintenance of hippocampal neurons 54

2.3.2 Transfection of hippocampal neurons 54

2.4 Preparation of Plasmid DNA 54

2.4.1 Transformation of competent DH5α bacterial cells 54

2.4.2 Small scale preparation of plasmid DNA 55

2.4.3 Large scale (maxi) preparation of plasmid DNA 55

2.5 Fluorescent Labelling of Synapses 55

2.5.1 Electrical stimulation of hippocampal neurons 55

2.5.2 Styryl dye labelling of synaptic vesicles 57

2.5.3 Stimulus independent labelling of synaptic vesicles 57

2.5.4 Identification of glutamate receptors 58

Expression of EGFP-tagged glutamate receptors 58

Live antibody labelling of glutamate receptors 58

2.6 Fluorescence Imaging 58

2.6.1 Epifluorescence microscopy 58

2.6.2 Confocal microscopy and FRAP 59

Imaging 59

Fluorescence recovery after photobleaching 59

2.6.3 Image analysis 59

Puncta movement 59

FRAP 60

Kymograph 60

2.7 Electron Microscopy 60

2.7.1 Photoconversion of FM1-43 60

2.7.2 Preparation of neurons for sectioning 61

Secondary fixation 61

Embedding 61

Removal of coverslips 61

2.7.3 Correlative light and electron microscopy 62

2.7.4 Ultrathin Sectioning of Samples 62

Serial sectioning 62

Section contrast staining 62

Formvar coating slot grids 62

2.7.5 Image acquisition 63

2.7.6 Analysis of electron micrographs 63

2.7.7 Three dimensional reconstruction of electron micrographs 64

2.8 Collaborations 64

Chapter 3 | Fluorescence Study of Synaptic Vesicle Dynamics in Hippocampal Neurons 65

3.1 Introduction **65**

3.2 Visualizing Hippocampal Synapses **66**

3.3 The Dynamic Nature of Recycling Pool Vesicles **69**

3.3.1 Time-lapse imaging of FM dye-labelled vesicles 69

The axonal movement of fluorescently labelled vesicles 69

Relationship between extent of recycling pool labelling and movement 72

3.3.2 Jasplakinolide inhibits vesicle transport 73

3.4 Stable Incorporation of Non-native Recycling Pool Vesicles **76**

3.4.1 FRAP of FM4-64 at mature synapses 76

The relationship between FRAP and neighbouring boutons 80

3.4.2 Imported vesicles join the recycling pool of synapses 83

3.5 Neuronal Stimulation and Vesicle Movement **86**

3.5.1 Dual labelling of vesicles with FM4-64 and SypI-EGFP 86

3.5.2 FM dye loading stimulus does not affect FRAP 88

3.6 Movement of Recycling Vesicles in Organotypic Hippocampal Slices 89

3.6.1 Observing vesicle movement in organotypic hippocampal slices 89

3.6.2 FRAP of FM1-43 in organotypic slices 90

3.7 Discussion **92**

Chapter 4 | Ultrastructural Analysis of the Presynaptic Terminal **98**

4.1 Introduction **98**

4.2 Ultrastructural Visualization of Synaptic Vesicles **99**

4.2.1 Photoconversion of FM1-43 99

4.2.2 Correlation of light and electron microscopy 100

4.2.3 Visualizing FM1-43 labelled vesicles by EM....102

4.3 Ultrastructural Characteristics of the Presynaptic Vesicle Cluster...105

4.3.1 Quantification of synaptic vesicle number....105

4.3.2 Spatial characteristics of recycling pool....107

4.3.3 Photobleaching FM1-43 and ultrastructural analysis....111

4.4 Discussion....115

Chapter 5 | Ultrastructural Analysis of Synaptic Vesicle Mobility....120

5.1 Introduction....120

5.2 Departure of Recycling Pool Vesicles from Synapses....121

5.2.1 Exit of fluorescently labelled vesicles from synapses....121

Identification of mobile units of fluorescence in EM....123

5.2.2 Mobile vesicle clusters....126

5.3 Ultrastructural Analysis of Vesicle Incorporation....128

5.3.1 Quantification of vesicle incorporation....128

5.3.2 Spatial distribution of newly imported vesicles....131

5.3.3 Shedding and incorporation viewed simultaneously by electron microscopy....134

5.3.4 Non-cluster based vesicle movement....137

5.4 Discussion....139

Chapter 6 | Concluding Remarks....144

Bibliography 152

Table of Figures

Figure 1.1– Schematic representation of the presynaptic grid 14

Figure 1.2– Characteristics of Type I and Type II synapses 16

Figure 1.3– The molecular organization of the presynaptic cytomatrix 20

Figure 1.4– Illustration of FM dye loading protocol 31

Figure 1.5–Multiple modes of vesicle retrieval 33

Figure 2.1– Calibration of field stimulation chamber 56

Figure 3.1 – Visualizing synapses of hippocampal neurons 68

Figure 3.2 – Inter-bouton movement of vesicles 71

Figure 3.3– Differential vesicle pool labelling and movement 73

Figure 3.4 – Jasplakinolide inhibits axonal transport 75

Figure 3.5 – FRAP of FM4-64 at mature synapses 78

Figure 3.6 – Analysis of vesicle incorporation 80

Figure 3.7– Kymograph plots of FM FRAP 82

Figure 3.8– Relationship between FRAP and neighbouring boutons 83

Figure 3.9 – Incorporated vesicles enter the recycling pool 85

Figure 3.10 – FRAP of EGFP-SypI and FM4-64 labelled vesicles 87

Figure 3.11 FM loading protocol does not influence vesicle incorporation 88

Figure 3.12 – Vesicle movement in organotypic slice cultures 91

Figure 4.1 – Photoconversion of FM1-43 100

Figure 4.2– Correlation of light and EM images 102

Figure 4.3 – Ultrastructural identification of FM1-43 positive vesicles. 104

Figure 4.4– Defining the boundaries of the vesicle cluster 106

Figure 4.5– Identification of photoconverted vesicles.....107

Figure 4.6– Defining regions within the vesicle cluster.....109

Figure 4.7– Spatial distribution of vesicle pools within boutons.....110

Figure 4.8– Preventing the photoconversion of FM1-43 by photobleaching.....113

Figure 4.9– Synapse viability following photobleaching.....114

Figure 5.1– Shedding of fluorescent packets from synapses.....123

Figure 5.2– Identification of mobile packets using CLEM techniques.....125

Figure 5.3– Ultrastructural detail of mobile packets.....127

Figure 5.4– Vesicle incorporation visualized by electron microscopy.....131

Figure 5.5– 3-dimensional reconstruction of FRAP bouton.....132

Figure 5.6– Analysis of the spatial distribution of newly incorporated vesicles within boutons.....134

Figure 5.7– Vesicle shedding and incorporation at the ultrastructural level.....136

Figure 5.8– Non-clustered movement of vesicles.....138

Abbreviations

µ	Micro
AP	Action potential
APV / AP-5	DL-2-Amino-5-phosphonovaleric acid
AraC	Cytosine arabinoside
BME	Eagle's Basal Medium
CLEM	Correlative light and electron microscopy
CNQX	6-cyano-2,3-dihydroxy-7-nitro-quinoxaline
cDNA	Complementary DNA
DAB	3,3' Diaminobenzidine
DIC	Differential interference contrast
DMSO	Dimethylsulphoxide
DNA	Deoxyribonucleic acid
DNase	Deoxyribonuclease
EDTA	Ethylenediaminetetra-acetic acid
EGFP	Enhanced green fluorescent protein
EM	Electron Microscopy
FCS	Fetal Calf Serum
FRAP	Fluorescence recovery after photobleaching
GluR	Glutamate receptor
Hz	Hertz
Ig	Immunoglobulin
Kb	Kilobase
kD	Kilo Dalton
L	Litre
m	Metre
M	Molar
n	Nano
PBS	Phosphate buffered saline
PC^+	Photoconverted
PC^-	Non-photoconverted
PDL	Poly-D-Lysine
S.E.M.	Standard error of the mean
Syp-I	Synaptophysin I
UV	Ultraviolet
V	Volt

Chapter 1 | Introduction

Since the conception of the neuron doctrine by Ramon y Cajal and the realization that the nervous system consists of many independent but inter-connected cells, efforts have been ongoing to better understand these connections (Glickstein, 2006). The primary mode of communication between neurons in the nervous system is mediated by the release and reception of chemical neurotransmitters onto target neurons at specialized intercellular contacts, synapses, as coined by Charles Sherrington (Eccles, 1982) (Cowan et al., 2001). Neurotransmission involves the calcium-dependent fusion of neurotransmitter-containing vesicles with the presynaptic membrane and the release of neurotransmitters into the synaptic cleft where they can bind to postsynaptically localized receptors. Synaptic vesicle exocytosis occurs repeatedly over the lifetime of synapses and it is the retrieval of vesicles after fusion by endocytosis that maintains the vesicle cluster at synapses and ensures the fidelity of synaptic transmission over long periods of time.

Over the course of the 1950's and 1960's some of the fundamental aspects of synaptic neurotransmission were elucidated in studies on the frog neuromuscular junction. Electrophysiological studies established the quantal nature of neurotransmitter release (Katz, 1969), while electron microscopy provided evidence for the physical basis of these quanta. Visualizing vesicles at synaptic terminals detailed their fusion at active zones and re-uptake via clathrin mediated endocytosis (Heuser and Reese, 1973). In the intervening years the molecular basis of these events has been elucidated by a combination of biochemical and genetic tools, such that now many of the proteins and their interactions involved in the priming, fusion and retrieval of vesicles as well as the postsynaptic actions of the neurotransmitters are known. Along with determining the ultrastructural (Peters et al., 1991) and molecular architecture of synapses (Dresbach et al., 2001), researchers have studied the formation of synaptic contacts. This involves the delivery of both pre- and postsynaptic elements by motor proteins along axonal and dendritic processes using the actin and microtubule cytoskeletal network, with the

components becoming localized at putative synapses by the coordination of diffusible and extracellular cues at these sites (Waites et al., 2005).

1.1 Synapse Structure

Chemical synapses facilitate the propagation or cessation of action potentials between electrically isolated neurons by converting potential changes in the membrane to a chemical signal that induces a similar or opposite potential change in the membrane of the target neuron (Eccles, 1982; Squire, 2003). The different synapses formed between the many neurons of the nervous system, across many species, share common structural characteristics as visualized by electron microscopy (Palay and Palade, 1955) (De Robertis and Bennett, 1955). The asymmetric nature of synapses and the directionality of signalling are apparent from these electron micrographs. At two opposing neuronal membranes, neurotransmitter containing vesicles are arranged along the presynaptic side opposite to a postsynaptic membrane specialization, called the postsynaptic density (PSD) (Peters et al., 1991).

1.1.1 The presynaptic compartment

Ultrastructural detail

In electron micrographs, the most striking feature of synapses is the vesicles of the presynaptic compartment. The first ultrastructural studies of synapses identified and classified many vesicle types on the basis of their diameter and lumenal density (Cowan et al., 2001). The most abundant vesicles at CNS synapses are electron lucent, 35-50 nm in diameter (Palay, 1956) and store neurotransmitters such as glutamate, GABA, glycine and acetylcholine (Cowan et al., 2001). These vesicles are usually located at single release sites or active zones in discrete clusters that can range in size from 10's to 100's of vesicles, displaying varying degrees of compactness (Harris and Sultan, 1995). The number of vesicles seen attached or docked at the active zone can vary from 2-16 and depends on the size of the vesicle

cluster (Harris and Sultan, 1995). At specialized synapses, such as mossy fibre terminals, 1000's of vesicles are present, but are distributed between multiple release sites (Amaral and Dent, 1981; Henze et al., 2000). Aminergic neurotransmitters are contained in 40-60 nm diameter electron dense vesicles, which can be released from synapses or the soma of neurons (De-Miguel and Trueta, 2005). In contrast, peptidergic neurotransmitters are stored in large dense core vesicles of 80-200 nm diameter. Peptidergic vesicles are usually distributed throughout the axons and cell bodies of neurons and are generally excluded from synaptic vesicle clusters (Hokfelt et al., 1984; Nusbaum et al., 2001). These vesicles release their contents in response to elevated calcium levels, though release events, in general, are rarer compared than those of small synaptic vesicles. They are not recycled locally and new vesicles are formed and filled with neurotransmitters in the soma and trafficked out to release sites in the axon. Because of the overall slow nature of their release and reuse these vesicles have neuromodulatory functions within the nervous system (Nusbaum et al., 2001).

The active zone region of synapses is an electron dense portion of the cytoplasmic membrane that varies between synapses depending on their type and function (Cowan et al., 2001). A presynaptic array of electron dense particles, found close to the plasma membrane as observed by electron microscopy, is known as the presynaptic grid and is thought to play a role in arranging the vesicles for release (Pfenninger et al., 1972) (Figure 1.1). Quick-freeze, deep-etch electron microscopy has revealed fibrillar projections from the active zone back into the vesicle cluster. These fibrils are believed to organize and tether the non-docked vesicles to the synapse (Hirokawa et al., 1989). Ultrastructural and biochemical studies of rat synaptosomes have shown the presynaptic cytomatrix to be made up of 50 nm particles regularly spaced at 50-100 nm distances with fine (10 nm) fibrils in between (Hirokawa et al., 1989; Landis et al., 1988). The regular spacing of the filamentous network is thought to be organized by the actin binding proteins spectrin (Phillips et al., 2001).

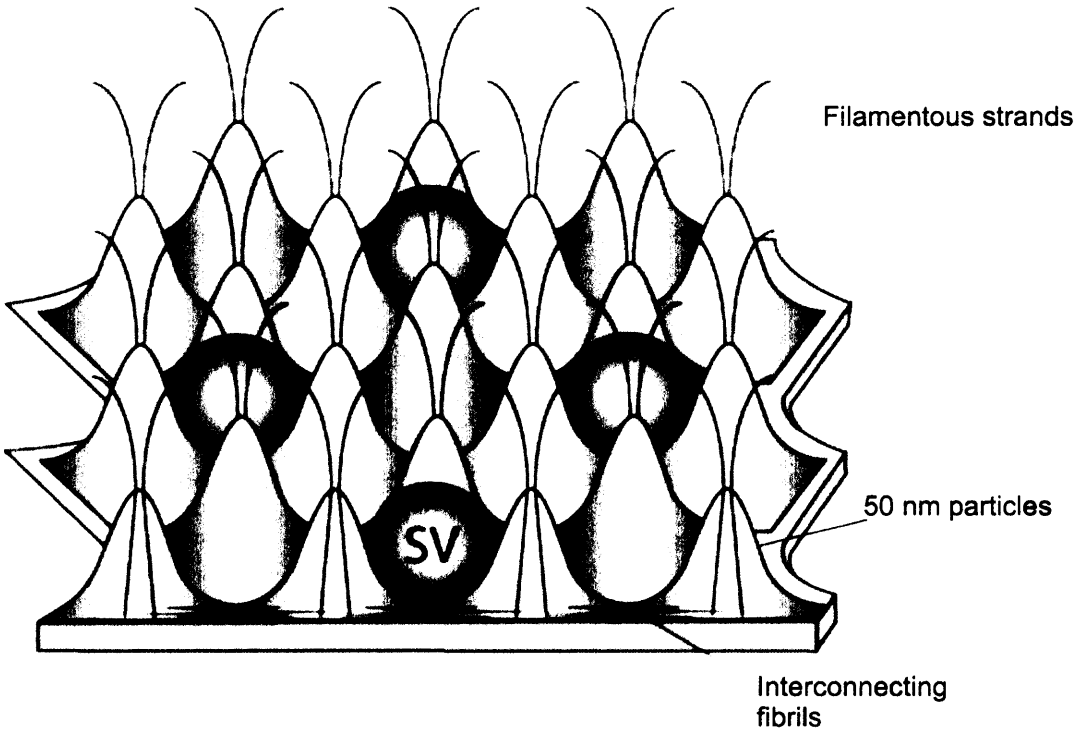

Figure 1.1– Schematic representation of the presynaptic grid

Vesicle docking sites are thought to be defined by 50 nm particles regularly spaced along the presynaptic plasma membrane. Fine interconnecting fibrils run between these particles, while filamentous strands extend further back into the vesicle cluster. This figure was adapted from (Gundelfinger et al., 2006).

A similar type of organization has been reported at the frog NMJ where EM tomograms have revealed an orderly array of pegs, ribs and beams at the active zone (Harlow et al., 2001). The proteins of the presynaptic density are thought to function by organizing the vesicle cluster, localizing Ca^{++} channels and release machinery, as well as maintaining the recycling vesicle pool during sustained bouts of release (Dresbach et al., 2001). The prominence of presynaptic membrane thickenings and the morphological appearance of vesicles at synapses have given rise to a simplified method of classification. Synapses with an obvious presynaptic density containing spherical vesicles are termed asymmetric or type I and are usually functionally classified as excitatory (Gitler et al., 2004; Megias et al., 2001). Inhibitory synapses have less prominent presynaptic densities and ovoid vesicles,

thought to be due to osmolarity-related artefacts during fixation, and are called symmetric or type II synapses (Figure 1.2), (Bodian, 1966) (Cowan et al., 2001). At other synapses presynaptic densities can take on more distinct shapes, in line with their proposed function. At the ribbon synapses of photoreceptors and hair cells of the inner ear, presynaptic densities appear as a bar or ribbon perpendicular to the membrane, and vesicles are docked along the length of the ribbon (Rao-Mirotznik et al., 1995; Townes-Anderson et al., 1985). This structure is thought to ensure a rapid supply of new vesicles to the active zones in order to sustain the tonic neurotransmission seen at these synapses (Sterling and Matthews, 2005). While some of the fundamental aspects of presynaptic function can be deduced from electron micrographs, a full understanding of neurotransmission at synapses requires a description of the proteins present and an analysis of their function.

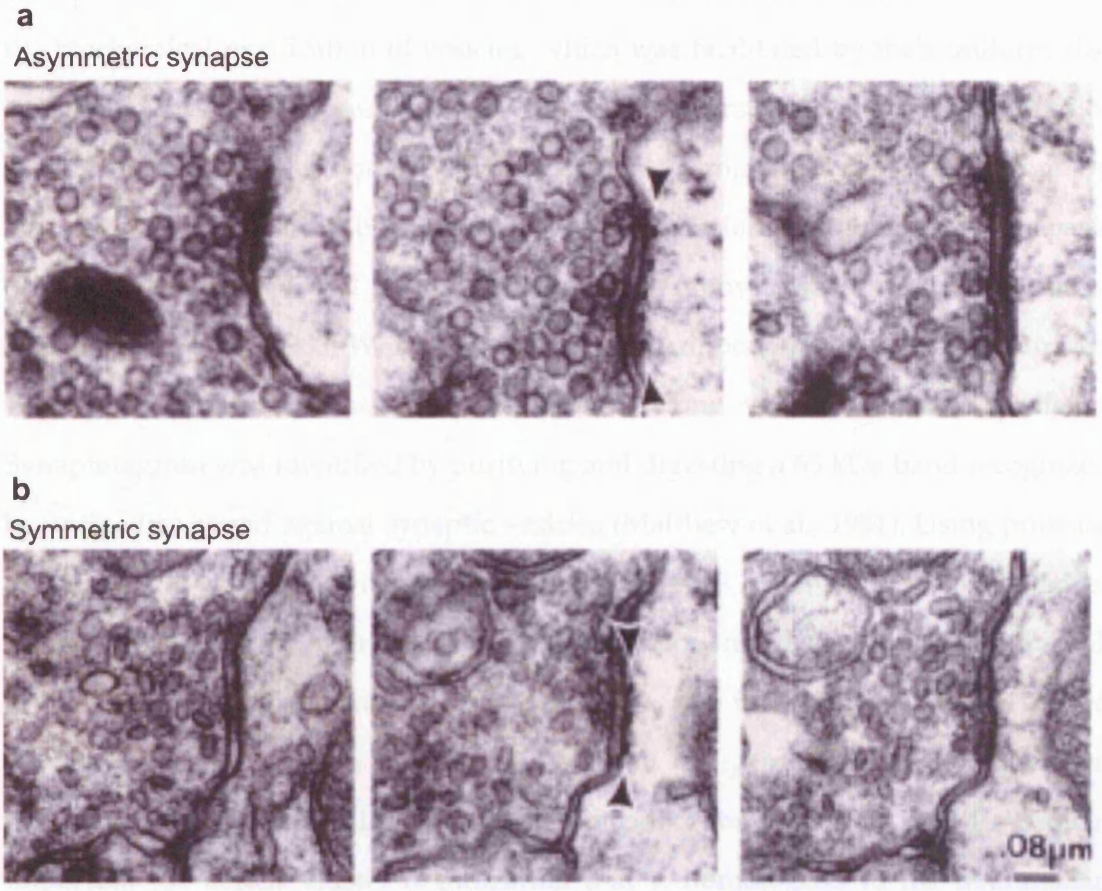

Figure 1.2– Characteristics of Type I and Type II synapses

Consecutive sections through synapses in the cat dorsal lateral geniculate nucleus. (**a**) Three consecutive sections through a Type I or asymmetric synapse displaying characteristic round vesicles and prominent membrane specializations. (**b**) Consecutive sections through a Type II or symmetric synapse containing ovoid vesicles and less obvious membrane thickening at release sites. This figure was adapted from (Rapisardi and Lipsenthal, 1984).

Molecular components

The identification and characterization of presynaptic cytomatrix proteins followed the biochemical purification of vesicles, which was facilitated by their uniform size and abundance at synapses. Vesicles were purified first from the electric organ of the elasmobranch fish *Torpedo californica* and later from rat brain preparations by homogenization followed by sucrose gradient separation of organelles on the basis of density differences, and permeation chromatography to separate on the basis of size (Huttner et al., 1983; Whittaker et al., 1972). Antibodies raised against purified vesicles could then be used to isolate and clone vesicle-associated proteins. Synaptotagmin was identified by purifying and digesting a 65 kDa band recognized by antibodies raised against synaptic vesicles (Matthew et al., 1981). Using protease digestion and degenerate oligonucleotides, fragments of DNA were generated to screen a cDNA library in order to obtain the full sequence of the protein (Perin et al., 1990). Forward genetic screens in *C.elegans* have also identified and characterized key molecules in synapse function. A series of *C.elegans* mutants displaying an uncoordinated phenotype identified genes encoding for example, Unc-10, a protein important for vesicle cluster organization that is homologous to the mammalian protein RIM (Koushika et al., 2001) and Unc-13 a protein involved in vesicle priming and known as Munc-13 in mammals (Brose et al., 2000; Richmond et al., 1999). Synaptosomes are produced by the homogenization of rat brain in isotonic buffers. This results in the pinching off of presynaptic nerve terminals to yield spherical units of membrane that are rich in synaptic vesicles, presynaptic proteins and a fragment of the postsynaptic membrane including the postsynaptic density (Whittaker et al., 1964). While synaptosomes have been used to study vesicle release *in vitro*, this rich source of synaptic proteins combined with immunoprecipitation and *in vitro* binding assays has helped to identify various protein-protein interactions within the presynaptic cytomatrix. These studies have led to the discovery of other vesicle-associated proteins and non-vesicular proteins that interact with synaptic vesicles. (Bellen, 1999).

In neurons forming *en passant* synapses, presynaptic specializations are usually seen as out-pockets along the axon from which microtubules are generally excluded. Actin filaments are the major cytoskeletal element present within the presynaptic compartment and are thought to play a scaffolding role at synapses, giving structure to the presynaptic cluster (Landis et al., 1988). This is most evident at the lamprey synapses where actin filaments are seen to surround the vesicle cluster (Shupliakov et al., 2002). In hippocampal neurons EGFP-tagged actin has been used to study the localization and behaviour of actin at these synapses (Colicos et al., 2001). EGFP-actin is seen localized to presynaptic sites, and disrupting its filamentous nature with actin destabilizing agents can affect vesicle release (Morales et al., 2000). Other cytoskeletal proteins, such as microtubules and spectrin at the *Drosophila* NMJ, have been shown to be important for synapse maintenance (Pielage et al., 2005; Roos et al., 2000) as well as in organizing the presynaptic density as discussed previously. Some proteins associated with synaptic vesicles presumably function to maintain their positions within the cluster and mediate their recruitment and fusion with the active zone, and will be discussed in more detail later. Other vesicle proteins are involved in the regeneration of functional vesicles following endocytosis. The multi-subunit vacuolar H^+-ATPase pump (v-ATPase) on vesicles is responsible for generating a pH of ~5.6 in vesicles, and the resulting electrochemical gradient plays a role in the uptake of neurotransmitter into the vesicles (Jahn and Sudhof, 1994). Aside from mediating the entry of protons into vesicles, the V_0 subunit of the v-ATPase may also function downstream of the SNARE complex in vesicle cycle, facilitating the formation of a fusion pore between vesicles and the plasma membrane (Hiesinger et al., 2005; Morel, 2003). Each class of neurotransmitter has an associated group of transporters which function by using either the proton gradient, the membrane potential differences or both (Ahnert-Hilger et al., 2003). In the case of glutamate, three transporters, VGLUT1-3, have been cloned and these principally use membrane potential differences to function. The transporter VGAT, moves GABA and glycine by using both proton and membrane potential differences (Ahnert-Hilger et al., 2003).

The meshwork of proteins that make up the presynaptic specialization are collectively called the cytomatrix at the active zone (CAZ). The major proteins of this presynaptic molecular complex identified so far include the large multi-domain proteins Piccolo and Bassoon and other active zone components, CAST, RIM1/2 and Munc-13 isoforms (Dresbach et al., 2001). Piccolo and Bassoon are present at both excitatory and inhibitory synapses of hippocampal neurons from early stages in synaptogenesis (Zhai et al., 2000; Zhai et al., 2001). These proteins have regions of homology in their N-termini which include Zn^{++} finger repeats and coiled-coiled domains (Dresbach et al., 2001), but the C-terminus of Piccolo contains PDZ domains and two C2 domains which are not present in Bassoon (Fenster et al., 2000). The proteins that can interact with Piccolo include the v-SNARE VAMP, the small GTPase proteins Rab5 and Rab3 through Piccolo's interaction with the rab acceptor protein PRA1 (Fenster et al., 2000), and the profilins, which regulate actin dynamics (Wang et al., 1999). Deletion analysis has suggested that the central region of Bassoon is important for its association with the CAZ, while the first 600 amino acids in the N-terminal region of the protein have been postulated to mediate Bassoon's association with synaptic vesicles; but as of yet no direct biochemical evidence for this interaction exists (Altrock et al., 2003; Dresbach et al., 2003). The many molecular interactions identified for these large proteins have led to the notion that Piccolo and Bassoon are the key organizer molecules of the presynaptic cytomatrix (Figure 1.3).

The CAZ proteins RIM1/2, contain Zn^{++} finger repeats, a PDZ domain and two C2 domains. These proteins interact with the vesicle associated small GTPase Rab3 in a GTP-dependent manner and Munc-13 via Zn^{++} finger domains (Dresbach et al., 2001). RIM proteins may function to tether vesicles at the active zone region through Rab3 binding. The protein CAST forms a complex with RIM1 and Munc-13-1 by binding RIM1. CAST also associates with Piccolo and Bassoon. It has been suggested that this large multi-molecular complex and or part of the complex functions in regulating vesicle release at synapses (Figure 1.3) (Martin, 2002; Takao-Rikitsu et al., 2004).

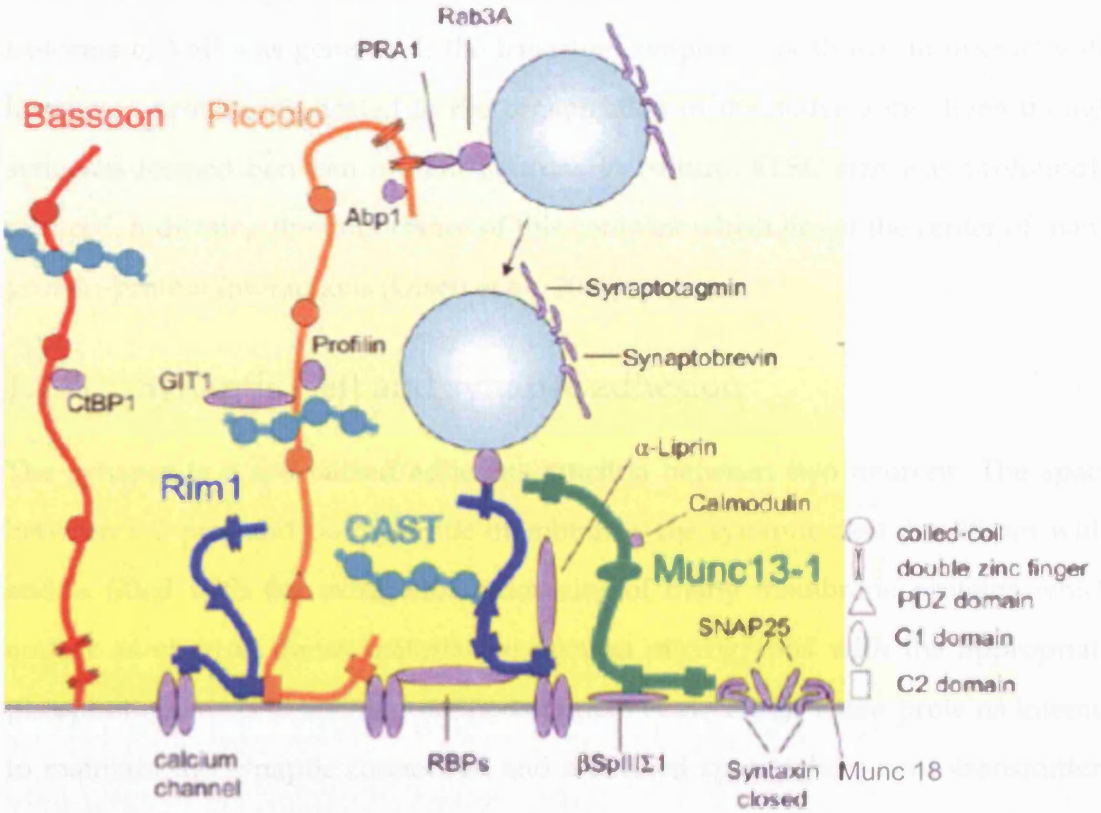

Figure 1.3– The molecular organization of the presynaptic cytomatrix
The multi-domain proteins RIM, Bassoon, Piccolo and the CAST proteins are shown as the major scaffolding proteins of the presynaptic cytomatrix. These proteins are thought to function in tethering vesicles in preparation for release as well as recruiting a variety of effector proteins, highlighting their role in both the structural and functional organization of the presynaptic region. This figure was adapted from (Gundelfinger et al., 2006).

The tripartite complex of CASK, Mint and Mals/Veli/Lin-7 is another major component of the presynaptic cytomatrix. CASK is a member of the membrane guanylate kinase (MAGUK) family of PDZ domain proteins. It binds to Mint though its CaMK domain (Butz et al., 1998) and to β-neurexin, a transmembrane protein, through its PDZ domain (Hata et al., 1996). These interactions may act to align the pre- and postsynaptic elements via the trans-synaptic association of β-neurexin and its counterpart neuoligin. The tripartite complex has also been implicated in the localization of calcium channels to the active zone through the SH3 and PDZ binding motifs of calcium channels, and Mint and CASK proteins

(Maximov and Bezprozvanny, 2002). In a study where a mouse lacking all three isoforms of Veli was generated, the tripartite complex was shown to interact with liprin-α, a protein implicated in the organization of the active zone. Even though synapses formed between mutant neurons in culture, EPSC size was profoundly reduced, indicating the importance of this complex which lies at the center of many protein-protein interactions (Olsen et al., 2005).

1.1.2 Synaptic cleft and synapse adhesion

The synapse is a specialized adherens junction between two neurons. The space between the pre- and postsynaptic membranes, the synaptic cleft, is ~20 nm wide and is filled with the extracellular domains of many membrane proteins which appear as electron dense material in electron micrographs with the appropriate phosphotungstic acid staining methods (Peters et al., 1991). These proteins interact to maintain the synaptic connection and a defined space where neurotransmitters bind receptors to elicit postsynaptic responses. The synaptic connection is quite strong given that postsynaptic elements remain attached to synaptosomes (Cowan et al., 2001). The adhesion molecules which are expressed both pre- and postsynaptically have a role in axodendritic target recognition and the recruitment of synaptic components during synaptogenesis (Garner et al., 2002; Scheiffele, 2003), synapse maturation (Ziv and Garner, 2004) and maintenance, as well as in structural modulation associated with functional synaptic plasticity (Lippman and Dunaevsky, 2005).

Cadherins are single transmembrane calcium-dependent adhesion molecules with five ectodomain (EC) repeats in their extracellular domains (Shapiro et al., 1995). At synapses, N-cadherins are localized to the peri-active zone region (Uchida et al., 1996) and lateral or *cis*-binding clusters the cadherins on one side of the membrane. This clustering, combined with Ca^{++} binding to EC domains ensures that the homophilic, *trans*-interactions between cadherins across the synaptic cleft are very stable (Shapiro et al., 1995). Cadherins are linked to the actin cytoskeleton by the interaction of their cytoplasmic domain with α and β-catenins (Nagafuchi et al.,

1994; Ozawa et al., 1990), and this connection is essential to the cadherins' role in controlling synapse structure, number and postsynaptic spines (Takeichi and Abe, 2005; Togashi et al., 2002). Cadherin-related neuronal receptors (CNR) are a large family of proto-cadherins shown to be localized to synapses (Kohmura et al., 1998). These molecules have variable numbers of EC repeats which are similar to conventional cadherins, but show large variations in their cytoplasmic tails. This diversity has been postulated to underlie synapse specificity in nervous system (Shapiro and Colman, 1999). The cytoplasmic tails of proto-cadherins don't associate with catenins, but do interact with downstream signalling cascades, as in the case of CNR1 and its interaction with the non-receptor tyrosine kinase fyn (Hamada and Yagi, 2001; Kohmura et al., 1998).

The immunoglobulin-superfamily of proteins also functions at synaptic connections. The extracellular domains of these proteins contain cysteine loop Ig domains and fibronectin type III repeats which mediate trans-synaptic adhesion through homophilic and heterophilic interactions (Vaughn and Bjorkman, 1996). N-CAM has five Ig-domains and three fibronectin repeats (Vaughn and Bjorkman, 1996) and is implicated in determining synapse number and certain types of synaptic plasticity (Murase and Schuman, 1999; Rougon and Hobert, 2003), while the best described role for the polysialylated form of N-CAM is in axon pathfinding (Rutishauser and Landmesser, 1996). Other Ig-protein families present at synapses include Syn-CAM, sidekicks and nectins which also function in synapse formation (Scheiffele, 2003).

Neurexins are a presynaptically localized family of cell surface proteins that are expressed exclusively in neurons, with many different isoforms generated by alternative splicing (Ullrich et al., 1995). They can bind to postsynaptically localized neuroligins to form a trans-synaptic bridge implicated in synapse formation (Cline, 2005). Another set of heterophilic interactions at synapses are mediated the Eph family of receptor tyrosine kinases and their ephrin ligands. These proteins are divided into A and B sub-groups. Ephrin-A ligands are attached to the membrane by a GPI-anchor and bind to EphA receptors, while ephrin-B ligands are

transmembrane proteins which bind to EphB receptors (Murai and Pasquale, 2004). EphB receptors are localized to axonal growth cones and function as repulsive cues in axon guidance (Flanagan and Vanderhaeghen, 1998). At mature synapses, however, Eph receptors are restricted to the postsynaptic region. Receptor-ligand interactions occur extracellularly, and the intracellular kinase and PDZ-binding domains of the Eph receptors are thought to mediate intracellular signalling and glutamate receptor clustering (Torres et al., 1998; Yamagata et al., 2003).

Integrins are a diverse family of heteromeric proteins consisting of α and β-subunits that can localize to synapses both pre- and postsynaptically (Chavis and Westbrook, 2001; Schwartz, 2001). As well as attaching to the actin cytoskeleton, ligand binding to extracellular domains can activate intracellular signalling cascades, involving a host of protein kinases including focal adhesion kinase and phosphoinositide 3-kinase (PI3K) (Schwartz, 2001). An inside-out signalling capability can translate intracellular changes to these proteins to the extracellular domains and alter their adhesive nature and interactions (Ginsberg et al., 2005; Tadokoro et al., 2003). The establishment of neural networks and synaptogenesis relies on integrin function (Jones, 1996) while at mature synapses integrins play a role in synaptic transmission (Kramar et al., 2003), LTP as well as memory formation (Chan et al., 2003; Chan et al., 2006).

The extracellular interactions of adhesion molecules maintain a regularly-spaced and stable synaptic cleft that is likely to be essential for synaptic transmission. Modulation of intracellular signalling and protein-protein interactions by the cytoplasmic tails of these molecules help to organize a stable multi-molecular matrix at the pre- and postsynaptic junction and regulate synaptic transmission (Murase and Schuman, 1999).

1.2 The Synaptic Vesicle Cycle

The basic principles of the synaptic vesicle cycle are derived from early freeze-fracture EM studies and correlative electron miroscopy where synaptic vesicles seen docked along the presynaptic membrane at rest, appear to undergo exocytosis as well as endocytosis upon nerve stimulation (Heuser and Reese, 1973). Our understanding of the molecular mechanisms of this process has been aided by the biochemical purification of synaptic vesicle proteins and elucidation of their interactions as well as functional studies in a large range of synapses and organisms.

1.2.1 Exocytosis and neurotransmitter release

In order for synapses to achieve neurotransmitter release within 0.1 ms of calcium influx (Sabatini and Regehr, 1999) vesicles need to be organized and prepared for exocytosis. Specialized interactions between synaptic vesicle proteins and the active zone work to tether the vesicles in place and prime them for release (Lin and Scheller, 2000). The energetically unfavourable fusion between the lipid bilayers of vesicles and the plasma membrane during exocytosis was first studied *in vitro* and in yeast to yield what is termed the SNARE hypothesis of membrane fusion (Bennett and Scheller, 1993; Sollner et al., 1993; Rothman and Orci, 1992). SNARE is derived from SNAP receptor, where SNAP stands for soluble NSF attachment protein, and NSF, an ATPase, in turn, stands for N-ethylmaleimide-sensitive fusion protein. At resting synapses a small number of vesicles are closely associated or docked at the active zone. The interaction between the vesicle specific GTPase Rab3 and the active zone protein RIM1 is thought to be important for this association (Rosenmund et al., 2003). Following the docking of vesicles at the active zone they can become primed for release in a process mediated by the SNARE complex (Sudhof, 2004). The vesicle-associated SNARE protein synaptobrevin/VAMP 1/2 interacts with the target SNARE proteins syntaxin and SNAP-25 on the presynaptic membrane to form a *trans*-SNARE core-complex. This interaction brings the two membranes close together via the formation of a parallel, four-helical bundle

(Sollner et al., 1993). Fusion is driven by the zippering of this protein complex into a *cis* form, which is promoted by the influx of calcium (Jahn et al., 2003). SNARE protein recycling after vesicle fusion is required for the ongoing release of vesicles at synapses, and the SNARE complex disassembly from the *cis*-state is mediated by SNAPs and NSF (Hanson et al., 1997).

While the three SNARE proteins are believed to be the minimal machinery required for membrane fusion, other presynaptic proteins are also critical for this process (Jahn et al., 2003). In studies where genes encoding VAMP (Schoch et al., 2001) and SNAP-25 (Washbourne et al., 2002b) were knocked-out in mice, synaptic vesicle exocytosis was not completely inhibited in mutant synapses. However, the genetic ablation of Munc 18-1, a syntaxin-interacting protein, abolished neurotransmitter release entirely (Verhage et al., 2000). Munc 18-1 is a cytosolic protein which binds to the closed conformation of syntaxin (Hata et al., 1993) and prevents SNARE complex formation. Inhibition of exocytosis in its absence indicates that Munc18-1 must have some additional function during exocytosis other than this inhibitory interaction with syntaxin. A similar inhibitory interaction has been observed between the vesicle proteins VAMP, synaptophysin and the V_0 subunit of the V-ATPase (Calakos and Scheller, 1994; Galli et al., 1996). VAMP must dissociate from synaptophysin in order to participate in the SNARE complex formation, raising the possibility that the release from synaptophysin may be a regulatory step in vesicle exocytosis (Edelmann et al., 1995).

The vesicle associated synaptotagmins contain two C2 domains, C2A and C2B, which can bind calcium, the SNARE complex and phospholipids (Sudhof, 2004). The binding of synaptotagmins is thought to be aided by the stabilizing action of complexin proteins on the SNARE complex (Murthy and De Camilli, 2003) (Marz and Hanson, 2002; Reim et al., 2001). Synaptotagmin proteins act as a calcium sensor to trigger the final stages of vesicle fusion. Synaptotagmin I is believed to be the calcium sensor involved in fast or synchronous release at synapses (Geppert et al., 1994; Yoshihara et al., 2003). Other isoforms of synaptotagmin with differing affinities for calcium have been postulated to be responsible for slow or

asynchronous release (Hui et al., 2005). Synaptotagmin proteins can bind the SNARE complex of primed vesicles (Chapman et al., 1995; Li et al., 1995), and following an action potential driven rise in calcium concentration the affinity of the C2 domains of synaptotagmin for phospholipids in the cell membrane increases. This interaction is thought to encourage the SNARE complex to undergo a *trans* to *cis* conversion that drives the full fusion of vesicles with the membrane (Sudhof, 2004).

Munc-13, first described in *C. elegans* as Unc-13 (Maruyama and Brenner, 1991), has a critical role in exocytosis as demonstrated by the lack of vesicle fusion in Munc-13 KO mice (Augustin et al., 1999b) and *unc-13* mutant worms (Richmond et al., 1999). The Munc-13 null mice showed no reduction in the number of docked vesicles, indicating a role for this protein in priming rather than docking (Augustin et al., 1999b). The single C1 domain and two C2 domains of these proteins mediate binding to diacyl glycerol (DAG) and phorbol ester, and to Ca^{++} in a phospholipid-dependent manner (Betz et al., 1998). Munc-13-1 is essential for synaptic vesicle priming at ~90% of glutamatergic synapses, while Munc-13-2 functions at the remainder (Augustin et al., 1999a; Augustin et al., 1999b). The interactions of Unc-13/Munc-13 with RIM1 through its N-terminal region, and the SNARE protein syntaxin are thought to be important for its function in vesicle priming and release (Betz et al., 2001; Madison et al., 2005). The C1 domain of Munc-13 binds DAG and is responsible for its role in plasticity-related and phorbol ester mediated increases in neurotransmitter release (Rhee et al., 2002; Rosenmund et al., 2002; Betz et al., 1998).

Calcium entry to the presynaptic terminal in response to action potentials triggers the fusion of vesicles primed at active zones. The voltage sensitive $Ca_v2.1$ (P/Q) and $Ca_v2.2$ (N-type) calcium channels mediate the local and transient rise in calcium concentration from 100 nM to over 100 μM (Reid et al., 2003). Calcium channels are present close to docked vesicles and the low Ca^{++} affinity of the calcium sensors in the fusion complex combined with the Ca^{++} buffering capacity of the presynaptic region confines release to locally situated vesicles (Sudhof, 2004). The different

classes of calcium channels can be distinguished on the basis of their electrophysiological properties as well as their pharmacological profiles (Catterall, 2000). P/Q-type channels are blocked by the spider toxin ω-agatoxin IVA (Mintz et al., 1992) and N-type channels are sensitive to ω-conotoxin GVIA (McCleskey et al., 1987). The SV2 proteins, of which there are three, were initially thought to act as pumps that helped to clear calcium from the presynaptic area following release (Janz et al., 1999). However more recent data would suggest that these proteins function to facilitate vesicle release and regulate the size of the readily releasable pool (RRP) at synapses (Custer et al., 2006; Xu and Bajjalieh, 2001).

The Rab3 family of small GTP-binding proteins can associate with synaptic vesicles in a reversible manner (Darchen and Goud, 2000). The GTP bound form of Rab3 binds vesicles in the presynaptic cluster, and during exocytosis GTP hydrolysis mediates its dissociation from the vesicles (Fischer von Mollard et al., 1991). In general, Rab3 proteins are thought to play a role in vesicle docking though the genetic ablation of all four isoforms of the protein resulted in just a 30% reduction in EPSCs (Schluter et al., 2004). Rab3 proteins are also proposed to function in the late stages of exocytosis after docking (Darchen and Goud, 2000). Rab3a binds the presynaptic cytomatrix protein rabphillin in a GTP-dependent fashion. This interaction was thought to underlie the role of rabphillin in mediating Rab3 effects on exocytosis. However, rabphillin knock-out (Schluter et al., 1999) and over-expression studies (Chung et al., 1999) have undermined this conclusion and have left the function of this interaction unclear (Sudhof, 2004). Rab3a binding to RIM 1/2 proteins along with the RIM protein's association with Munc13-1 is important for maintaining synaptic strength, possibly by preserving vesicle cluster organization (Schoch et al., 2002). In addition, Rab3a has been implicated in mossy fibre LTP (Castillo et al., 1997).

1.2.2 Vesicle cluster organization

Ultrastructural studies of synaptic terminals have shown that vesicles are largely uniform in size and apart from those docked at the active zone there is little to

distinguish the vesicle population (Peters et al., 1991). While the biochemical isolation of vesicles has led to a characterization of their molecular components, such an approach lacks the resolution to identify differences between individual or groups of vesicles within and amongst individual presynaptic compartments. However, functional studies have suggested the existence of different groups or pools of vesicles within presynaptic terminals, as exemplified by the rapid depression of neurotransmitter release to a steady-state level during repetitive stimulation (Elmqvist and Quastel, 1965). While presynaptic changes in calcium sensitivity or postsynaptic receptor desensitization could account for the depression, the initial decline in the response to stimulation is thought to reflect the depletion of a small proportion of the vesicle population, called the readily releasable pool (RRP) of vesicles. The subsequent steady-state response to stimulation reflects the balance of exocytosis with vesicle recycling and the recruitment of vesicles from a reserve pool (Sara et al., 2002). The vesicles that participate in exocytosis, within the RRP and reserve pool, together constitute what is known as the recycling pool (RP) (Rizzoli and Betz, 2005). The RRP of hippocampal synapses contains 5-20 vesicles (Rizzoli and Betz, 2005; Sudhof, 2000) which can be specifically released by the application of a hyper-osmotic solution (Rosenmund and Stevens, 1996) or brief bursts of stimulation (Murthy and Stevens, 1999). At the ultrastructural level, the RRP at hippocampal synapses is believed to be preferentially localized to regions closer to the active zone and this spatial positioning may underlie its preferential use (Schikorski and Stevens, 2001; Sudhof, 2000). However, at the frog neuromuscular junction there is no such spatial localization of the RRP; therefore, molecular cues may identify these vesicles as members of this pool (Rizzoli and Betz, 2004). Under sustained stimulus conditions, close to 80% of the vesicles within the frog NMJ are released (Henkel et al., 1996a; Richards et al., 2000). However, at hippocampal synapses a large proportion of the vesicle population, called the resting pool, does not participate in the vesicle cycle under any conditions (Harata et al., 2001a; Sudhof, 2000). The non-recycling or resting pool vesicles have been thought of as non-functional vesicles undergoing some form of maturation or repair. However, another proposed function for these vesicles is that they act as a reservoir

for the recycling pool, which when accessed could rapidly increase the size of the RP to enhance the efficacy of neurotransmitter release without a need for a change in the overall size of the vesicle population (Harata et al., 2001a). This scenario is suggested from the observation that the neuromodulator serotonin can increase the size of the recycling pool at the crayfish NMJ (Wang and Zucker, 1998).

1.2.3 Endocytosis and synapse maintenance

Monitoring vesicle release and reuptake

Several methods are available to study neurotransmitter release mechanisms at synapses. The release of neurotransmitter can be detected indirectly by monitoring postsynaptic receptor activation. For example, in hippocampal slices, extracellular recordings measure the population responses, while intracellular patch clamp techniques detect current flow in individual neurons (Shepherd, 1994). Direct detection of neurotransmitter release from terminals by electrochemical probes is possible when the molecules in question can be readily oxidized or reduced. In this way dopamine and serotonin release can be detected, while more electrochemically stable transmitters such as glutamate and GABA cannot (Travis and Wightman, 1998). At sufficiently large presynaptic terminals, vesicle fusion or reuptake can be detected as membrane capacitance fluctuations that result from changes in membrane surface area (Neher and Marty, 1982). More recently, the development of fluorescent probes combined with advances in a variety of microscopy techniques, epifluorescence, confocal and total internal reflection, have allowed for the direct visualization of vesicle cycling within the presynaptic terminals of small CNS neurons (Ryan, 2001). In an earlier study, the fluorescent labelling of recycled vesicles was achieved by the bath application of fluorescently tagged antibodies to the lumenal domain of synaptotagmin (Matteoli et al., 1992). While this technique specifically labels synaptic vesicles, it has been superseded by the FM family of fluorescent styryl dyes as a means of studying synaptic vesicle dynamics. The FM dyes were first used to study vesicle uptake and release at the frog NMJ and later in many other preparations including cultured hippocampal neurons, where they

have been used most extensively (Cochilla et al., 1999), and to a lesser degree in hippocampal slices (Pyle et al., 1999). FM dyes have a lipophilic hydrocarbon tail that encourages an association with membranes, while the positive charge on their head group prevents them from crossing the plasma membrane. Dyes with longer tail groups have an increased affinity for membranes, and as such, slower rates of departitioning from the membrane (Cochilla et al., 1999). The fluorescence of FM dyes is based on a conjugated ring structure in the head group and the link between the head and tail group governs the fluorescence properties of the molecules. The dyes exhibit very little fluorescence when in the aqueous phase, but show a strong enhancement of fluorescence (~350 fold) upon insertion into plasma membrane (Brumback et al., 2004). In the study of membrane dynamics, the green emitting FM1-43 (excitation peak 479 nm, emission peak 598 nm) and the red-shifted FM4-64 (excitation peak 506 nm, emission peak 750 nm) are most commonly used. The reversible association of FM dyes with membranes allows for the detection of both endocytosis and exocytosis. FM dyes are taken up into vesicles via stimulus-coupled endocytosis and washing away excess surface dye reveals the fluorescent labelling of functional presynaptic sites (Figure 1.4). Upon the fusion of dye-labelled vesicles, dyes are departitioned from the membrane, and the resulting reduction in fluorescence is a measure of vesicle exocytosis. FM dyes can be photoconverted to an electron-dense product to allow the ultrastructural identification of recycled vesicles in electron micrographs (Henkel et al., 1996a). Another popular method of monitoring the rate of vesicle exocytosis and endocytosis uses proteins fused to pH-sensitive GFP variants. Synapto-pHluorin (spH) is a synaptic vesicle protein produced by fusing the lumenal tail of VAMP to a pH-sensitive GFP, ecliptic pHluorin (Miesenbock et al., 1998). The pHluorin molecules, by virtue of their localization to the lumen of vesicles, are quenched by the low pH values. Upon exocytosis and exposure to the extracellular medium their fluorescence increases, but is quenched once again upon endocytosis (Ryan et al., 1997). These transient changes in fluorescence have been used to measure vesicle turnover most successfully in hippocampal cultures that express exogenous spH (Fernandez-Alfonso and Ryan, 2004). The high level of surface expression of spH and associated

low signal-to-noise ratio has made the use of these molecules in slice preparations more technically challenging (Li et al., 2005).

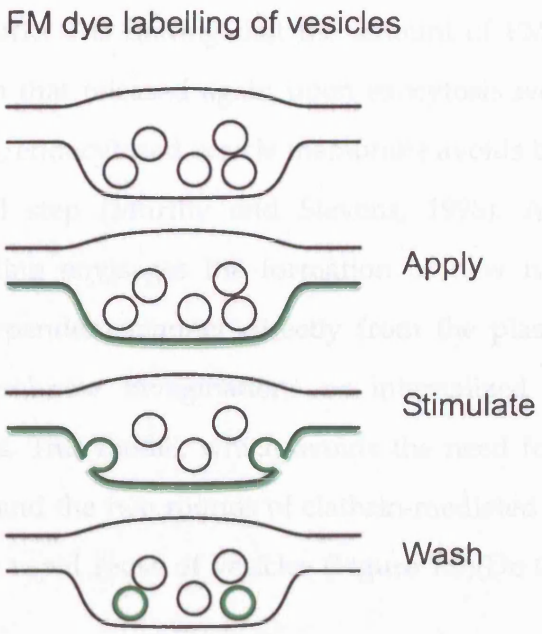

Figure 1.4– Illustration of FM dye loading protocol

The synaptic vesicle cycle is activated following the application of FM dye to the outer leaflet of the plasma membrane. Non-endocytosed dye is washed from the membrane after stimulation to reveal discrete fluorescent puncta representing synaptic vesicle clusters. .

Modes of recycling

The importance of endocytosis as a key feature of synapse function is most clearly demonstrated in temperature-sensitive *Drosophila* mutant *shibire*, where at restrictive temperatures the inhibition of endocytosis results in paralysis and a depletion of vesicles at synapses (Koenig and Ikeda, 1989). The precise mechanism by which synapses retrieve vesicular membrane is however more contentious. The model proposed by Heuser and Reese involves the uptake of vesicles by clathrin-mediated endocytosis at peri-synaptic regions and their transport to and sorting in endosomal intermediates from which new vesicles are formed (Heuser and Reese, 1973). At the same time Ceccarelli et al suggested the existence of an alternative form of release at synapses, where vesicles can briefly form fusion pores with the presynaptic membrane and release their contents without the need for full collapse,

in a mechanism that has become known as kiss-and-run (Ceccarelli et al., 1973; Fesce et al., 1994). In this way, vesicles can be rapidly retrieved directly from the active zone without the need for a clathrin-mediated endocytosis and intermediate endosomal vesicular traffic. The finding that the amount of FM dye taken up in endocytosis is similar to that released again upon exocytosis would suggest that, under certain conditions, endocytosed vesicle membrane avoids being diluted in an intermediate endosomal step (Murthy and Stevens, 1998). Another suggested means of vesicle recycling envisages the formation of new functional synaptic vesicles in a clathrin-dependent manner directly from the plasma membrane or from deep plasma membrane invaginations or internalized cisternae rich in synaptic vesicle proteins. This model, which avoids the need for an intermediate endosomal sorting step and the two rounds of clathrin-mediated vesicle formation, would allow for a more rapid reuse of vesicles (Figure 1.5)(De Camilli and Takei, 1996; Takei et al., 1996).

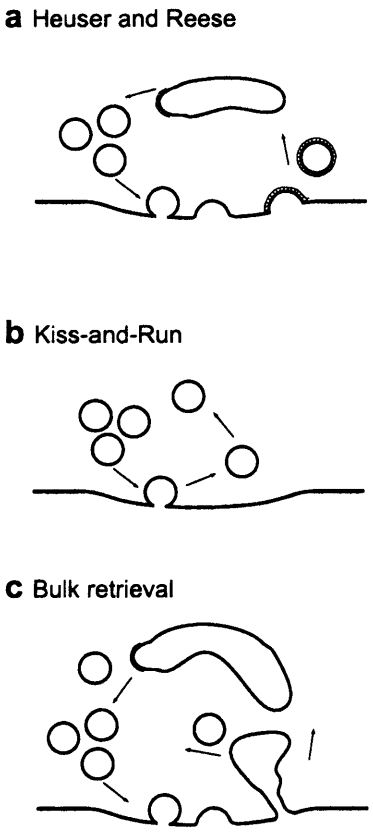

Figure 1.5–Multiple modes of vesicle retrieval

(**a**) A schematic of the Heuser and Reese model of endocytosis. Vesicles undergo fusion and full collapse on the presynaptic membrane. After this vesicles are retrived via clathrin mediated endocytosis and may go through endosomal compartments before rejoining the vesicle cluster. (**b**) Kiss-and-run release does not require the full collapse of vesicles for the release neurotransmitter. Instead neurotransmitter is released through a transiently formed fusion pore and are subsequently retrieved from this site of fusion. (**c**) In the bulk retrieval model large invaginations are formed following release. New vesicles may bud directly from these or from the internalized cisternae which they form, once pinched off from the plasma membrane. Adapted from (Royle and Lagnado, 2003).

Whether it occurs directly from plasma membrane or from endosomal intermediates, the mechanisms of clathrin-mediated endocytosis are so far the best understood. Clathrin-dependent vesicle formation requires the recruitment of the adaptor molecule AP-2 to the membrane. This is mediated by the concentration of vesicle proteins containing tyrosine binding motifs, which may include synaptotagmin (Zhang et al., 1994), along with PI(4,5)P2 (Haucke and De Camilli, 1999). The binding of clathrin triskelia to AP-2 forms a clathrin lattice on the membrane and the proteins amphiphysin, endophilin and epsin are all thought to

play a role in inducing membrane invagination, in some cases by penetrating and locally destabilizing the plasma membrane to generate lattice curvature. Such actions produce uniformly sized vesicles (Murthy and De Camilli, 2003). The scission of deeply invaginated clathrin-coated pits to form coated vesicles is mediated by the GTPase dynamin (Brodsky et al., 2001). When its GTPase function is inhibited with GTPγS, vesicle populations are depleted following stimulation and there is an increase in the number of coated pits at synapses (Takei et al., 1995). Dynamin may also function in non-clathrin mediated vesicle retrieval to sustain fast endocytosis, as suggested by studies in ribbon synapses of retinal bipolar neurons (Jockusch et al., 2005). The dissociation of clathrin from vesicles requires the binding of Hsc70 and auxilin to clathrin in order to destabilize the icosahedral cage structure (Schmid, 1997). The phosphatase action of synaptojanin on PI(4,5)P2 is thought to help remove adaptor proteins from newly formed vesicles (Cremona et al., 1999).

The observation that the rate of membrane re-upake can vary has led to the suggestion that fast and slow modes of vesicle recycling, with different mechanisms, exist at synapses. At the *Drospohila* NMJ, two modes of endocytosis have been noted. In the first, the uptake of vesicles directly from the active zone is thought to be a rapid clathrin-independent process involved in kiss-and-run release, while a second re-uptake mechanism from the periphery of the synapse uses clathrin-mediated endocytosis (Koenig and Ikeda, 1996; Verstreken et al., 2002; Verstreken et al., 2003). A more recent report has called into question the existence of kiss-and-run release at the *Drospohila* NMJ and suggests that inefficient clathrin-dependent mechanisms account for the persistence of neurotransmitter release at the synapses of *endophilin* and *synaptojanin* mutant flies (Dickman et al., 2005). Capacitance measurements at retinal bipolar neurons have revealed fast and slow mechanisms of endocytosis at these synapses. Vesicles can be retrieved for reuse quickly (~1 s) following a brief stimulation but after a sustained stimulus train membrane re-uptake occurs at much slower rates (Neves and Lagnado, 1999). At small central synapses multiple methods of vesicle recycling are also thought to co-exist (Murthy and De Camilli,

2003). In a number of FM dye-labelling studies the time taken for vesicles to become available for reuse following fusion has been measured. Estimates range from 30-60 s, for relatively slow reuse (Ryan and Smith, 1995), to ~1 s in cases of fast vesicle recycling (Klingauf et al., 1998; Pyle et al., 2000). As an alternative to FM dyes, synapto-pHluorin measurements of endocytosis at hippocampal synapses revealed a variable rate of vesicle uptake depending on the duration of the stimulus (Sankaranarayanan and Ryan, 2000) and the temperature of the preparation (Fernandez-Alfonso and Ryan, 2004). Fast recycling vesicles are thought to be those in the RRP that undergo preferential release at synapses (Pyle et al., 2000). Studies in hippocampal cultures using both FM dyes (Aravanis et al., 2003) and synapto-pHluorin (Gandhi and Stevens, 2003) have demonstrated a kiss-and-run mode of release at synapses that could account for the rapid reuse of vesicles. It is possible that kiss-and-run is the most prevalent means of release at synapses during low frequency stimulation (Harata et al., 2006), or at synapses with a low release probability (Gandhi and Stevens, 2003), while in cases of extensive stimulation, clathrin-based modes of vesicle retrieval contribute more to the vesicle cycle. Consistently, repeated stimulation of hippocampal neurons expressing spH in the presence of bafilomycin (an inhibitor of vesicular proton pump) to trap re-endocytosed vesicles in a fluorescent state, resulted in a continuous step-wise increase in fluorescence at boutons. This suggests that the RRP is repopulated with vesicles from the reserve pool rather than through an immediate reuse of endocytosed vesicles under conditions of sustained stimulation. (Li et al., 2005).

The number of vesicles present at the majority of central synapses has been estimated to be ~200 (Schikorski and Stevens, 1997). However, of this total population, the RP described above, has been reported to contain from between 25 to 127 vesicles (Harata et al., 2001a). While these estimates differ greatly, they indicate the reduced capacity of the RP and highlight the requirement for the efficient recycling of vesicles to ensure the fidelity of sustained release at these synapses. The concerted efforts of the multiple recycling mechanisms discussed above must fufill these requirements.

Modulation of vesicle pool organization

The number of vesicles in the RRP as estimated by stimulus trains (Rosenmund and Stevens, 1996), prolonged membrane depolarization (Mozhayeva et al., 2002) or hyper-osmotic shock (Stevens and Tsujimoto, 1995), is believed to be related to the release probability of synapses (Rosenmund and Stevens, 1996). During prolonged stimulation the release probability of synapses decreases and this may be linked to the depletion of the RRP (Moulder and Mennerick, 2006). In addition, RRP size and release probability have been correlated to the size of the RP, which can vary between synapses within the same neuron (Murthy et al., 1997). This relationship between release probability and the size of the RP, as assessed by FM dye intensity and the rates of destaining, is dependent on the rate of stimulation. At low frequencies the correlation between size and release is less than at higher frequencies (Waters and Smith, 2002). A possible target for the presynaptic modulation of synaptic efficacy may be the RRP or the RP. The size of the RRP has been shown to increase in hippocampal neurons following treatment with phorbol esters (Nagy et al., 2004; Stevens and Sullivan, 1998). The presynaptic actions of phorbol esters include modulating the calcium sensitivity of the vesicle release machinery (Lou et al., 2005), binding to munc-13 to alter RRP pool size and vesicle release (Rhee et al., 2002) as well as regulating release probability by activating PKC (Malenka et al., 1986). An increase in the turnover of synaptic vesicles has been observed in hippocampal neurons following the induction of LTP by either chemical (Malgaroli et al., 1995) or stimulus protocols (Ryan et al., 1996) in both cultures and acute slice preparations (Zakharenko et al., 2001). These changes occur in less than an hour, and the modulation of vesicle release at individual synapses is believed to contribute to the increased synaptic strength. An increase in the size of the entire RP or more specifically the RRP could underlie the presynaptic modifications. Whether this occurs by recruitment of vesicles from the resting pool or by an overall increase in the size of the vesicle cluster has yet to be determined.

1.3 Transport of Synaptic Components

Neurons are highly polarized cells usually with a single axon and many branching dendrites which can extend for great distances from the cell body (Craig and Banker, 1994). Synaptic components are distributed from the soma to the outer-lying synapses by an energy-dependent transport mechanism, mediated by motor proteins moving along cytoskeletal filaments (Bradke and Dotti, 2000). The movement of proteins and organelles away from (anterogradely) and towards the cell body (retrogradely) is essential for the establishment of synaptic contacts and the long-term maintenance of neuronal function (Bradke and Dotti, 2000). This section will describe the basic mechanisms of axonal transport and focus on the movements of synaptic vesicles along axons as well as within established synaptic vesicle clusters.

1.3.1 Axonal transport

The movements of axonally transported proteins can be classified according to the overall rate of movement and their directionality. Early studies of axonal movement using radioisotope pulse-labelled proteins in live animals, identified three distinct groups of proteins and classified them according to their rates of movement: a fast component and two slower components called SCa and SCb, respectively (Brown, 2000).

Fast axonal transport

The fast component of axonal transport involves the anterograde and retrograde movement of membranous organelles along cytoskeletal filaments at rates of up to 200-400 mm/day or 0.5-5 μm/s (Brown, 2003). These organelles contain many of the proteins required for synaptic function such as SNAREs, ion channels and adhesion molecules (Hirokawa and Takemura, 2005). In axons, microtubule filaments are organized in a polarized manner with the pointed or plus ends directed towards the periphery and the barbed or minus ends towards the soma (Baas et al., 1988). These

dynamic and unstable polymers of α– and β-tubulins are ~25 nm in diameter and arranged parallel to one another with a spacing of ~20 nm between each filament. Microtubule associated proteins (MAPs), including the axon-specific MAP, tau, control the spacing between filaments and their stability by modifying the rates of assembly and disassembly (Desai and Mitchison, 1997; Squire, 2003).

The kinesin and dynein families of molecular motors are responsible for the movement of cargo along microtubules (Vale, 2003). The majority of the kinesin (KIF) proteins are plus-end directed motors that move cargo anterogradely (Hirokawa and Takemura, 2004), while dynein motors are involved in retrograde transport(Vale, 2003). There are 45 human and mouse KIF genes which can be classified into 14 large families, kinesin 1-14, based on their evolutionary relatedness. KIFs can also be classified according to the position of the motor domain, be it amino-terminal, middle or carboxy-terminal as N-, M- or C-kinesins, respectively. N- and M-kinesins are plus-end directed motors and C-kinesins carry cargo towards the minus end of microtubules (Hirokawa and Takemura, 2005). Kinesins are rod-shaped proteins, approximately 80 nm in length, and are made up of heavy (115-130 kDa) and light (62-70 kDa) chains (Vale, 2003). The conserved globular or motor domains of kinesins in the heavy chain head region are responsible for microtubule binding and ATP-dependent movement (Hirokawa and Takemura, 2005). The tail regions, containing the light chains, bind membranous cargo and are highly variable between different kinesin proteins. This variability may be the basis for cargo selectivity and the differential regulation of motor proteins (Hirokawa and Takemura, 2005; Seiler et al., 2000). The retrograde transport of cargo to the soma is mediated by minus-end directed KIF proteins, such as members of the kinesin 14 family, and those of the dynein family (Vale, 2003). Dyneins are large (1-2 MDa) double-headed proteins with two heavy chains that contain the motor domain and multiple light chains (King, 2000). There is less diversity amongst members of the dynein family and their binding to many different accessory intermediate and light chain proteins is thought to confer cargo specificity (Goldstein and Yang, 2000). An example of this type of interaction is that

of dynein motors with the dynactin protein complex which occurs via the p150 ^{glued} subunit; this association can mediate motor binding to microtubules and cargo while at the same time enhancing the processivity of the motor proteins (Welte, 2004). The dynactin complex is also thought to be key in facilitating the bi-directional transport of cargo in axons. The addition of p150 antibodies to extruded squid axoplasm resulted in a block of both retrograde and anterograde movement (Waterman-Storer et al., 1997). The molecular basis for the dual role of dynactin seems to lie in its ability to interact with both the anterograde motor kinesin II as well as cytoplasmic dynein (Deacon et al., 2003).

Fast axonal transport of cargo over long distances primarily occurs along microtubules. However, axonally transported organelles are also moved along actin filaments by myosin motors (Bridgman, 2004; Brown, 1999). Actin filaments are 4-6 nm in diameter and are generally shorter and less uniformly organized than microtubules (Alberts, 2002). The primary actin-based motor in neurons is myosin-V, a double headed protein consisting of two dimerized heavy chains forming three domains: a head/neck domain, a middle proximal/medial tail domain and a distal globular tail domain (Langford, 2002). The head/neck domain contains actin and ATP binding sites, while the middle domain is the site of heavy chain dimerization (Vale, 2003). A large protein complex of light chains and other accessory proteins exists at the tail or globular end of the motor protein where cargo binds (Langford, 2002). Myosin-V has been shown to carry synaptic and endosomal vesicles in axons (Bridgman, 2004).

The interplay between the microtubule and actin based transport was first demonstrated in studies of squid giant axoplasm where vesicles were seen to move alternately along actin filaments and microtubules (Kuznetsov et al., 1992). An ultrastructural demonstration of the close association between actin and microtubule filaments in the squid giant axon supports the dual dependency of axonal transport on both the actin and microtubule cytoskeleton (Bearer and Reese, 1999). The interaction of kinesin family proteins with myosin-V motors, via their tail domains, is thought to form a heteromotor complex capable of movement on both

actin and microtubules. The activation of a given motor by binding to its substrate may inhibit the function of the other motor, and as such, allow the same vesicle to be carried efficiently along both actin and microtubules (Huang et al., 1999; Langford, 2002). The fast axonal retrograde transport of cargo in motor neuron axons is another example of the dual role of filamentous actin and microtubules in this process. In this situation, the efficient retrograde movement of cargo is facilitated by cooperation between the myosin-Va and cytoplasmic dynein motor proteins, possibly through a dimerization based interaction (Lalli et al., 2003). In addition, pigment granules in *Xenopus laevis* melanophores have been observed to associate with myosin, dynein and kinesin motors (Nascimento et al., 2003). The importance of the actin cytoskeleton for competent axonal transport is further evidenced by the effects of actin disrupting agents on cargo movement. The actin binding protein gelsolin, which acts to sever and cap actin filaments (dos Remedios et al., 2003), can inhibit fast axonal transport in the axoplasm of squid giant axons (Brady et al., 1984). The actin depolymerizing effects of DNaseI has similar effects on axonal transport (Goldberg et al., 1980), while the actin stabilizing agent jasplakinolide can also disrupt axonal transport in hippocampal neurons (Hiruma et al., 2003).

Slow axonal transport

Certain proteins, cytoskeletal proteins in particular, have been reported to move along axons at much slower rates compared to proteins contained in membranous organelles (Brown, 2000). In the original radio-isotope labelling studies that characterized the speed of axonal protein traffic (Lasek et al., 1984), slow moving proteins were placed in either of two categories SCa or SCb. SCa included microtubules, neurofilaments and associated proteins which moved together at a rate of 0.3-3 mm/day. Actin and related proteins moved at a slightly faster rate of 2-8 mm/day and were placed in the SCb category (Lasek et al., 1984). These early studies suggested that cytoskeletal proteins moved slowly and continuously *en masse* along the axon in an exclusively anterograde manner. Subsequent live-imaging experiments, in which microtubules in a narrow cross section of an axon

were marked by selective photobleaching of fluorescently labelled microtubules (Lim et al., 1990; Lim et al., 1989) or by photoactivation (Okabe and Hirokawa, 1992; Reinsch et al., 1991), have provided conflicting results depending on the preparation studied. These imaging experiments were carried out using rates of acquisition ranging from 1 frame per 10 min to 1 frame per 30 s and in a few cases the slow coherent axonal movement of stripes of proteins marked in this way was observed, while in others a non-directional recovery of fluorescence was seen with little movement of the stripe. Recent live-cell imaging studies, using higher rates of acquisition (one frame per 2-4 s) of fluorescently labelled microtubules (Wang and Brown, 2002) and neurofilaments (Wang et al., 2000) have shown that they can move quickly as polymers in intermittent bursts, with rates similar to that observed for membranous cargo in fast axonal transport. These studies have led to the idea that the motors involved in slow transport are likely to be the same as those used for fast axonal transport, and that the long intervals between bursts of movement could account for the overall reduced rate of movement observed (Baas and Buster, 2004).

1.3.2 Synaptic vesicle movements

Sorting synaptic components

In order for synaptic components, unique to axons and dendrites, to be delivered efficiently to their targets, a mechanism of cargo sorting is required. Proposed mechanisms for the selective localization of proteins to axons include, the differential packaging of axonal and dendritic bound cargo at the TGN, selective transport along axonal or dendritic microtubules, the selective fusion of transport packets at destinations, as well as the selective retrieval of incorrectly targeted proteins (Winckler, 2004). Axonal proteins are known to become packaged into tubulovesicular organelles at the Golgi for transport to the cell membrane (Nakata et al., 1998). The preferential association of KIF5 motor proteins with the microtubules in the initial segment of the axon provides one mechanism for selective targeting of organelles bound to KIF5 (Nakata and Hirokawa, 2003). The

destination of the motor protein can also be affected by the cargo it binds. When the C-terminal tail of KIF5 binds to AMPA receptor-containing vesicles through GRIP-1, these vesicles are targeted to the dendrites (Setou et al., 2002). However, when KIF5 binds vesicles containing amyloid precursor protein, indirectly through the interactions of kinesin light chains with the scaffolding protein JIP, these organelles are targeted to the axon (Verhey and Rapoport, 2001). An example of presynaptic protein transport is the sorting and targeting of the synaptic vesicle protein VAMP. The axonal localization of this protein is achieved by its selective endocytosis along the dendritic surface (Sampo et al., 2003). The importance of the VAMP cytoplasmic domain for its target localization was demonstrated in an experiment where the cytoplasmic domain of VAMP was fused to the NH_2-terminus of the transferrin receptor. Whereas the transferrin receptor is normally exclusively targeted to dendrites, this chimeric protein localized to presynaptic sites, but not to synaptic vesicles. The signal sequence contained within the cytoplasmic portion of VAMP was sufficient for the inclusion of this protein into transport organelles bound for the presynaptic terminal but not for its insertion into synaptic vesicles, indicating that additional signals are required for correct targeting (West et al., 1997).

Vesicle formation

The blockade of axonal transport in neurons and subsequent ultrastructural examination of the regions proximal to the site of blockade revealed an accumulation of tubulovesicular membrane structures rather than vesicles (Tsukita and Ishikawa, 1980). This data was taken to suggest that synaptic vesicles are formed either in the axon or at synapses rather than directly from the TGN in the soma. Consistently, live cell imaging of the anterograde movement of fluorescently labelled synaptic proteins, combined with post-hoc electron microscopy demonstrated SNAP-25 and synaptophysin moving out of the soma in large tubulovesicular structures (Nakata et al., 1998). A separate study also showed the accumulation of GFP-labelled VAMP in tubulovesicular organelles at new sites of axo-dendritic contact (Ahmari et al., 2000). Further evidence for the non-somal production of synaptic vesicles comes from studies demonstrating that synaptic

vesicle components are delivered to synapses separately by different motor proteins. The monomeric kinesin motor protein KIF1A, associates with synaptophysin and synaptotagmin but not SV2 (Okada et al., 1995), while VAMP has been shown to be transported by KIF5 (Nakata and Hirokawa, 2003).

The formation and maturation of synaptic vesicles may occur at already established synapses with newly arriving components being assimilated into the synaptic vesicle cycle or through a process of fusion with non-synaptic axonal membrane and recycling though endosomal intermediates (Hannah et al., 1999). The possibility of vesicle fusion at non-synaptic sites was indicated by the observation of neurotransmitter release in immature motor neuron (Sun and Poo, 1987; Young and Poo, 1983). Subsequently, the incubation of immature hippocampal neurons with antibodies directed against the lumenal domain of synaptotagmin revealed the constitutive and evoked exo-endocytic recycling of vesicles in isolated axons (Kraszewski et al., 1995; Matteoli et al., 1992). The repeated fusion of synaptic vesicle precursor organelles with the axonal plasma membrane may act to filter synaptic vesicle proteins and facilitate their distribution into newly forming vesicles. Evidence for this proposal is seen in Drosophila neurons deficient in the exocyst protein sec5. The exocyst complex is known to be involved in the polarized exocytosis of transport vesicles in non-neuronal cells (Grindstaff et al., 1998) but is not required for synaptic vesicle fusion at synapses (Murthy et al., 2003). In sec5 mutant axons, synaptotagmin proteins were transported as normal but excluded from vesicles (Murthy et al., 2003). It was then suggested that the inability of synaptotagmin precursor vesicles to fuse with the plasma membrane, due to the lack of sec5, resulted in the exclusion of these components from precursor vesicles. In neurons the exocyst complex, thus appears to play a role in the formation of nascent vesicles.

Localizing synaptic vesicles

In developing neurons both axons and dendrites form filopodial extensions, presumably in search of apposing partners (Goda and Davis, 2003). The proteins involved in the stabilization and maintenance of synaptic contacts, which include

transsynaptic homophilic and heterophilic adhesion molecules, may also function to localize synaptic components to nascent synapses. A number of adhesion molecules have been shown to have an instructive role in synapse formation. When HEK-293 cells expressing syn-CAM were co-cultured with hippocampal neurons, synaptic vesicle clusters formed along axons at points of contact with HEK cells (Biederer et al., 2002). Neuroligin, which binds to presynaptic β-neurexin, can also induce the clustering of presynaptic vesicles and proteins in axons when expressed in non-neuronal cells (Scheiffele et al., 2000). These molecules are thought to interact with presynaptic cytomatrix proteins through PDZ binding motifs. The multi-domain protein CASK can bind to neurexins and promote the polymerization of actin at these sites (Biederer and Sudhof, 2001). The interaction of CASK with other presynaptic scaffolding proteins through a cascade of protein-protein binding events may then act to recruit proteins required for presynaptic differentiation (Biederer and Sudhof, 2000). N-cadherin, while not essential for synapse formation, has been proposed to stabilize early axo-dendritic contacts and allow other molecular interactions which promote the maturation of the contact into a synapse (Togashi et al., 2002). Another adhesion molecule, NCAM, has been reported to interact with TGN-derived organelles by binding, through its cytoplasmic domain, the cytoskeletal protein spectrin. Imaging studies have revealed the movement of NCAM-associated organelles along axons and their eventual localization to nascent sites of synaptic contact (Sytnyk et al., 2002). These complexes, while not initiating the axo-dendritic contact, may help to rapidly recruit presynaptic components during synaptogenesis. The disruption of the actin cytoskeleton by latrunculin A in the early stages of synaptogenesis results in the loss of presynaptic sites (Zhang and Benson, 2001). This effect may be indicative of a role for actin in stabilizing vesicles at nascent synapses, possibly through its interaction with the synaptic vesicle protein synapsin I (Valtorta et al., 1992). However, as synapses mature they become more resistant to perturbations of actin filaments. After 18-20 DIV, latrunculin has little effect on the structural integrity of synapses (Zhang and Benson, 2001), suggesting that other molecular interactions supersede the role of actin in maintaining the synapses.

Movement of synaptic packets

Neurons in the early stages of network formation are thought to be quite dynamic with the predominant features being neurite extension and the creation of synaptic contacts (Waites et al., 2005). In hippocampal neurons the movement of synaptic components have been studied with respect to its role in synapse formation. In developing neurons, within a short time of axo-dendritic contact, vesicle recycling is evident at nascent synapses (Zhen and Jin, 2004). The time-course and sequence of protein recruitment to nascent synaptic sites in hippocampal neurons in culture has been elucidated by a combination of repeated FM dye labelling and post hoc immunostaining (Friedman et al., 2000). Over the first 30 mins following contact, both presynaptic scaffolding proteins and vesicles are recruited, and within two hours, functional synapses form at axo-dendritic contacts (Friedman et al., 2000). The association of certain presynaptic proteins in dedicated transport packages has been suggested to facilitate the formation of synapses. The presynaptic cytomatrix proteins Piccolo and Bassoon are known to travel along axons together with syntaxin and SNAP-25 in 80 nm dense core vesicles called presynaptic transport vesicles (PTV's). These vesicles have been proposed to be part of a modular mechanism of synapse formation, with 2-3 PTV's being sufficient to form a presynaptic site (Shapira et al., 2003). Mobile synaptic vesicles, most probably generated by non-synaptic exo-endocytosis as discussed previously, have been identified in isolated axons as well as in filopodia and growth cones (Dai and Peng, 1996; Kraszewski et al., 1995; Sabo and McAllister, 2003). These non-synaptic recycling events are different from those at bona fide synapses, in that they display an increased sensitivity to brefeldin A (Zakharenko et al., 1999), a decreased sensitivity to tetanus toxin (Verderio et al., 1999a) and different calcium channel properties to those at mature synapses (Verderio et al., 1995). The mobile clusters of synaptic vesicles, moving at rates of between 0.1-1 $\mu m\ s^{-1}$, provide further evidence for the notion that components of synapses are pre-assembled prior to their arrival at the synapse, so as to facilitate the rapid formation of functional synapses (Matteoli et al., 2004). In more mature neurons, orphan presynaptic sites lacking appropriate postsynaptic partners have been identified (Krueger et al., 2003). In

some cases, these immature synapses seem to arise from mobile synaptic vesicles that are associated with the scaffolding protein Bassoon. These results extend the idea of pre-assembled synaptic units to mature synaptic networks, where under certain conditions the rapid formation of synapses may be required. The movement of synaptic vesicle packages has also been linked to synapse disassembly in developing neurons. Following a protocol that induces synaptic depression, an NMDA-dependent decrease in presynaptic function was correlated with an increase in the disassembly of fluorescently labelled synapses (Hopf et al., 2002).

A similar quantal mechanism of assembly for postsynaptic units has been proposed, following the observation that mobile packets of NMDA and AMPA receptors move along microtubules in the dendrites of cortical neurons (Washbourne et al., 2002a). NMDA receptors and PSD-95 proteins seemingly accumulated concurrently shortly after axo-dendritic contact, while AMPA receptor recruitment proceeded at a slower rate. In hippocampal neurons, the formation of the postsynaptic density has been propsed by some researchers to occur by the gradual, non-packet based, recruitment of proteins to locations opposite already established presynaptic sites (Bresler et al., 2004; Friedman et al., 2000). However, in a more recent report mobile packets of postsynaptic proteins, including the scaffold protein PSD-95, have been observed in hippocampal neurons. In contrast to the previous studies, when these mobile postsynaptic packets became stationary, they seemingly recruited presynaptic proteins and formed functional synapses at these sites (Gerrow et al., 2006). A more detailed examination of the early events in synaptogenesis are required to define categorically whether the inductive power in synapse formation resides pre- or postsynaptically.

Maintaining vesicle clusters

The actin cytoskeleton has been thought of as a scaffold or a restraining cage tethering the reserve pool of vesicles to the synapse via its interactions with synapsin I (Dillon and Goda, 2005; Dunaevsky and Connor, 2000; Greengard et al., 1993). The activity-dependent phosphorylation of synapsin I is believed to release the vesicles from actin filaments and engage them in exocytosis (Chi et al., 2003;

Huttner et al., 1983). Accordingly, the injection of synapsin I antibodies into presynaptic terminals caused a reduction in the size of the recycling pool and an impairment of release during high frequency stimulation (Bloom et al., 2003; Pieribone et al., 1995). In addition, fluorescently labelled synapsin I appears to dissociate from the vesicle cluster and transiently disperse into the axon upon stimulation (Chi et al., 2001). Other molecules may also play a role in regulating the vesicle cluster. The presynaptic scaffolding molecules Piccolo and Bassoon, which are distributed throughout the vesicle cluster, may act to maintain cluster integrity through an indirect interaction with the vesicle protein Rab3 (Murthy and De Camilli, 2003). Beta-catenin has also been implicated in vesicle cluster maintenance. In β-catenin null mice, synapse formation or the number of docked vesicles was not adversely effected. However, there was a marked reduction in the overall size of vesicle clusters. The rescue of this phenotype by expressing wild-type or mutant β-catenin required its interaction with protein partners via PDZ-binding motifs but was independent of β-catenin's link to actin or wnt signalling activities (Bamji et al., 2003).

Intra-bouton vesicle movements

Whereas upon stimulation, vesicles are mobilized within terminals for release, at resting synapses, vesicle movements are thought to be minimal. This lack of mobility was suggested in early reports from frog NMJ and hippocampal cultures, where the photobleached subsections of FM dye loaded presynaptic boutons showed little fluorescence recovery (Henkel et al., 1996b; Kraszewski et al., 1996). The application of okadaic acid, a protein phosphatase inhibitor, or stimulation promoted the movement of fluorescence material back into the photobleached regions. Okadaic acid disrupts the interaction of synaptic vesicles with release sites, resulting in their dispersal into axons (Betz and Henkel, 1994; Kraszewski et al., 1995). In contrast, staurosporine, a kinase inhibitor, reduces the movement of vesicles within the cluster, thus blocking the recruitment of vesicles from reserve pools and preventing the intermixing of vesicles after endocytosis (Becherer et al., 2001; Kraszewski et al., 1996). These results indicate that phosphorylated proteins,

such as synapsin I, regulate vesicle mobility at synapses. More recently the movement of synaptic vesicles within hippocampal boutons has been addressed using more sensitive fluorescence detection and analysis approaches. In one study, a combination of FM dye labelling of vesicles, spot photobleaching and fluorescence correlative spectroscopy (FCS) (Shtrahman et al., 2005), or in another study, minimal FM dye loading protocols to label single vesicles along with a modified form of FCS called fluorescence fluctuation analysis (FFS) (Jordan et al., 2005; Lemke and Klingauf, 2005), have tracked the movement of vesicles within boutons. These studies reported that while the majority of vesicles at a synapse are immobile, at any time there is also a small proportion of the population capable of moving through the cluster in a stop-and-go fashion as though they were making and breaking tethering links. In addition, as described in previous studies, okadaic acid treatment was seen to increase the mobility of vesicles while staurosporine had the opposite effect. These results would suggest that presynaptic vesicle clusters in resting neurons are more dynamic than previously thought.

Concluding comments

Many studies in a number of different synapses and model systems have helped to elucidate the molecular interactions and transport mechanisms required for synapse formation as well as the long-term maintenance of these connections. It is generally believed that synapses are independent stable units of transmission, with the local recycling of synaptic components via the synaptic vesicle cycle underpinning their autonomous nature. However, reports of the movement of vesicles in neurons, discussed previously in this chapter, could point to a less stable arrangement of synapses within established networks. The subsequent chapters of this thesis characterize the redistribution of recycling pool vesicles between established synapses and investigate the implications of such movements on synaptic function in hippocampal neurons.

Aims

The aims of this thesis were to examine the fate of endocytosed vesicles, specifically to test the classical model of a compartmentalized synaptic vesicle cycle in cultured hippocampal neurons. To achieve this:

- The movements of recently endocytosed vesicles were examined by time-lapse imaging.
- Fluorescence recovery after photobleaching and FM styryl dye destaining protocols were used to assess the fate of mobile recycling pool vesicles.
- The nature of mobile vesicles and their incorporation into non-native synapses were studied at the ultrastructural level using correlative light and electron microscopy along with FM dye photoconversion.

Chapter 2| Materials and Methods

Materials

2.1 Chemicals/Reagents/Products

All chemicals/reagents used that are not listed below were obtained from Sigma-Aldrich or BDH/Merck.

Product	Company	Address
Acetic acid	Sigma-Aldrich	Dorset, UK
Advasep-7	Biotium	Hayward, CA, US
AP-5	Tocris Bioscience	Bristol, UK
Bromophenol Blue	BIO-RAD	Hemel Hempstead, UK
Cytosine arabinoside	Sigma-Aldrich	Dorset, UK
CNQX	Tocris Bioscience	Bristol, UK
Cy2 G-anti-rabbit	Jackson ImmunoResearch	Pennsylvania, US
DAB	DAKO	Cambridgeshire, UK
DDSA	TAAB Laboratories Equipment Ltd	Berkshire, UK
DMP30	TAAB Laboratories Equipment Ltd	Berkshire, UK
DNase I	Calbiochem	California, US
Eagle's Basal Medium	Invitrogen	Paisley, UK
Fetal Calf Serum	Sigma-Aldrich	Dorset, UK
FITC G-anti-mouse	Jackson ImmunoResearch	Pennsylvania, US
Fluo-4	Molecular Probes/Invitrogen	Paisley, UK
FM1-43FX	Molecular Probes/Invitrogen	Paisley, UK
FM4-64	Molecular Probes/Invitrogen	Paisley, UK
16% Formaldehyde	Agar Scientific	Essex, UK
Formvar	Agar Scientific	Essex, UK
GluR-1 antibody rabbit	Calbiochem	California, US
Glutamax	Gibco/Invitrogen	Paisley, UK
25% Glutaraldehyde	Agar Scientific	Essex, UK
Hank's Balanced Salt Solution	Invitrogen	Paisley, UK
HEPES	Sigma-Aldrich	Dorset, UK
Lead Nitrate	Fisher Scientific	Leicestershire, UK

Metamorph software	Molecular Devices LTD	Berkshire, UK
MNA	TAAB Laboratories Equipment Ltd	Berkshire, UK
Osmium tetroxide	TAAB Laboratories Equipment Ltd	Berkshire, UK
PBS	Gibco/Invitrogen	Paisley, UK
Potassium ferrocyanide	Sigma-Aldrich	Dorset, UK
Propylene oxide	Agar Scientific	Essex, UK
QIAGEN® Plasmid Maxi Kit	Qiagen	Crawley, UK
QIAprep® Spin Miniprep Kit	Qiagen	Crawley, UK
Picrotoxin	Sigma-Aldrich	Dorset, UK
Sodium Cacodylate	TAAB Laboratories Equipment Ltd	Berkshire, UK
Sodium Citrate	Sigma-Aldrich	Dorset, UK
Sodium Pyruvate	Gibco/Invitrogen	Paisley, UK
TAAB 812	TAAB Laboratories Equipment Ltd	Berkshire, UK
Tannic Acid	TAAB Laboratories Equipment Ltd	Berkshire, UK
Tissue culture plastics	Beckton Dickinson or Corning	California, US, New York, US
Trypan Blue	Gibco/Invitrogen	Paisley, UK
Trypsin/EDTA	LMCB	UCL, UK

2.2 Buffers and Solutions

All buffers and solutions were made as described below. 'RT' indicates room temperature; 'Filter' indicates sterilization using a 0.2 μm filter.

Buffer/Solution	Ingredients	Storage	Sterilization
Astrocyte Growth Medium	Eagle's Basal Medium (BME), 20 mM Glucose, 10 mM HEPES buffer, 1 mM sodium pyruvate, Glutamax, 10 % fetal calf serum	4°C	Filter
Dissection Solution	Hank's Balanced Salt Solution (HBSS) with 10 mM HEPES	4°C	Filter
Enzyme Solution	Dissection solution containing 1.5 μM calcium chloride, 2 mg/ml L-cysteine, 0.1 μg/ml DNase I, 0.5 mM EDTA 30 units papain.	4°C	Filter
EPON	TAAB 812, DDSA, MNA, DMP30 in a ratio of 24:9.5:16.5:1, respectively	RT	-

EPON/PO	1:1 EPON and propylene oxide	RT	-
External Bath Solution	137 mM NaCl, 5 mM KCl, 2.5 mM CaCl2, 1 mM MgCl2, 10 mM D-glucose, 5 mM HEPES, 0.1 mM picrotoxin	-20°C	Filter
Formaldehyde-Glutataldehyde Fixative	2% glutaraldehyde and 2% formaldehyde in PBS	On ice	-
2x Hepes-buffered saline (2x HBS)	274 mM NaCl, 10 mM KCl, 1.4 mM Na2HPO4.7H2O, 15 mM dextrose (D-glucose) 42 mM Hepes	-20°C	Filter
L-agar	1% bacto-tryptone, 0.5% yeast extract, 170mM NaCl, 15% agar	RT	Autoclave
L-broth	1% bacto-tryptone, 0.5% yeast extract, 170 mM NaCl	RT	Autoclave
Lead Citrate solution	80 mM lead citrate, 120 mM sodium citrate and 0.8 ml 10 N NaOH in 50 ml of H_2O. Centrifuge	RT	-
Neuronal Growth Medium	Eagle's Basal Medium (BME), 20mM Glucose, 10mM HEPES buffer, 1mM sodium pyruvate, Glutamax, 2% fetal calf serum	4°C	Filter
Osmium fixative	1% osmium tetroxide, 1.5% potassium ferrocyanide	RT	-
PDL-Collagen	Acetic acid (0.025%), 1:8 dilution rat tail collagen, 5 μg/ml Poly-D-Lysine in dH_20.	RT	-
Sodium Cacodylate buffer	0.2 M stock: sodium cacodylate in dH_20, pH adjusted with HCL	4°C	-
Sodium sulphate solution	1% w/v sodium sulphate in 0.05 M sodium cacodylate	-	-
Tannic Acid solution	1% w/v in 0.05 M sodium cacodylate	-	-
Transfection medium	Eagle's Basal Medium (BME), 20 mM Glucose, 10 mM HEPES buffer, 1 mM sodium pyruvate, Glutamax	4°C	Filter

2.3 Dissociated Hippocampal Cell Culture

2.3.1 Growth and maintenance of hippocampal neurons

Preparation of coverslips

12 mm glass coverslips were washed overnight in nitric acid, then rinsed thoroughly with deionised water for 2-3 hr, and stored in 100% ethanol. As required, coverslips were placed in 24-well plates and sprayed lightly with a Poly-D-Lysine (PDL)-collagen mix. PDL-collagen coated coverslips were used for up to two months after spraying.

Preparing astrocyte feeder layer

As a source of astrocytes for the feeder layer on which neurons were plated, surplus cells from a dissection were grown in T-25 flasks in astrocyte growth medium. After the cells had attached to the flask, neuronal growth was discouraged by shaking the flask for 4-5 hr at 250 rpm. When astrocytes were close to confluency, they were removed by trypsinization and plated onto PDL-collagen coated coverslips at between 4,000 and 7,000 cells per well in astrocyte growth medium. After a period of 4-5 days growth a suitable feeder layer had developed.

Dissection and plating of hippocampal neurons

Dissociated hippocampal cultures were prepared from P0 rats. The hippocampus was removed into cool dissection solution, cut into small pieces and placed in the papain-based enzyme solution for 35 min at 37°C. The enzyme solution was then replaced with neuronal growth medium and the tissue triturated with a flame polished pipette. Cell number was estimated by adding 40 μl of the cell solution to 4 μl of 0.4 % trypan blue (to identify dead cells) and cells were counted in a Hawkesly Hemacytometer. Neurons were plated at between 10,000 and 20,000 cells

per well in 500 µl of neuronal growth medium onto an astrocyte feeder layer plated 4-5 days earlier.

Maintenance of hippocampal neurons

Within 12 hrs of plating, neuronal growth medium was exchanged completely with fresh medium containing 4 µM cytosine arabinoside in order to inhibit astrocyte proliferation. Neuronal cultures were fed every 7 days after plating by removing 100 µl of neuronal growth medium from each well and replacing it with 200 µl of fresh neuronal growth medium which had been conditioned over-night in a flask of astrocytes.

2.3.2 Transfection of hippocampal neurons

Neurons were transfected with plasmid DNA at between 8 and 10 DIV using a modified calcium phosphate protocol (Xia et al., 1996). In brief, for each well to be transfected 1-2 µg of DNA was mixed with 1.5 µl of 2.5 M $CaCl_2$ and an appropriate volume of ultra-pure water to give a final volume of 15 µl. The DNA-$CaCl_2$ mix was then added drop-wise to the same volume of 2x-Hepes-buffered saline and incubated at room temperature in the dark for 20 min. In each well to be transfected the neuronal growth medium was replaced with transfection medium and stored for later use. 30µl of calcium phosphate-DNA solution was added to each well of neurons. After 20-30 min or at a time when a sandy precipitate was visible the neurons were washed gently with fresh transfection medium and the neuronal growth medium was replaced. Neurons were used for experiments after a further 4-6 days.

2.4 Preparation of Plasmid DNA

2.4.1 Transformation of competent DH5α bacterial cells

2-10 µl of plasmid DNA at 1 ng/µl was added to 50 µl of competent DH5α cells on ice and left for 30 minutes. The bacteria were heat shocked at 42°C for 1 minute

before being placed back on ice for 2 minutes. 500µl of L-broth was then added to the bacteria which were subsequently cultured for 45 minutes at 37°C with shaking at 150rpm. 150-400µl of bacterial culture was spread out using sterile techniques on to L-agar plates containing either 50µg/ml ampicillin or kanamycin as appropriate.

2.4.2 Small scale preparation of plasmid DNA

Single colonies of antibiotic resistant bacteria were picked from L-agar plates using sterile pipette tips and used to inoculate 5 ml of L-broth containing the appropriate antibiotic. Cultures were grown overnight at 37°C while shaking at 250 rpm.

2.4.3 Large scale (maxi) preparation of plasmid DNA

500µl of small scale bacterial culture was used to inoculate 200 ml of L-broth supplemented with antibiotic. The culture was grown overnight at 37°C with shaking at 250 rpm. Plasmid DNA was isolated from the culture using a QIAGEN® Plasmid Maxi Kit according to the manufacturer's instructions. DNA was dissolved in TE or EB buffer to a concentration of 1mg/ml and stored at -20°C.

2.5 Fluorescent Labelling of Synapses

2.5.1 Electrical stimulation of hippocampal neurons

A custom made slotted field stimulation chamber with two parallel platinum electrodes lying 1 cm apart and a glass coverslip base was used to stimulate hippocampal neurons. A gravity-flow perfusion system and vacuum pump-driven suction allowed for the efficient exchange of solutions. The platinum electrodes were connected to a Grass stimulator (Astro-Med Inc, USA) which was used to generate field potentials, the number and frequency of which could be varied. The field stimulation set-up was calibrated to determine the potential changes required to generate action potentials in the neurons. To do this, neurons were bathed in the calcium sensitive dye Fluo-4-AM (5 µM) in external bath solution (EBS) for 5 mins, during which time it crossed the cell membrane into cytoplasm. The cells were

placed in the field stimulation chamber and washed with fresh EBS containing 20 μM CNQX and 50 μM AP-V to prevent recurrent activity in the cultures, but allow action potential generation upon stimulation. The neurons were stimulated for 2 seconds at a time with 1 ms pulses at 10 Hz at increasing voltage with at least 20 s rest between stimulations, as outlined in the schematic in Figure 2.1a. The increase in intracellular calcium concentration in response to action potentials in the neuron was measured as an increase in Fluo-4 fluorescence intensity (Figure 2.1b). A maximal response was observed at 25V (Figure 2.1c). In subsequent experiments requiring the generation of action potentials in neurons a voltage setting of between 20 and 25 volts was used.

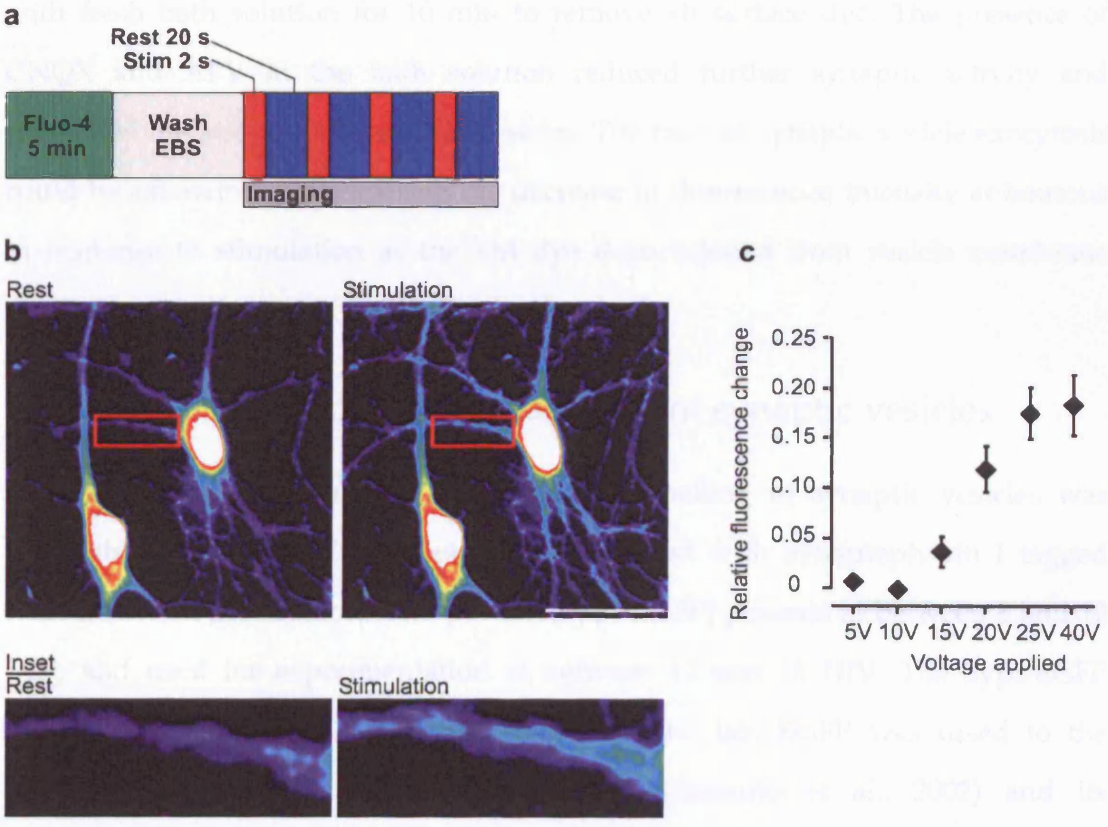

Figure 2.1– Calibration of field stimulation chamber

(**a**) Schematic describing the labelling of hippocampal neurons with fluo-4-AM and subsequent stimulation and imaging protocol. (**b**) Fluorescence images of fluo-4-AM labelled neurons before and during a stimulus train. Inset shows fluorescence intensity changes in response to stimulation in a single process. (**c**) Plot of the relative change of fluo-4-AM fluorescence intensity in neurons following 2 s stimulus trains of varying voltage.

2.5.2 Styryl dye labelling of synaptic vesicles

All experiments were carried out in EBS containing 20 μM CNQX and 50 μM AP5 at 35°C. The osmolarity of the EBS was adjusted with sorbitol to match that of the neuronal growth medium. The temperature of the EBS was regulated by either an in-line solution heater (Warner Instruments, USA) attached to the perfusion system or by an objective heater (Bioptech, USA). Synaptic vesicles were labelled by field stimulation in the presence of FM4-64 (10 μM) or FM1-43FX (10 μM), a fixable analog of FM1-43. A 600 AP train at 10 Hz was used to load the recycling pool of vesicles at synapses with FM dyes. The neurons were left in the FM dye for 45 s after stimulation, washed with 1 mM Advasep-7 in EBS for 1 min and then rinsed with fresh bath solution for 10 min to remove all surface dye. The presence of CNQX and APV in the bath solution reduced further synaptic activity and prevented the loss of FM dye from vesicles. The rates of synaptic vesicle exocytosis could be estimated by measuring the decrease in fluorescence intensity at boutons in response to stimulation as the FM dye departitioned from vesicle membrane during exocytosis.

2.5.3 Stimulus independent labelling of synaptic vesicles

In experiments where a stimulus-dependent labelling of synaptic vesicles was unsuitable, hippocampal cultures were transfected with synaptophysin I tagged with enhanced green fluorescent protein (SypI-EGFP) plasmid at between 8 and 10 DIV, and used for experimentation at between 12 and 16 DIV. The SypI-EGFP construct was made by Alessandra Ferrari in the lab. EGFP was fused to the cytosolic, carboxy-terminal of synaptophysin (Pennuto et al., 2002) and its expression was driven by the platelet derived growth factor promoter as described previously for the chick β-actin gene (Morales et al., 2000).

2.5.4 Identification of glutamate receptors

Expression of EGFP-tagged glutamate receptors

Hippocampal cultures were transfected with EGFP-GluR2 as described previously. The EGFP-GluR2 construct was a kind gift from Dr. Y. Hayashi. EGFP was fused to the extracellular, NH_2-terminus of the glutamate receptor 2 subunit (Shi et al., 2001; Shi et al., 1999).

Live antibody labelling of glutamate receptors

An alternative method for labelling glutamate receptors by a rabbit antibody directed against the extracellular domain of GluR1 was also used. In this case cultured neurons were incubated with 12.5 μg/ml of anti-GluR1 antibody (Calbiochem) in culture medium at 37°C for 45 min, washed with fresh culture medium, incubated with goat anti-rabbit Cy-2 secondary antibody (1:200 dilution; Jackson Immunoresearch) for 30 min, and then washed with fresh culture medium. These cultures could then be used in experiments where the pre-synaptic terminals were labelled with FM4-64.

2.6 Fluorescence Imaging

2.6.1 Epifluorescence microscopy

An Olympus BX50WI upright microscope was used for both live cell imaging and viewing fixed tissue. 4x (0.13NA) air and 10x (0.3NA), 40x (0.8NA) and 60x (0.9NA) water immersion objectives were used to view samples. 12-bit images were acquired using a Princeton Instruments 1392 x 1040 cooled-CCD camera controlled by Metamorph software (Universal Imaging Corp.). Brightfield images were acquired with DIC optics. Fluorophores were excited by light from a mercury burner lamp. GFP, FM1-43 and Cy-2 fluorescence was viewed using a 475/40 nm excitation filter, a 505LP dichroic and a 535/45 nm emission filter. FM4-64 was viewed using a 535/30 nm excitation filter, a 595LP dichroic and a 645/75 nm emission filter.

2.6.2 Confocal microscopy and FRAP

Imaging

Experiments involving the photobleaching of fluorophores were carried out using a confocal laser scanning unit (BioRad Radiance 2100) mounted on a Nikon microscope with a 60x 1.0NA dipping objective (Nikon). Excitation was provided by a 488 nm argon laser, and 512 x 512 pixel, 8 bit images were collected using BioRad Laser Sharp software. FM1-43 fluorescence was collected using a 528/50 nm filter set. In experiments requiring simultaneous imaging of EGFP-tagged constructs and FM4-64, the emitted light was split by a 560 nm dichroic mirror and collected with a 515/30 nm filter for EGFP and a 660 nm LP filter for FM4-64.

Fluorescence recovery after photobleaching

Synapses fluorescently labelled with either FM4-64 or SypI-EGFP were photobleached to within ~8% of their original fluorescence by repeated localized scans of the laser at high power, using the ROI-zoom function of BioRad Laser Sharp software. Images were acquired at 0.1 Hz for a brief period before photobleaching, and fluorescence recovery monitored for up to 600s after photobleaching. In experiments using the fixable analog of FM1-43 to examine the ultrastructural nature of vesicle movement, regions of interest were scanned 10 times at maximum laser power to effectively remove all FM1-43 derived photoconversion products.

2.6.3 Image analysis

Metamorph image analysis software was used to analyse fluorescent signals in raw unfiltered images.

Puncta movement

Fluorescent puncta movement was quantified using the track objects function; the positions of fluorescent puncta along a length of axon were identified in each frame of a time-lapse sequence to quantify the average displacement of puncta over time.

FRAP

Fluorescence signals at individual synapses were quantified by measuring the average pixel intensity within a region circumscribing the bouton of interest in both FRAP and fluorescence destaining experiments. Values obtained from Metamorph were further analysed and displayed graphically using either Excel (Microsoft) or Origin (Microcal Software, Inc.).

Kymographs

Kymographs were produced using the 'kymograph' function in Metamorph. A line of 5 pixels width (x-dimension) was drawn along the length of axon (y-dimension). The line was analysed by the Metamorph software, and the average value of the pixels in the x-dimension displayed for each point along the y-dimension. This process was carried out for each time point and the results placed one after another, from top to bottom, in order to display the changes in intensity along the line over time.

Two-tailed *t*-tests were used to compare data sets where data was normally distributed. Pearson R test was used for correlation analysis. Values in the text represent mean ± SEM, unless otherwise stated. Statistical significance was considered to have been achieved when $P < 0.05$.

2.7 Electron Microscopy

2.7.1 Photoconversion of FM1-43

FM1-43FX labelled cultures were fixed with 2% paraformaldehyde/2% glutaraldehyde in phosphate-buffered saline (PBS) at room temperature for 15 min and then washed with 100 mM glycine in PBS for 1 h followed by 100 mM NH_4Cl for 1 min and then rinsed in PBS. Target regions from fluorescence experiments were re-identified by transmitted light microscopy with the help of a gridded coverslip attached to the underside of the imaging chamber using an Olympus BX50WI upright microscope. For photoconversion, cells were pre-incubated in 1

mg/ml DAB in PBS for 10 min. FM1-43FX was photoconverted by illuminating a region of interest with 475/40 nm light from a mercury lamp, with all neutral density filters disengaged, for 10-15 mins in the presence of fresh DAB solution. Following photoconversion neurons were rinsed with PBS and a series of images at 4x, 10x and 60x magnifications were acquired, these would be used later to help identify the region of interest in EM.

2.7.2 Preparation of neurons for sectioning

Secondary fixation

Aldehyde fixed and photoconverted samples were treated with a 1% osmium tetroxide/1.5% potassium ferrocyanide solution for 1 hr, to fix lipids and enhance the contrast of membrane staining later. Samples were rinsed with 0.1 M sodium cacodylate buffer and stored at 4°C.

Embedding

Samples were stained with a 1% solution of tannic acid in 0.05 M sodium cacodylate buffer for 45 min. A 1% solution of anhydrous sodium sulphate in 0.05 M sodium cacodylate was used to neutralize the tannic acid. Samples were then rinsed in deionised water and dehydrated step-wise with 70%, 90% and 100% ethanol. Samples were placed in a 1:1 EPON/propylene oxide mix for 1 hr and then transferred into EPON alone for 4 h with one exchange of EPON after 2 h. Coverslips were then inverted onto a capsule/block of EPON with the region of interest towards the centre of the block. The EPON was allowed to harden overnight at 60°C.

Removal of coverslips

Coverslips were removed by a combination of submersion in liquid nitrogen and applying pressure to the edge of the coverslip with metal tongs.

2.7.3 Correlative light and electron microscopy

Once the glass coverslip had been removed, the embedded neurons could be viewed using a stereo microscope and a fibre optic illuminator. A composite of 4x, 10x and 60x brightfield DIC images of the region of interest, taken after photoconversion, was used to locate the region on the EPON block. The region to be serial sectioned was then marked out using a scalpel.

2.7.4 Ultrathin Sectioning of Samples

Serial sectioning

EPON blocks were mounted in the microtome and excess resin trimmed using a strong blade up to the scalpel marked region. Care was taken that the edges of the region were clean and sharp, and that the long edges were parallel for ease of alignment with the diamond knife and good ribbon formation when sectioning began. The EPON block was then aligned with the edge of the diamond knife and sectioned at a rate of 0.8 mm/s. Sections were collected in the water boat attached to the knife, stretched with chloroform and placed onto formvar-coated slot grids.

Section contrast staining

Sections were contrast stained by inverting the slot grids onto a drop of lead citrate solution for 10 min and washing repeatedly with ultrapure water.

Formvar coating slot grids

Enough formvar solution was added to an open ended separatory funnel such that 2/3 of the height of a microscope slide, standing in the funnel, was submerged. Glass slides were cleaned with a lint-free cloth and dust removed with pressurized air. The flow rate of formvar solution through the funnel and the concentration of the formvar determined the thickness of the formvar coating on the glass slide. The flow rate was adjusted to give silver-gold thickness film. The coated slide was allowed to dry for 45 s and the edges were scored with a razor-blade. The slide was "frosted" by exhaling heavily on it and the film removed from the slide by

immediately touching the bottom edge of the slide onto the surface of an overfilled staining dish of water and slowly lowering the slide into the bath, perpendicular to the water surface. Copper slot grids were gently laid onto the floating film, which was picked up using a glass slide with an address label trimmed to the size of the slide attached to one side. The slide was placed perpendicular to the water surface at one end of the formvar film and pushed into the water again perpendicular to the surface, picking up the formvar film on the way as it adhered to the address-labelled side of the glass slide. The coated grids were then allowed to dry before storage.

2.7.5 Image acquisition

Samples were viewed using a Phillips EM420 electron microscope. Images were acquired on film and digitally scanned at 20,000 d.p.i. or with a 1392 x 1040 cooled CCD camera (Roper Scientific, Inc.). Target boutons were identified by aligning electron micrographs with brightfield DIC images of the same area. Once identified target synapses were then found on each section where they appeared and imaged. In this way a complete ultrastructural representation of synapse was obtained.

2.7.6 Analysis of electron micrographs

For quantification of vesicle numbers and distribution at synapses, digital images of serial sections for each bouton were aligned using multiple membrane and organelle landmarks. This and further analysis was carried out using Metamorph and XARA (Pantone Inc.) and is described in detail in Chapter 4. Two-tailed *t*-tests were used to compare data sets where data was normally distributed. Kruskal-Wallis ANOVA was applied for group comparisons when data did not meet the requirements for a parametric ANOVA test. Distributions were compared using Kolmogorov-Smirnov two-sample test. Values in the text represent mean ± SEM, unless otherwise stated. Statistical significance was considered to have been achieved when $P < 0.05$.

2.7.7 Three dimensional reconstruction of electron micrographs

For serial reconstructions, a digital overlay, marking the positions of vesicles and active zones, was generated for each of the aligned sections. Vesicle diameter was assumed to be 50 nm, based on the average diameter of the vesicle population. The overlays were then stacked in sequence and reconstructed using three-dimensional rendering software (Volocity, Improvision), assuming a section depth of 60 nm.

2.8 Collaborations

All the experiments presented in this thesis were carried out by me. However, Dr. Kevin Staras provided valuable discussions and collaborations on many of the experiments. Dr. Lucy Collinson provided serial sectioning expertise. Dr. Alexandra Ferrari supplied organotypic hippocampal slice cultures and SypI-EGFP constructs. Lily Yu carried out a blind analysis of synaptic vesicle numbers.

Chapter 3 | Fluorescence Study of Synaptic Vesicle Dynamics in Hippocampal Neurons

3.1 Introduction

Hippocampal neurons form synapses *en passant* such that axons harbor multiple release sites along their length, while individual release sites mediate synaptic transmission by the fusion of neurotransmitter containing vesicles in response to action potentials. Fast synaptic transmission is sustained by the local endocytic retrieval of vesicles back into synapses following exocytosis. Local recycling, by lessening the need for new proteins or vesicles, ensures the long-term maintenance of function at synapses that sometimes lie at great distances from the cell body (Sudhof, 2004). The synapse-specific reuse of vesicles would imply that presynaptic compartments function essentially as autonomous vesicle recycling units, which act more or less independently of neighbouring release sites in maintaining their synaptic vesicle clusters. However, recent work examining the behaviour of fluorescently labelled synaptic components, particularly in developing systems, suggests that synaptic vesicles may be more mobile than previously thought (Ahmari et al., 2000; Hopf et al., 2002; Kraszewski et al., 1995; Krueger et al., 2003). Thus far mobile presynaptic proteins and vesicles have been viewed as a means of rapid synapse formation (Matteoli et al., 2004) and there has been little investigation of the stability of synaptic vesicle clusters in mature systems. In particular, the likelihood or extent of synaptic vesicle sharing between mature synapses in quiescent networks has not been addressed. The instability of synaptic vesicle clusters would call into question the assumption that the synaptic vesicle cycle is restricted to individual release sites. This and subsequent chapters investigate the stability of vesicle clusters at mature synapses and the implications of the observed

mobility of recycling pool vesicles on both the function and ultrastructure of established, stable synapses.

3.2 Visualizing Hippocampal Synapses

Hippocampal neurons grown in culture develop in a stereotyped way to create a synaptic network of interconnected neurons (Dotti et al., 1988). The discrete localization of presynaptic components and vesicle recycling has been demonstrated after as little as 3 days in culture (van den Pol et al., 1998). Following 12-14 days in culture, the majority of synapses have undergone maturation, and show more efficient excitation-secretion coupling than seen in younger cultures as well as the discrete postsynaptic apposition of glutamate receptors (Renger et al., 2001). Figure 3.1a is a DIC image of a neuronal network formed on an astrocyte feeder layer. Figure 3.1b illustrates in more detail an individual neuron within the network, while in Figure 3.1c the synapses formed onto this cell have been marked by loading the vesicles with FM1-43 by field stimulation. The live labelling of synapses in culture can also be achieved by transfecting neurons with the cDNA of synaptic vesicle-associated proteins fused to EGFP or its variants. In Figure 3.1d vesicles have been labelled with both synaptophysin I-EGFP (SypI-EGFP) and FM4-64. The observed co-labelling of most synapses implies that the majority of SypI-EGFP labelled synapses are functional and that protein over-expression is not detrimental to cell health. Whereas these methods concentrate wholly on identifying the presynaptic compartment, the simultaneous expression of postsynaptic glutamate receptors allows the identification of bona fide synapses as shown in Figure 3.1e. Alternatively, fluorescently conjugated antibodies directed against the extracellular domain of the GluR1 subunit, as in Figure 3.1f, can be used to identify mature postsynaptic domains. In Figure 3.1e and f the presynaptic compartments were identified by the activity-dependent labelling of synaptic vesicles with FM4-64. The majority of FM4-64 puncta are co-apposed to glutamate receptor-associated fluorescence, indicating that in these cultures most synapses are

in a mature state. The *en passant* nature of hippocampal synapses can be seen in the images shown in Figure 3.1 where synapses form as beads on a string along an axon apposed to a dendrite. These different methods of identifying mature synapses avoid the need for post-hoc immunostaining, thus readily permitting the study of the dynamic nature of recycling pool vesicles in live neuronal culture preparations presented in this thesis.

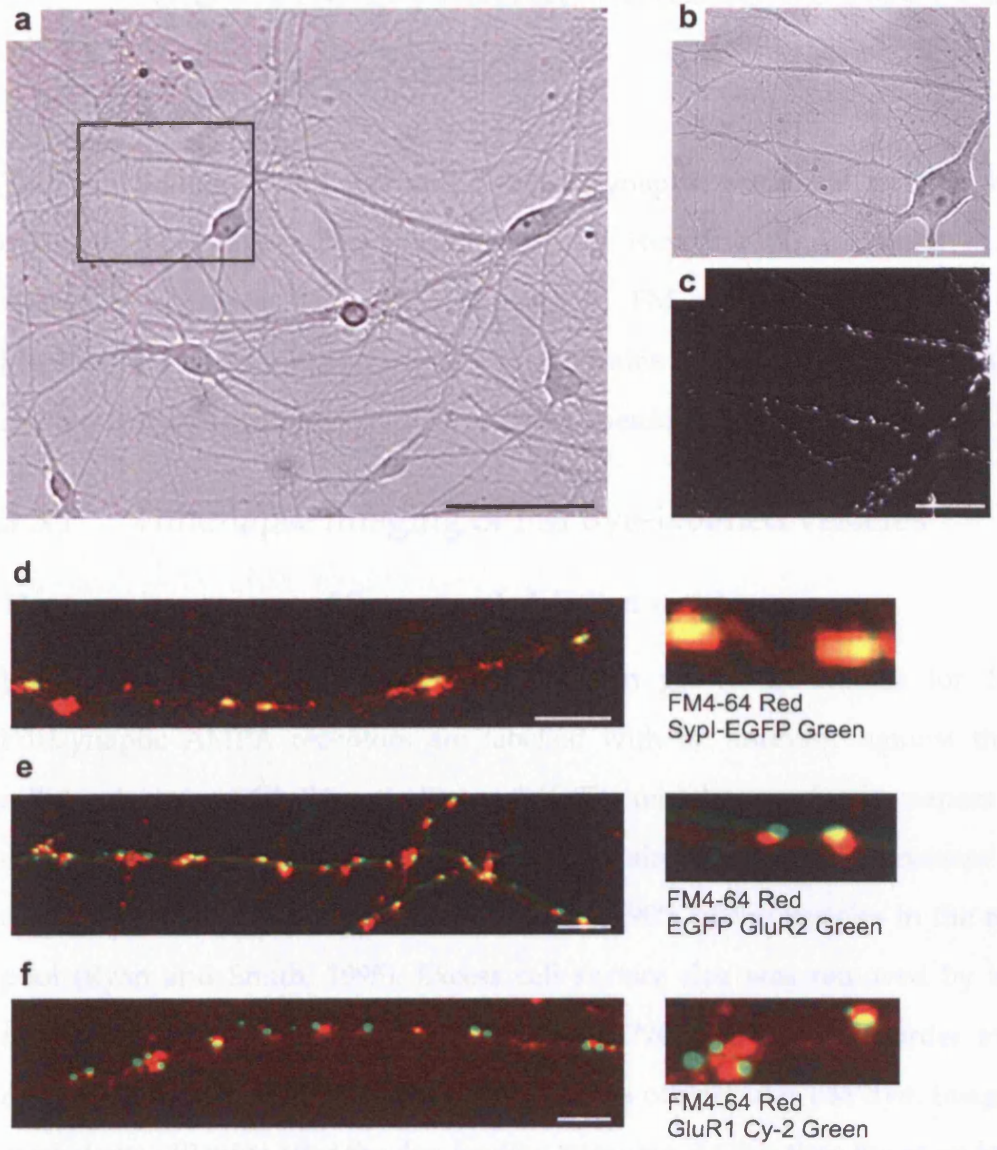

Figure 3.1 – Visualizing synapses of hippocampal neurons

(**a**) Low magnification brightfield DIC image of hippocampal neurons grown on an astrocyte feeder layer, after 14 days in culture. Scale bar 80 μm. (**b**) Higher magnification brightfield DIC image of an individual neuron from **a**. Scale bar 20 μm. (**c**) A fluorescence image of the neuron in **b** labelled with FM1-43 using a 600AP 10 Hz stimulus. Scale bar 20 μm. (**d**) Presynaptic boutons labelled with both FM4-64 (red) by field stimulation (600 APs 10 Hz) and SypI-EGFP (green) by transfection, Scale bar 10 μm. A higher magnification image showing the extent of co-labelling is shown on the right. (**e**) Fluorescence image of neurons transfected with EGFP-GluR2 (green) and subsequently labelled with FM4-64 (red) as in **d**, Scale bar 10 μm. A more detailed image demonstrating the juxtaposition of signal is also shown (right). (**f**) Synapses identified by the live labelling of postsynaptic receptors with anti-GluR1 primary antibody and Cy-2 conjugated secondary antibody (green) followed by the presynaptic labelling of vesicles with FM4-64 (red), Scale bar 10 μm. A higher magnification image detailing the labelling is shown on the right.

3.3 The Dynamic Nature of Recycling Pool Vesicles

The combination of FM dye and live postsynaptic glutamate receptor labelling outlined above allows the identification of recycling pool vesicles at mature excitatory synapses. Time-lapse imaging of FM dye-labelled vesicles at such identified synapses makes it possible to determine the stability of functional vesicle clusters at the presynaptic boutons of resting neurons.

3.3.1 Time-lapse imaging of FM dye-labelled vesicles

The axonal movement of fluorescently labelled vesicles

Figure 3.2 shows the synapses of a neuron grown in culture for 14 days. Postsynaptic AMPA receptors are labelled with an antibody against the extracellular domain of GluR1, as in Figure 3.1f. The recycling pools of synapses in these cultures were labelled by delivering a 600 AP train at 10 Hz in the presence of FM4-64. This protocol is believed to access close to 90% of the vesicles in the recycling pool (Ryan and Smith, 1995). Excess cell surface dye was removed by repeated exchanges of bath solution which contained CNQX and APV in order to reduce recurrent synaptic activity and prevent the loss of vesicular FM dye. Imaging was carried out ~10 mins after the dye-loading stimulus. At this time the re-endocytosed vesicles should have reclustered back at the synapse, given that endocytosed vesicles can be re-primed for release within 15 s of re-uptake (Ryan and Smith, 1995). A sample time-lapse sequence, acquired at 1 frame per 5 s, reveals the dynamic nature of recently recycled vesicles with FM4-64 fluorescence being transported in both anterograde and retrograde directions along mature axons (Figure 3.2a). Kymograph analysis of axonal segements also reveals the movement of FM4-64 packets. Stable boutons appear as vertical lines whereas mobile packets of fluorescence appear as diagonal lines between these (yellow arrowheads, Figure 3.2b). Fluorescence movement seems to occur in two modes: a modular or packet-like exchange is highlighted with yellow arrowheads in Figure 3.2a left panel, while

the more diffuse fluorescence signal seen to arise between the two synapses in the right panel of Figure 3.2a, highlighted with green arrowheads, may represent the flux of individual or non-clustered vesicles between synapses. The movement of synaptic vesicles was reflected in the changes in fluorescence intensity recorded at individual FM4-64 labelled boutons (Figure 3.2c). At the majority of boutons examined the positive and negative fluctuations in intensity appeared to approximately balance over time. The observed changes in fluorescence at individual boutons may reflect the movement of FM4-64 packets through the region of interest without them having any actual impact on the synapse itself. However, these fluctuations might also reflect the intermittent, but non-synchronized addition and loss of labelled vesicles at these synapses. This could suggest that the population of vesicles at a synapse may be changing over time while the actual size of the vesicle cluster is maintained. The contribution and implications of the movement of recycling pool vesicles on stable synapses will be further investigated in later sections.

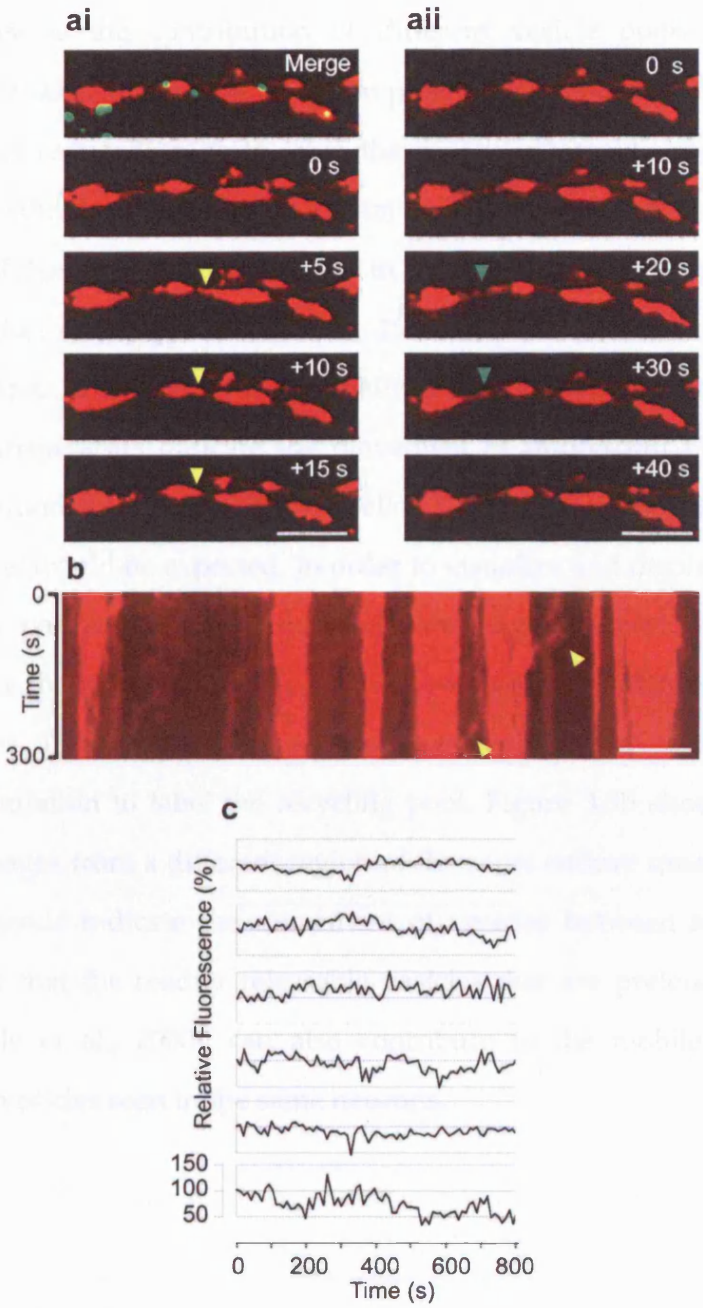

Figure 3.2 – Inter-bouton movement of vesicles

(**ai**) Merge, FM4-64 labelled synapses (red) co-apposed to postsynaptic antibody-labelled glutamate receptors (green), as in Figure 3.1f. Yellow arrowheads in time-lapse sequence highlight the transfer of a fluorescent packet between two mature synapses. (**aii**) A second time-lapse sequence of the same boutons shows a more diffuse spread of FM4-64 derived fluorescence signal (green arrowheads) between two mature synapses. Scale bars, 2.5 μm. (**b**) Kymograph of an axon containing FM4-64 labelled boutons, detailing fluorescence movement between boutons over time. Mobile packets appear as diagonal lines whose slopes are related to their velocity (yellow arrowheads). Scale bar, 5 μm. (**c**) Typical sample traces of the temporal fluctuations in FM4-64 fluorescence intensity (normalized to the first five points in the sequence) at six individual boutons.

Relationship between extent of recycling pool labelling and movement

In order to assess the contribution of different vesicle pools to the mobile population of vesicles, the number of action potentials delivered to neurons by field stimulation was reduced so as to label the readily releasable pool at synapses. Neurons were stimulated with a 40AP train at 20Hz in the presence of FM1-43, a condition which has been used previously to label the readily releasable pool in the same preparation (Murthy and Stevens, 1999; Rosenmund and Stevens, 1996). Sample time-lapse images from a minimally loaded culture are shown in Figure 3.3a. Orange arrowheads indicate the movement of fluorescent packets between synapses. The fluorescence intensity of labelled synapses was considerably lower in these cultures as would be expected. In order to visualize and display the exchange of fluorescent packets between synapses, the digital contrast was adjusted accordingly. At the end of imaging the neurons were stimulated to destain the labelled vesicles. The same cultures were once more loaded with FM1-43 by a 600 AP 10 Hz stimulation to label the recycling pool. Figure 3.3b shows a time-lapse sequence of images from a different region of the same culture used in Figure 3.3a. Yellow arrowheads indicate the movement of vesicles between synapses. These results suggest that the readily releasable vesicles that are preferentially used in exocytosis (Pyle et al., 2000), can also contribute to the mobile population of recycling pool vesicles seen in the same neurons.

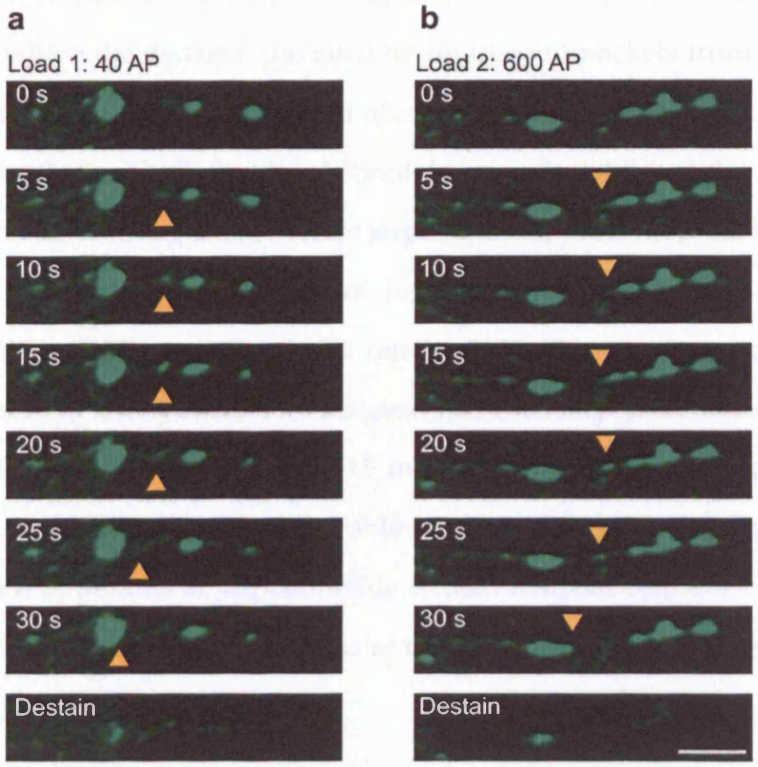

Figure 3.3– Differential vesicle pool labelling and movement

(**a**) A time-lapse sequence of a neuron labelled with FM1-43 using a minimal loading protocol of 40 APs at 20 Hz. Inter-bouton fluorescence movements are highlighted by yellow arrowheads. A stimulus was applied at the end of time-lapse imaging to destain the labelled vesicles. (**b**) A time-lapse sequence from a different region of the same neuron, re-labelled with FM1-43 by 600 AP 10 Hz stimulation. The movement of fluorescence between boutons is marked with yellow arrowheads. Images in **a** were scaled differently to those in **b** in order to visualize fluorescence movement in the minimally loaded neurons. Scale bar, 5 μm.

3.3.2 Jasplakinolide inhibits vesicle transport

In order to demonstrate that the observed vesicle movement is an active, transport-dependent process, the neurons were treated with the actin stabilizing agent jasplakinolide, a known inhibitor of fast axonal transport (Hiruma et al., 2003). The effects of 1 μM jasplakinolide were assessed by imaging the same regions of FM1-43 labelled cultures before and after treatment with the inhibitor. Figure 3.4a shows the dynamic nature of FM-labelled vesicles under control conditions with fluorescence passing along the region of axon denoted by the blue bar. The cultures were then treated with jasplakinolide for 15 mins and the same region imaged once more. Jasplakinolide noticeably blocked the movement of vesicles along the same

region of axon (blue bar, Figure 3.4b). Figure 3.4c summarizes the data from three experiments where the distance travelled by fluorescent packets from their point of origin was measured before (black) and after (red) the application of jasplakinolide. It is clear from this analysis that jasplakinolide severely inhibited the movement of FM4-64 fluorescence along axons. While jasplakinolide prevented the inter-synaptic movement of vesicles, the synapses of treated cultures were still functional as assessed by their ability to exocytically release FM1-43 in response to stimulation. Figure 3.4d shows the relative FM fluorescence intensity at boutons undergoing stimulation from cultures treated for 15 mins with jasplakinolide or DMSO as a control. The rate of dye loss is comparable between the two conditions, indicating that the release apparatus at jasplakinolide treated neurons remains functional and that vesicle mobilization within boutons at this particular stimulus frequency is not impaired by jasplakinolide treatment.

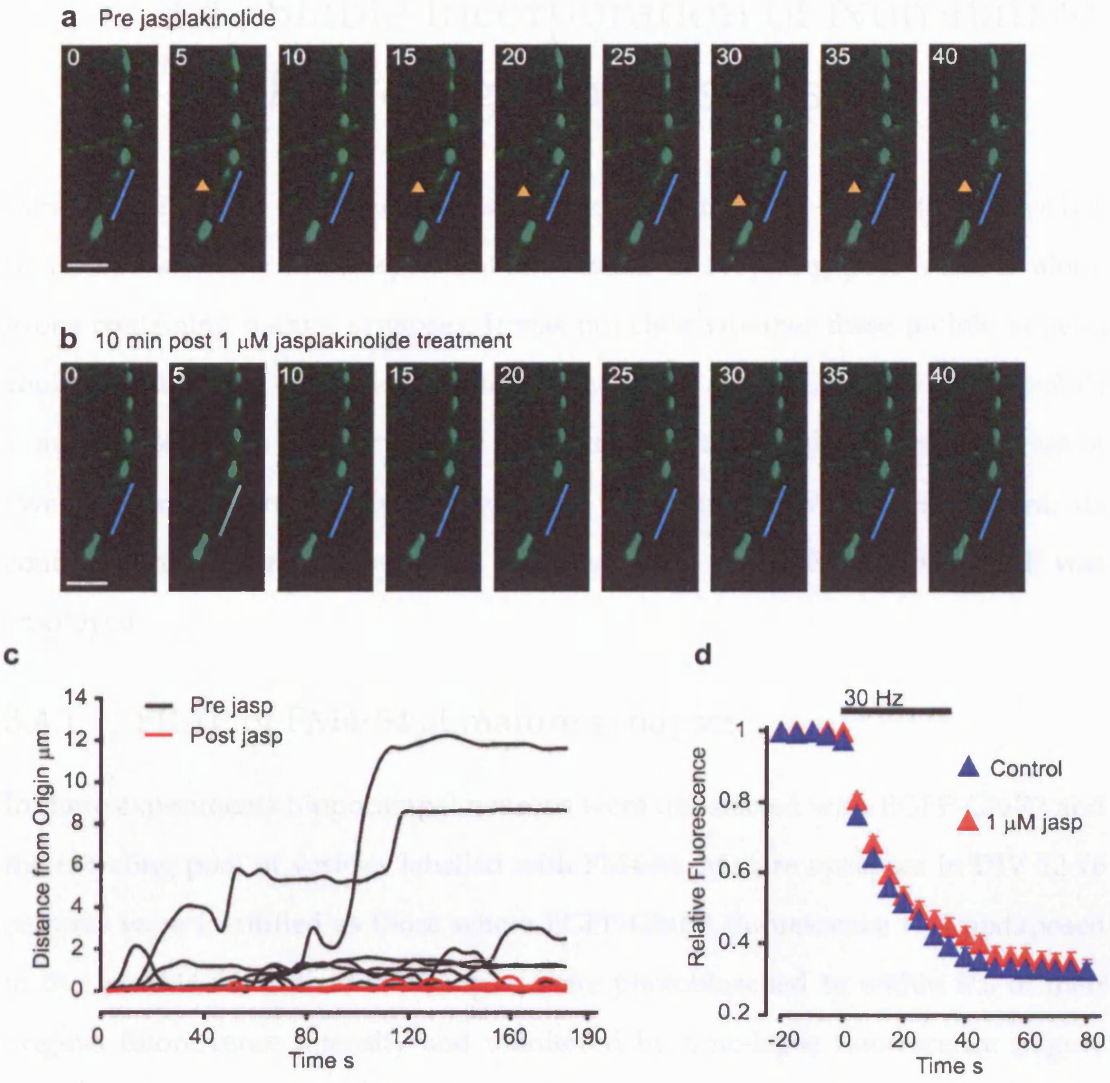

Figure 3.4 – Jasplakinolide inhibits axonal transport

(**a**) A sequence of time-lapse images from FM1-43 labelled neurons. Movement of fluorescence along the region of axon marked with the blue bar is highlighted with a yellow arrowhead. (**b**) Time-lapse images from the same region as **a**, following a 10 min treatment with jasplakinolide (1 μM). There is no evidence of fluorescence movement along the region of axon marked by the blue bar. Scale bars, 5 μm. (**c**) A summary of the distance moved by fluorescence packets before and after jasplakinolide treatment. (**d**) A comparison of the time-course of FM1-43 fluorescence destaining for untreated and jasplakinolide-treated cultures. Data are mean ± s.e.m.

3.4 Stable Incorporation of Non-native Recycling Pool Vesicles

Time-lapse imaging of neurons whose vesicles have been labelled with FM dye has so far revealed the actin-dependent movement of recycling pool vesicles along axons containing mature synapses. It was not clear whether these mobile vesicles could contribute to the vesicle clusters at synapses or whether they are a mobile subset of the vesicle population that have little relevance to the general function of synapses or neurons. To further address the nature of vesicle movement, its contribution to other synapses and its relevance to synapse function, FRAP was employed.

3.4.1 FRAP of FM4-64 at mature synapses

In these experiments hippocampal neurons were transfected with EGFP-GluR2 and the recycling pool of vesicles labelled with FM4-64. Mature synapses in DIV 12-16 cultures were identified as those where EGFP-GluR2 fluorescence was juxtaposed to that of FM4-64. Individual synapses were photobleached to within 8% of their original fluorescence intensity and monitored by time-lapse fluorescence (Figure 3.5). If indeed the mobile population of vesicles could contribute to the vesicle cluster at synapses, a recovery in fluorescence would be expected at these photobleached boutons. FM4-64 fluorescence was seen moving in both directions through the bleached portion of axon, and over time accumulated at the site of the photobleached synapse (yellow arrowhead Figure 3.5a). On average the FRAP signal at photobleached synapses was 22 ± 4% (mean ± sem) after 560 s. This synapse specific fluorescence recovery provides strong evidence that vesicles arising from sites of endocytosis outside the bleach region can move along the axon to become stably incorporated at non-native synapses. To confirm that axonal transport is required for the observed FRAP signal, cultures were treated with 1 μM jasplakinolide for 15 mins, to inhibit vesicle movement, prior to the photobleaching of synapses labelled with both EGFP-GluR2 and FM4-64 (see section 3.3.2). Little

FM4-64 fluorescence movement along the axon was observed and no FRAP signal accumulated at the site of the photobleached bouton, reflecting the requirement for the axonal transport of vesicles in the observed recovery (Figure 3.5b). Figure 3.6a summarizes the time-course of FM4-64 fluorescence recovery at photobleached boutons in untreated and DMSO treated cultures (red) and jasplakinolide treated cultures (blue). Fluorescence recovery was not significantly different between DMSO and untreated samples (*t*-test, 100 s post-FRAP: $P = 0.75$, untreated: $n = 6$, 13 ± 3%; DMSO: $n = 3$, 14 ± 2%; 500 s post-FRAP: $P = 0.57$, untreated; 23 ± 4%; DMSO: 18 ± 7%), and these groups were pooled.

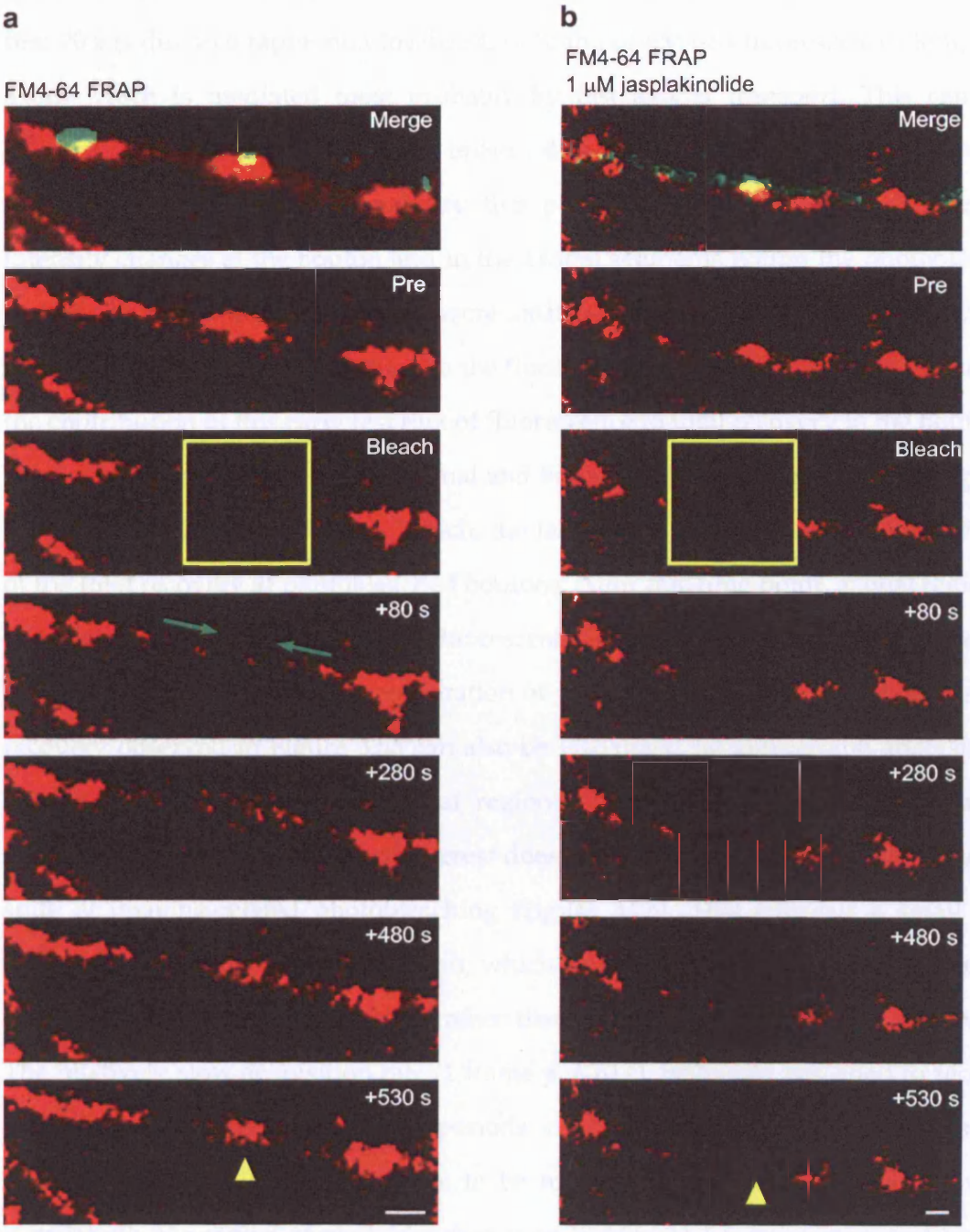

Figure 3.5 – FRAP of FM4-64 at mature synapses

(**a**) FRAP time-lapse images from FM4-64 and EGFP-GluR2 labelled hippocampal neurons. After photobleaching (yellow box), FM4-64 fluorescence recovers over time at the site of the bleached synapse (yellow arrowhead). Green arrows denote the fast axonal flux of fluorescence through the photobleach region. Scale bar, 2 µm. (**b**) FRAP time-lapse images of neurons as in **a**, following treatment with jasplakinolide (1 µM). There was little FM4-64 fluorescence recovery at the site of the photobleached synapse (yellow arrowhead). Scale bar, 2 µm.

The initial fast rise in fluorescence seen at untreated photobleached boutons in the first 70 s is due to a rapid, non-localized, in-filling of FM4-64 fluorescence along the axon, which is mediated most probably by fast axonal transport. This can be inferred from the sample time-lapse images shown in Figure 3.5a, highlighted with green arrows. However, to quantify this phenomenon, the initial fluorescence intensity changes at the bouton and in the axonal segments within the photobleach region adjacent to the target bouton were measured. Figure 3.6b shows the recovery curve for the axonal regions scaled to the fluorescence in target boutons to illustrate the contribution of this early fast flux of fluorescence to total recovery in the bouton. The initial phase of recovery for axonal and bouton regions (yellow shading Figure 3.6b) is similar, and at 70 s post bleach, the fast axonal recovery accounts for ~75% of the total recovery at photobleached boutons. After this time point, axonal regions show no further accumulation of fluorescence, while target boutons continue to recover, reflecting the stable incorporation of vesicles at synapses. The fluorescence recovery observed in Figure 3.5a can also be visualized by kymograph analysis of the bouton and surrounding axonal regions (Figure 3.7a). The total integrated fluorescence within the region of interest does not change significantly over time in spite of imaging-related photobleaching (Figure 3.7b). This suggests a small net gain of fluorescence within the region, which could be explained if vesicle sharing were to occur over a longer range rather than simply between adjacent synapses. The relatively slow acquisition rate (1 frame per 10 s), primarily designed to record fluorescence recovery over long periods of time, does not allow the rapid movements of small vesicle clusters to be monitored. Figure 3.7c is an example kymograph of a region of photobleached axon imaged at 1 frame per second for 60 s. The fluorescence recovery observed here should correspond to the early component of recovery seen in the plot in Figure 3.6b. With this rate of acquisition, it is possible to track the movement of small fluorescent particles through consecutive frames, seen in the kymograph as continuous diagonal lines capable of moving across the width of the photobleached region within 10 s. This data further supports the idea that the fast axonal flux of fluorescently labelled vesicles contributes to the early phase of recovery.

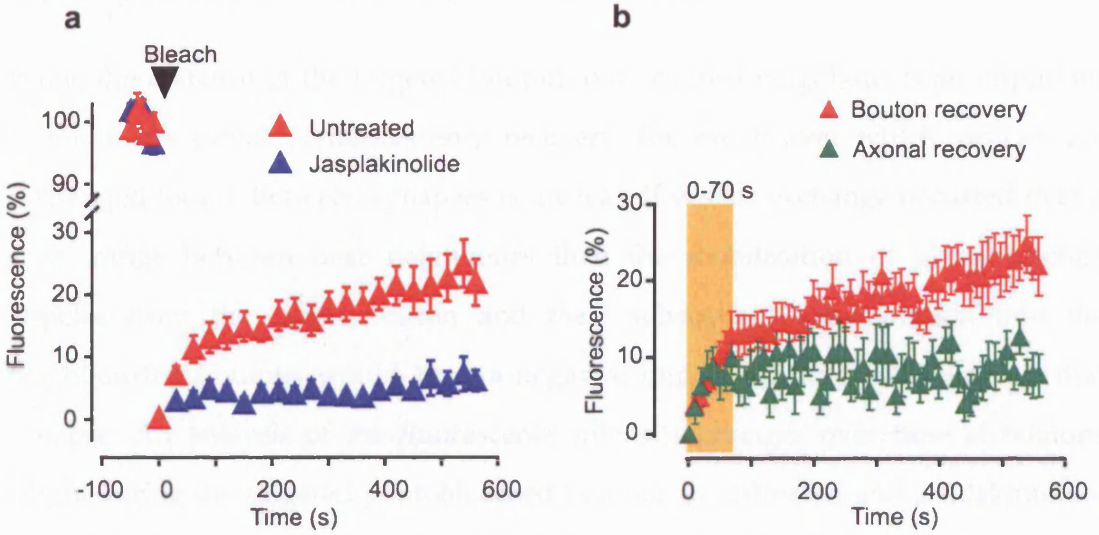

Figure 3.6 – Analysis of vesicle incorporation

(**a**) Average FRAP time-course of untreated (red triangle, n = 9) and jasplakinolide-treated cultures (blue triangle, n = 8). Boutons were photobleached to an average of 8.1 ± 1.1% of original fluorescence for untreated cultures and 7.7 ± 1.5% for jasplakinolide treated cultures. The data is normalized to the extent of bleach to illustrate clearly the degree of recovery. Data are mean ± s.e.m. (**b**) Fluorescence recovery curve for photobleached boutons (red triangles) and axonal segments adjacent to target boutons (green triangles) from the dataset in **a**. Both traces are scaled to the pre-photobleach fluorescence in target boutons to show the contribution of fast axonal flux to the total fluorescence recovery observed in the synapse. The initial phase of recovery (0-70 s) for axonal and bouton regions are highlighted with a yellow box. Data are mean ± s.e.m.

The relationship between FRAP and neighbouring boutons

The fluorescence recovery observed at photobleached synapses is consistent with the movement of FM4-64 from other synapses along the axon. As such, the distance between targeted photobleached boutons and their nearest fluorescently labelled neighbour would be expected to influence the FRAP signal. In experiments comparing the fluorescence recovery in jasplakinolide treated and untreated samples, all targeted synapses were within 7 μm of a neighbouring synapse. Over this range there was no correlation between the extent of fluorescence recovery and the distance to non-photobleached nearest-neighbour (Pearson R test, n = 11, r = -0.35, P = 0.289). However, when targeted synapses were located at greater distances from potential sources of fluorescence there was a significant negative correlation

between recovery of fluorescence and distance to nearest neighbour as shown in Figure 3.8a (Pearson R test, $n = 16$, $r = -0.70$, $P = 0.003$).

While the distance of the targeted bouton to its nearest neighbour is an important factor in the extent of fluorescence recovery, the range over which vesicles are exchanged locally between synapses is unclear. If vesicle exchange occurred over a short range between near neighbours then the mobilization of photobleached vesicles from the target bouton and their subsequent incorporation into the neighbouring boutons would have a negative impact on the fluorescence at that synapse. An analysis of the fluorescence intensity changes over time at boutons neighbouring the targeted photobleached boutons in untreated and jasplakinolide-treated cultures was carried out and is summarized in Figure 3.8b. In both cases an approximately linear imaging-related decrease in fluorescence is observed at neighbouring boutons. There is some evidence for a small additional decrease in fluorescence at neighbouring boutons in untreated cultures compared to jasplakinolide-treated cultures. This may represent the displacement of FM-labelled, host recycling pool vesicles by photobleached vesicles originating from target boutons. Nevertheless, the small size of this effect would indicate that vesicles arising from individual release sites are most likely distributed across multiple synapses. Indeed, fluorescent packets were seen to travel up to 14 μm from their origin over the time-course of imaging in earlier experiments (Figure 3.4c). Therefore any impact of photobleaching the recycling vesicle pool at a single bouton is likely to be only weakly apparent in the fluorescence intensity of other boutons within the neighbourhood.

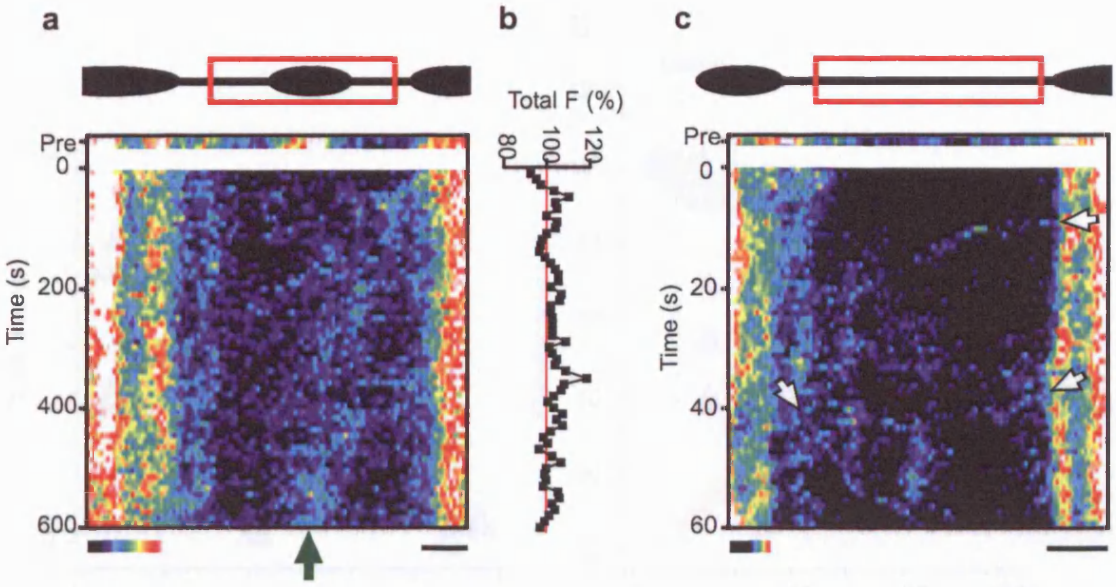

Figure 3.7– Kymograph plots of FM FRAP

(**a**) Kymograph of the region of axon, including the photobleached bouton and its neighbours (see schematic) from Figure 3.5a. Images were acquired at 0.1 Hz and demonstrate the temporal accumulation of fluorescence at the target synapse (green arrow). (**b**) A time-course of the integrated fluorescence of the line of interest from the kymograph in **a**. (**c**) A kymograph of a region of photobleached axon in an FM1-43 labelled neuron imaged at 1 Hz. The movement of small fluorescent packets along the axon through consecutive frames is seen in the kymograph as continuous diagonal lines (arrowheads). Scale bars, 2 μm

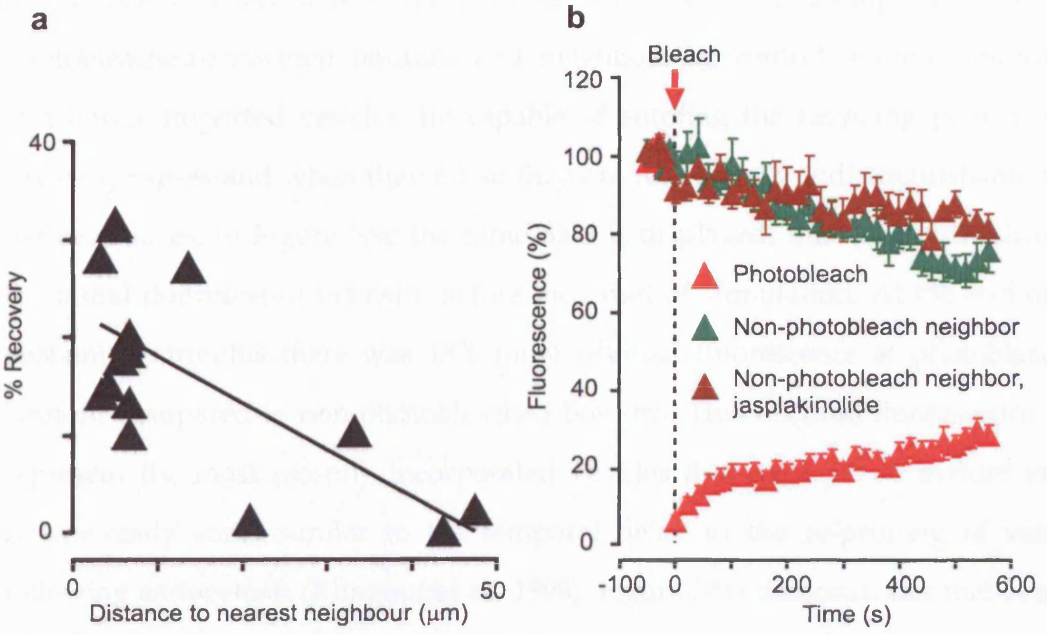

Figure 3.8– Relationship between FRAP and neighbouring boutons

(**a**) A comparison of FRAP signal at synapses at 600s post-bleach as a function of their distance to the nearest non-photobleached neighbour. There was a significant negative correlation between the extent of FRAP and distance to nearest neighbour over a 50 μm range (Pearson R test, n = 16, r = -0.70, P = 0.003) (**b**) Fluorescence intensity measurements for photobleached synapses, and those immediately adjacent to them outside the photobleach region from the dataset used in Figure 3.6a. Note, for comparative purposes, bleached synapses are not normalized to the extent of bleach as in Figure 3.6a.

3.4.2 Imported vesicles join the recycling pool of synapses

The data so far suggests that vesicles recycled at a given synapse can depart from the vesicle cluster and move along the axon to become stably incorporated at another synapse. However, it is not clear whether these newly imported vesicles contribute functionally to host synapses. To test this, mature synapses were photobleached as before (Figure 3.5) and images acquired immediately after photobleaching and again 900 s later to assess the extent of recovery. FRAP was not monitored by time-lapse imaging so as to minimize the loss of fluorescence signal. After the recovery period, a destaining stimulus of 1200 APs at 20 Hz was applied and the change in fluorescence at recovered and neighbouring non-photobleached synapses was recorded at a rate of 1 frame every 2 s (Figure 3.9a). The kinetics of dye loss, a measure of the rate of exocytosis, from both populations of boutons is presented in Figure 3.9b. Data was normalized to the initial fluorescence values and

to the extent of dye loss at the boutons. The rate of destaining was similar at photobleached-recovered boutons and neighbouring control boutons, indicating that newly imported vesicles are capable of entering the recycling pool of non-native synapses and when they do so they are functionally indistinguishable from native vesicles. In Figure 3.9c the same data is displayed, this time normalized to the initial fluorescence intensity before the onset of stimulation. At the end of the destaining stimulus there was 18% more residual fluorescence at photobleached boutons compared to non-photobleached boutons. This residual fluorescence may represent the most recently incorporated vesicles that have yet to mature into a release-ready state, similar to the temporal delay in the re-priming of vesicles following endocytosis (Klingauf et al., 1998). Figure 3.9d demonstrates that at some photobleached boutons the FRAP signal destains to a similar extent as neighbouring non-photobleached control boutons. This supports the possibility that the variability in the extent of destaining of newly imported vesicles might relate to their time spent at the host synapse before the onset of stimulation, rather than the inability of the synapse to competently release vesicles upon stimulation due to phototoxicity. Further experiments to confirm the non-toxic effects of photobleaching on synapse function are shown in later sections (see section 4.3.3).

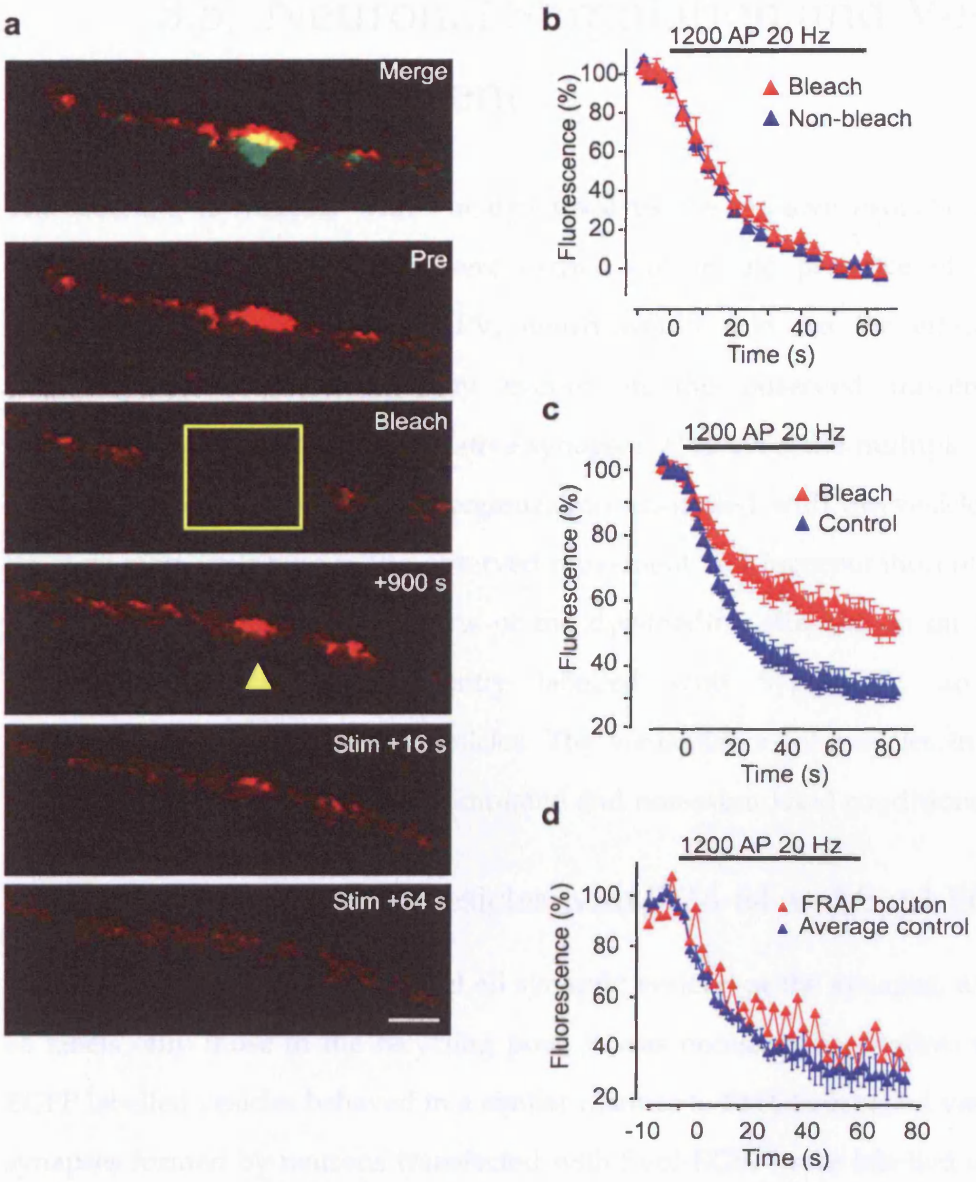

Figure 3.9 – Incorporated vesicles enter the recycling pool

(**a**) FM4-64 signal (red) is coapposed to EGFP-GluR2 (green), top panel. After photobleaching (yellow box), FM4-64 fluorescence recovers over time and is seen as a stably-localized signal at the site of the synapse after ~900 s (yellow arrowhead). Following stimulation, the recovered fluorescence at the photobleached bouton destains. (**b**) Average time-course of FM4-64 fluorescence during stimulation, normalized to total fluorescence lost, reveals similar destaining kinetics for recovered (red triangle, $\tau = 22.0 \pm 1.2$, $n = 7$) and non-bleached boutons (blue triangle, $\tau = 18.5 \pm 0.9$, $n = 35$). (**c**) Average time-course of FM4-64 fluorescence during stimulation, normalized to the initial fluorescence intensity. (**d**) The time-course of FM4-64 fluorescence destaining at a single recovered bouton compared to the average fluorescence intensity change of neighbouring non-photobleached boutons. Data are shown as mean ± s.e.m. Scale bar, 2 μm

3.5 Neuronal Stimulation and Vesicle Movement

The labelling of vesicles with Fm dye involves the massive exocytic release of neurotransmitter. Experiments were carried out in the presence of glutamate receptor blockers CNQX and APV, which would rule out the effects of any postsynaptically-derived plasticity events on the observed movement and incorporation of vesicles at non-native synapses. However, the multiple rounds of exocytosis and vesicle cluster re-organization associated with the vesicle labelling protocol may contribute to the observed movement and incorporation of recycling pool vesicles. To assess the effects of the dye-loading stimulation on the FRAP signal, vesicles were fluorescently labelled with SypI-EGFP, an activity-independent label of synaptic vesicles. The visualization of vesicles in this way allowed for their observation in stimulated and non-stimulated conditions.

3.5.1 Dual labelling of vesicles with FM4-64 and SypI-EGFP

Given that SypI-EGFP would label all synaptic vesicles at the synapse, while FM4-64 labels only those in the recycling pool, it was necessary to confirm that SypI-EGFP labelled vesicles behaved in a similar manner to FM4-64 labelled vesicles. The synapses formed by neurons transfected with SypI-EGFP were labelled with FM4-64 using a 600 AP 10 Hz load protocol (Figure 3.10a). The majority of SypI-EGFP positive terminals took up the FM4-64. From time-lapse images, EGFP signal was observed moving with FM4-64 fluorescence, indicating that the same mobile population of vesicles could be labelled with both fluorophores. There was also evidence for the movement of non-FM associated EGFP fluorescence along axons. As the excitation peaks for EGFP and FM4-64 are 498 nm and 506 nm respectively, it was possible to photobleach both signals at targeted boutons at the same time. Given that the emission spectra for these fluorophores are quite different, with peaks at 516 nm for EGFP and 751 nm for FM4-64, the fluorescence recovery of the two signals were monitored simultaneously with the appropriate filter settings

(Figure 3.10a). The time-course of fluorescence recovery is summarized in Figure 3.10b. While the fluorescence intensity of EGFP was greater than that of FM4-64, the extent of fluorescence recovery observed for both fluorophores was similar. This similarity validates the use of SypI-EGFP as a marker of vesicles to report the phenomenon of the inter-bouton exchange of vesicles. The activity-independent labelling of vesicles allowed the effect of the dye-loading stimulation on vesicle mobilization and incorporation to be studied.

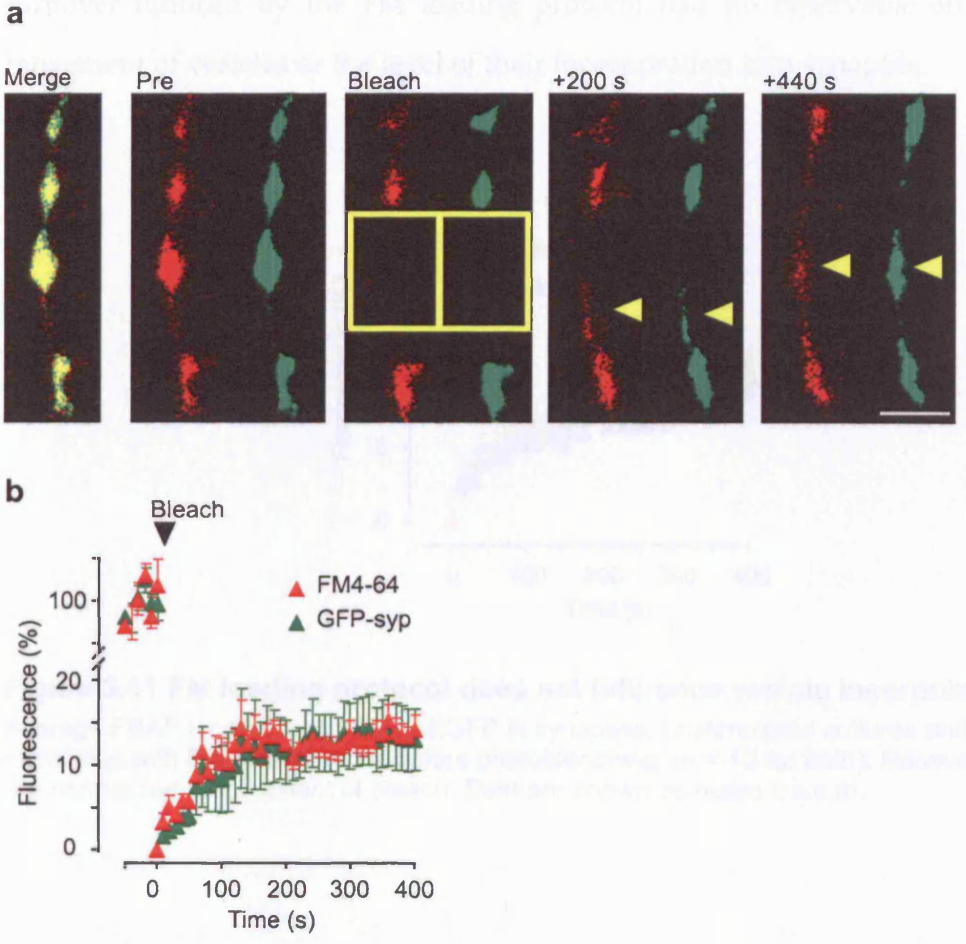

Figure 3.10 – FRAP of EGFP-SypI and FM4-64 labelled vesicles

(**a**) SypI-EGFP (green) and FM4-64 (red) fluorescence signals at co-labelled synapses show a similar recovery following photobleaching (yellow boxes). Yellow arrowheads highlight the movement and recovery of signal for both fluorophores. Scale bar, 2 μm. (**b**) Average FRAP time-course, normalized to the extent of bleach, for SypI-EGFP and FM4-64 in co-labelled synapses (n = 8). Data are shown as mean ± s.e.m.

3.5.2 FM dye loading stimulus does not affect FRAP

The fluorescence recovery of photobleached SypI-EGFP-positive boutons was measured in unstimulated, quiescent cultures and in others, 10 mins after a 600 AP 10 Hz stimulation. The 10 minute wait period mimicked the time taken to wash out FM dye in previous experiments. In both cases a recovery of fluorescence was observed, and the FRAP curves from both conditions are shown in Figure 3.11. The similarity in the rates and extents of fluorescence recovery demonstrates that vesicle turnover induced by the FM loading protocol had no observable effect on the movement of vesicles or the level of their incorporation into synapses.

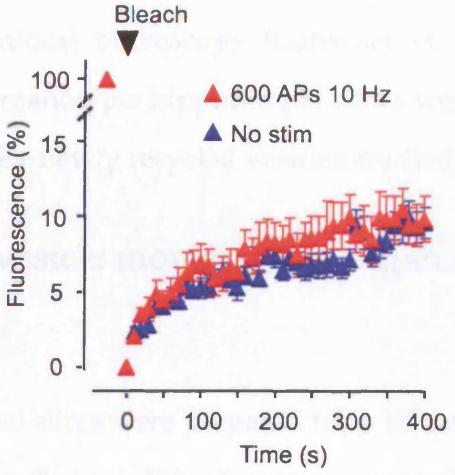

Figure 3.11 FM loading protocol does not influence vesicle incorporation
Average FRAP time-course of SypI-EGFP in synapses, unstimulated cultures and those stimulated with 600APs at 10 Hz before photobleaching, (n = 15 for both). Recovery curves are normalized to the extent of bleach. Data are shown as mean ± s.e.m.

3.6 Movement of Recycling Vesicles in Organotypic Hippocampal Slices

The movement of vesicles between the synapses of dissociated neurons grown in culture has been established using two different methods of vesicle labelling: FM4-64 or SypI-EGFP. One concern however, is that as the natural environment of the neurons is not preserved in dissociated neuronal cultures the results obtained here may be to some extent a product of this artificial system. Organotypic hippocampal slices provide a situation where the cyto-architecture of tissue is maintained to some degree, and yet the neurons are accessible for imaging with conventional epifluorescence and confocal microscopy (Gahwiler et al., 1997). The synaptic vesicles of neurons in organotypic hippocampal slices were labelled with FM1-43, and the behaviour of these newly recycled vesicles studied.

3.6.1 Observing vesicle movement in organotypic hippocampal slices

Organotypic hippocampal slices were prepared from P7 rats and maintained for up to 20 days by Alessandra Ferrari. Experiments were carried out after 15-20 days. Recycling pool vesicles of neurons were labelled by bathing the slices in a EBS containing 50 mM potassium and 10 μM FM1-43 for 2 minutess. Slices were then washed with EBS containing Advasep-7 for 5 minutes and for a further 20 minutes with fresh EBS. Fluorescence imaging of neuronal processes close to the surface of the slice revealed individual FM1-43 positive puncta distributed along these processes. Other seemingly non-process associated fluorescent puncta presumably belonged to axons lying out of the plane of focus (Figure 3.12a). Time-lapse imaging demonstrated the movement of small packets of FM1-43 fluorescence along processes between larger more stable fluorescent boutons (see yellow arrows Figure 3.12b). The FM dye represented fusion competent vesicles at presynaptic terminals, as bathing the slices with a solution containing 50 mM potassium induced destaining. The final two panels of the image sequence in Figure 3.12b show the

destaining of FM1-43 positive boutons in hippocampal slice culture in an example experiment.

3.6.2 FRAP of FM1-43 in organotypic slices

The results presented in the previous section report the mobility of newly recycled synaptic vesicles, as labelled with FM1-43 dye, in organotypic slices. These vesicles are capable of moving along axons in a manner similar to vesicles in dissociated hippocampal neurons. To continue the characterization of vesicle mobility in organotypic slices, the ability of these mobile recycling pool vesicles to stably incorporate into non-native synapses was assessed by FRAP as in dissociated hippocampal neurons (section 3.4.1). FM1-43 dye was loaded into the presynaptic terminals of organotypic slices with a high potassium solution as before. Fluorescently labelled boutons along neuronal processes were photobleached and images acquired immediately after bleaching and again 10 minutes later to assess the degree of recovery (Figure 3.12c). After this time a recovery in fluorescence was observed at the target boutons, an example of which is shown in Figure 3.12c, marked with a yellow arrow. The FRAP signal observed in organotypic slices, which was comparable to that seen at photobleached boutons in dissociated cultures, confirms that the dynamic nature of recycling pool vesicles is not a phenomenon restricted to dissociated cell culture systems. It was not feasible however, to carry out all experiments in organotypic slices due to imaging related issues such as high background fluorescence signal and restrictions in focal plane. In addition, technical problems with transfection and antibody penetration in slice culture preparations made the confirmation of the maturation state of boutons difficult.

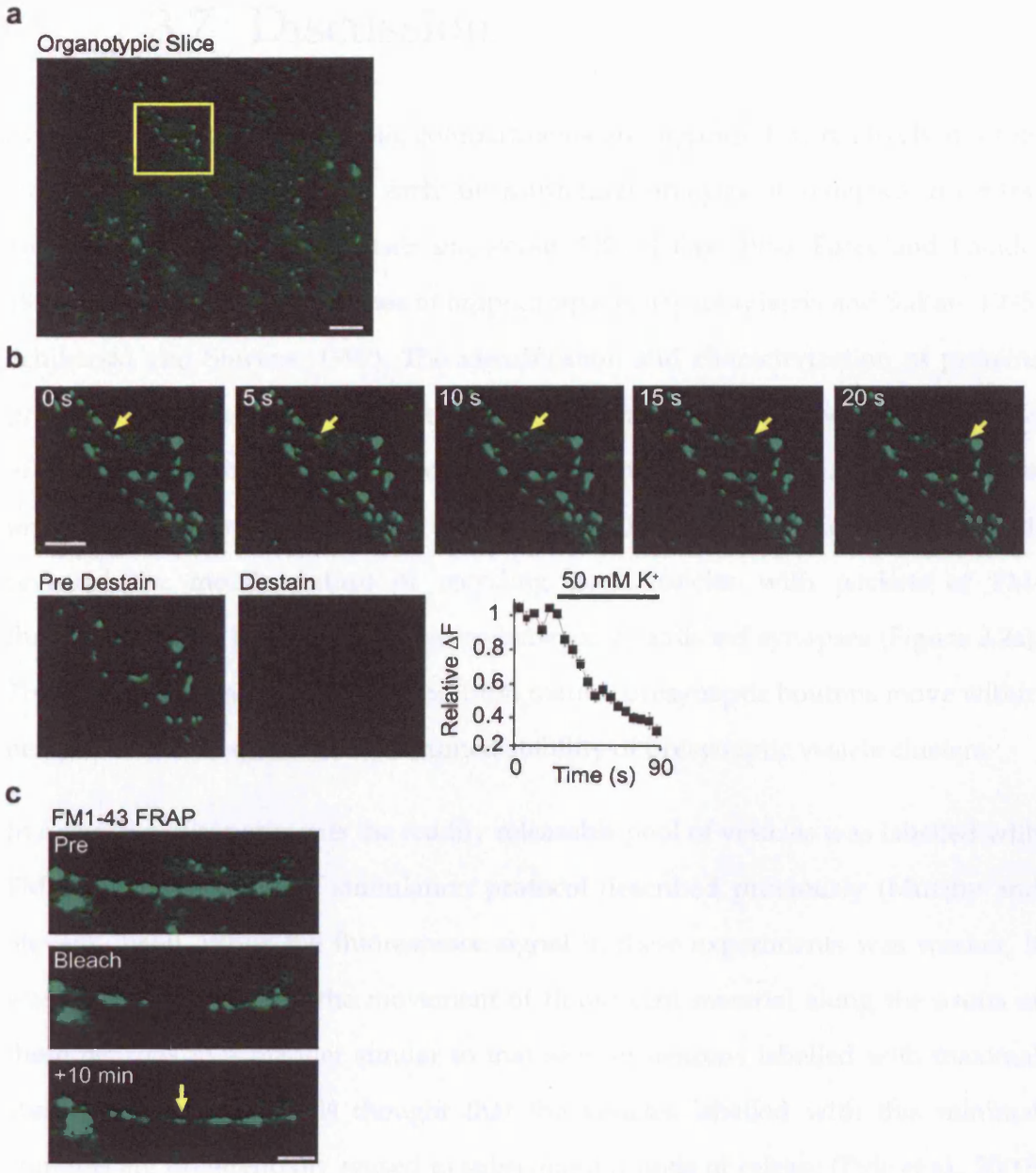

Figure 3.12 – Vesicle movement in organotypic slice cultures

(**a**) Low magnification image of an organotypic slice culture labelled with FM1-43 using hyperkalemic stimulation (50 mM K^+), following multiple washes with Advasep-7. Scale bar, 10 μm (**b**) A time-lapse sequence of the box region in **a**. The movement of fluorescent material between larger FM1-43 puncta is highlighted by yellow arrowheads. Further stimulation with a 50 mM potassium solution resulted in the loss of fluorescence from boutons and the time-course of fluorescence loss is summarized in the plot on the right. Scale bar, 5 μm (**c**) Axon in an organotypic slice containing FM1-43 positive boutons. Following photobleaching and a recovery of fluorescence was observed back into the site of the targeted bouton (yellow arrow). Scale bar, 5 μm.

3.7 Discussion

Synaptic vesicles in presynaptic compartments are organized in relatively discrete clusters, as demonstrated by early ultrastructural analysis of synapses in central and peripheral neurons (Heuser and Reese, 1973; Palay, 1956; Palay and Palade, 1955) and in more recent studies of hippocampal synapses (Harris and Sultan, 1995; Schikorski and Stevens, 1997). The identification and characterization of proteins present at presynaptic terminals has forwarded a framework for the molecular basis of vesicle clustering (Murthy and De Camilli, 2003). In this chapter, time-lapse imaging of mature synapses, in which vesicles had been labelled with FM4-64, revealed the mobile nature of recycling pool vesicles with packets of FM-fluorescence seen to move along axons between established synapses (Figure 3.2a). The observation that vesicles arising from mature presynaptic boutons move within neurons calls into question the assumed stability of presynaptic vesicle clusters.

In a number of experiments the readily releasable pool of vesicles was labelled with FM1-43 using a minimal stimulation protocol described previously (Murthy and Stevens, 1999). While the fluorescence signal in these experiments was weaker, it was possible to observe the movement of fluorescent material along the axons of these neurons in a manner similar to that seen in neurons labelled with maximal stimulation protocol. It is thought that the vesicles labelled with this minimal stimulus are preferentially reused in subsequent rounds of release (Pyle et al., 2000) and that they are either docked at or located close to the active zone (Schikorski and Stevens, 2001; Sudhof, 2000). The observation of vesicle movement in these conditions would indicate that vesicles from both the readily releasable and reserve pools are capable of moving away from the vesicle cluster, with probably only the vesicles tethered at the active zone not having the opportunity to exit the vesicle cluster laterally unless they were to become undocked (Murthy and Stevens, 1999). However, a study using synaptopHluorin-expressing hippocampal neurons suggests that vesicles released following a brief 40AP stimulus enter the reserve pool before gaining access to the releasable pool (Li et al., 2005). Taking this data

into account it is not possible to be certain that all of the vesicles labelled by the 40 AP stimulation in experiments in this chapter were part of the preferentially reused, readily releasable pool of vesicles. As such, while these results suggest that vesicles close to the active zone can exit the vesicle cluster in the manner described above, the evidence presented here is not conclusive.

The axonal transport of vesicles involves both the microtuble and actin cytoskelton as well as their associated motor proteins (Brady et al., 1984; Goode et al., 2000). Stabilization of the actin cytoskeleton has been shown to inhibit fast axonal transport in hippocampal neurons (Hiruma et al., 2003). It is thought that the polymerizing actions of jasplakinolide may lead to the formation of actin aggregates in axons which disrupt the transfer of cargo along and between the different elements of the cytoskeleton responsible for transport (Goode et al., 2000). In this chapter the treatment of neuronal cultures with jasplakinolide for 15 minutes caused a profound inhibition in the axonal movement of recycling pool vesicles labelled with FM1-43 (Figure 3.4a). The effect of jasplakinolide on vesicle movement was quantified by measuring the displacement of small units of fluorescence over time from their fluorescent puncta of origin which were usually larger and more stable (Figure 3.4c). It was difficult to track fluorescent packets over long distances as they frequently left the plane of focus or encountered other stable puncta. When a mobile packet was seen to pass though a more stable puncta, one could not be sure that the vesicles that exited were the same as those that had entered. However, the inhibition of the axonal transport was so profound that it was possible to observe and quantify its effect even with the shortcomings of this technique. Jasplakinolide-treated neurons were still capable of exocytosis as assessed by the destaining of FM dye from boutons upon stimulation (Figure 3.4d). The ability of neurons to respond to stimulation demonstrates their overall health following jasplakinolide treatment. However, the fact that the effect of jasplakinolide on axonal transport is irreversible would imply that it would eventually kill the neurons (Hiruma et al., 2003). This result also indicates that while the stabilization and/or polymerization of actin filaments inhibits the inter-bouton movement of

vesicles, possibly through the disruption of the cytoskeletal tracks used by the motor proteins, it does not affect the mobilization of vesicles within the presynaptic terminal during exocytosis, in agreement with previous work (Sankaranarayanan et al., 2003).

In order to establish that mobilized vesicles can become incorporated into non-native vesicle clusters and contribute functionally to these synapses, FRAP was carried out on individual mature FM dye-labelled boutons (Figure 3.5a). The observed axonal movement of FM4-64 fluorescence and the FRAP signal indicate that mobile vesicles originating from the recycling pool of synapses can contribute significantly to the vesicle clusters of other synapses. The persistent recovery of fluorescence in the axonal regions surrounding the photobleached bouton highlights the constitutive nature of vesicle movement (Figure 3.5b). This recovery represents the constant trafficking of fluorescently labelled vesicles through the photobleached region. A proportion of these vesicles become incorporated at the site of the photobleached synapse accumulating over time and giving rise to the observed FRAP signal at the bouton. As would be expected, the inhibition of axonal transport by jasplakinolide prevented a recovery in fluorescence following photobleaching. The results in Figure 3.8a illustrate the requirement for neighbouring non-photobleached synapses to act as a source of fluorescent vesicles for the FRAP signal in target boutons. While the proximity of a bouton to its closest source of fluorescence has an impact on the FRAP signal, the nearest neighbouring synapses are apparently not the only source of vesicles for the photobleached synapses (Figure 3.8b). If there were a preferential exchange of vesicles between neighbouring synapses then a more rapid decline in fluorescence would be expected at the nearest-neighbour synapses as mobilized fluorescent vesicles were replaced by photobleached vesicles from the target bouton. However, the decline of fluorescence at neighbouring non-photobleached synapses was similar in jasplakinolide-treated and untreated samples and was probably due to an imaging related photobleaching of signal. There was no evidence for a fast early reduction in signal which would correspond to the initial phase of recovery seen in

photobleached boutons (Figure 3.6b). Presumably, the axonal flux of photobleached vesicles out of the region of interest would only have a very transient effect on the overall fluorescence of the neighbouring bouton, since it need not necessarily localize at the synapse and therefore might not be detected by the relatively slow rate of image acquisition (0.1 Hz). Indeed, it seems from general observations in time-lapse studies that rather than vesicles being shuttled locally between neighbouring synapses, vesicles have a greater and variable range of movement up and down along the axon. The range across which the vesicles from one particular synapse can be distributed is not clear and warrants further study.

In neurons whose synapses had been labelled with both SypI-EGFP and FM4-64 the intensity of the EGFP signal at synapses was greater than that of FM4-64. This presumably relates to differences in the fluorescence quantum yield of each fluorophore and the fact that transfection will likely label the majority of vesicles while FM dye will only label the recycling pool. In synapses labelled with both SypI-EGFP and FM4-64 using a stimulus protocol to load the recycling pool, the extent of FRAP for both fluorophores was similar (Figure 3.10). These results suggest that non-recycling or resting pool vesicles are also mobilized from synapses. If vesicle movement were restricted solely to the recycling pool, then the proportional recovery of SypI-EGFP would be expected to be smaller than that of FM4-64.

The similar FRAP curves obtained at SypI-EGFP labelled boutons in both stimulated and unstimulated cultures (Figure 3.11) would suggest that the mobilization of synaptic vesicles during exocytosis has no long-term impact on the incorporation of non-native vesicles into synapses. There was no discernable difference in the amount of SypI-EGFP being trafficked in the axons of stimulated and unstimulated neurons, suggesting that the lateral departure of vesicles from the presynaptic cluster was not affected by this stimulation protocol. It has been shown previously that presynaptic proteins display greater mobility upon stimulation. The dispersion of EGFP tagged synapsin along axons and its subsequent reclustering at synapses (Chi et al., 2001) and a similar dispersal and reclustering of EGFP tagged

VAMP (Li and Murthy, 2001), though in this case along the surface of the axon, following vesicle exocytosis has been described. SypI-EGFP demonstrated a similar behaviour in response to stimulation as VAMP-EGFP in the study by Li et al. However, the time constant for reclustering for both synaptophysin and VAMP was close to 115 s while in this chapter FRAP experiments were carried out ~10 mins after stimulation. This rules out any effect of the activity-dependent dispersal of synaptic components on the observed fluorescence recovery.

The majority of the experiments so far in this chapter, and in subsequent chapters are carried out using dissociated hippocampal neurons grown in culture. To test for this phenomenon in a more intact preparation, similar experiments were carried out in organotypic hippocampal slices. This system, where the organization and connectivity of the hippocampus remains largely intact, has been used previously to study the stability of presynaptic terminals over time by culturing hippocampal slices from mice expressing SypI-EGFP under the *Thy 1* promoter (De Paola et al., 2003). In this chapter, synaptic vesicles were labelled with FM1-43, and fluorescence movements similar to those seen in cell culture-based experiments were observed (Figure 3.11). FRAP studies also revealed the incorporation of non-native vesicles into the synaptic boutons of these slices. Attempts were made to carry out FRAP experiments in acute hippocampal slices. There was some evidence of fluorescence recovery in photobleached synapses labelled with FM1-43. However, due to the high level of background and an inability to completely remove FM1-43 from the tissue surrounding the neurons, it was impossible to determine whether the recovery did indeed come from the intracellular transport of vesicles or from the diffusion of excess FM1-43 along the surface of the neurons.

This chapter makes use of multiple fluorescence-based synapse labelling methods to characterize the mobility of recycling pool vesicles in mature neurons. While it is implicit from these studies that FM-fluorescence relates to synaptic vesicles, the nature of these mobile fluorescence units is not clear. The contribution of some endosomal intermediates can not be ruled out from these fluorescence studies. FM dye destaining experiments revealed the functional nature of newly imported, non-

native vesicles. However, these findings raise the question as to how the imported vesicles are arranged with respect to the native vesicle cluster and how their spatial integration relates to their functionality at host synapses. The following chapters will describe the inter-bouton exchange of vesicles using a combination of fluorescence imaging and electron microscopy to detail vesicle incorporation at the ultrastructural level.

Chapter 4 | Ultrastructural Analysis of the Presynaptic Terminal

4.1 Introduction

The observed mobility of FM dye fluorescence described in the previous chapter raises questions about the nature of these mobile fluorescent signals that redistribute between synapses as well as the ultrastructural organization of synapses in such a dynamic system. Electron microscopy allows the detailed visualization of synapses and individual synaptic vesicles in neurons. For instance, the seminal evidence that synaptic vesicles form the physical basis for quantal release at synapses comes from EM studies (Heuser and Reese, 1973). The photoconversion of FM dye to an electron dense precipitate by prolonged excitation in the presence of DAB, has been used previously to confirm that FM1-43 labels synaptic vesicles in synapses (Henkel et al., 1996a). The correlation of light and electron microscopy (CLEM), allows for regions of interest imaged at the light level to be studied in more detail by EM. When CLEM is used in combination with photoconversion, fluorescence signals can be accounted for in electron micrographs. This was first demonstrated with lucifer yellow in crayfish nerve cells (Maranto, 1982), and more recently with FM1-43 in hippocampal neurons (Harata et al., 2001b). These powerful techniques permit the visualization of the recycling vesicle pool at identified synapses, making it possible to examine their ultrastructural organization.

4.2 Ultrastructural Visualization of Synaptic Vesicles

The techniques required to confidently correlate fluorescence and EM imaging data were first established in order to identify FM dye-labelled vesicles by electron microscopy.

4.2.1 Photoconversion of FM1-43

The excitation of fluorescent molecules in the presence of a reducing agent such as DAB, can give rise to an electron dense reaction product that is visible in EM, once treated with osmium tetroxide. More unstable fluorophores are more likely to emit free radicals and this makes their conversion to electron dense products in the presence of DAB more efficient. The photolabile nature of FM1-43, therefore, makes it a good substrate for photoconversion. To establish a photoconversion protocol the recycling pool of synapses in hippocampal neurons was first loaded with the fixable form of FM1-43 (FM1-43fx) and imaged as demonstrated in Figure 4.1 (see section 2.5.2). Neurons were then fixed with a glutaraldehyde/paraformaldehyde solution in PBS, and the samples prepared for photoconversion as detailed in section 2.7.1. A DIC image of the same region as in the fluorescence image was acquired prior to photoconversion. Neurons were then incubated in DAB and excited with maximal intensity light in the 455 nm to 495 nm range. Illuminating the area of interest for 36 min was found to be excessive, in that all of the neurites took on a dark appearance after this time, as seen in the DIC image in Figure 4.1a. A reduction in the duration of illumination to 19 min (Figure 4.1b) resulted in the darkening of regions of neurites that corresponded to previously fluorescent puncta (orange arrowheads). However, it was found that using an even shorter illumination time of less than 15 min, which had little effect on the appearance of neurites as observed by DIC imaging, was sufficient to photoconvert FM1-43 in vesicles to an electron dense product visible in EM (Figure 4.1c and Figure 4.3). In all subsequent experiments a photoconversion time of between 12 and 15 mins was used.

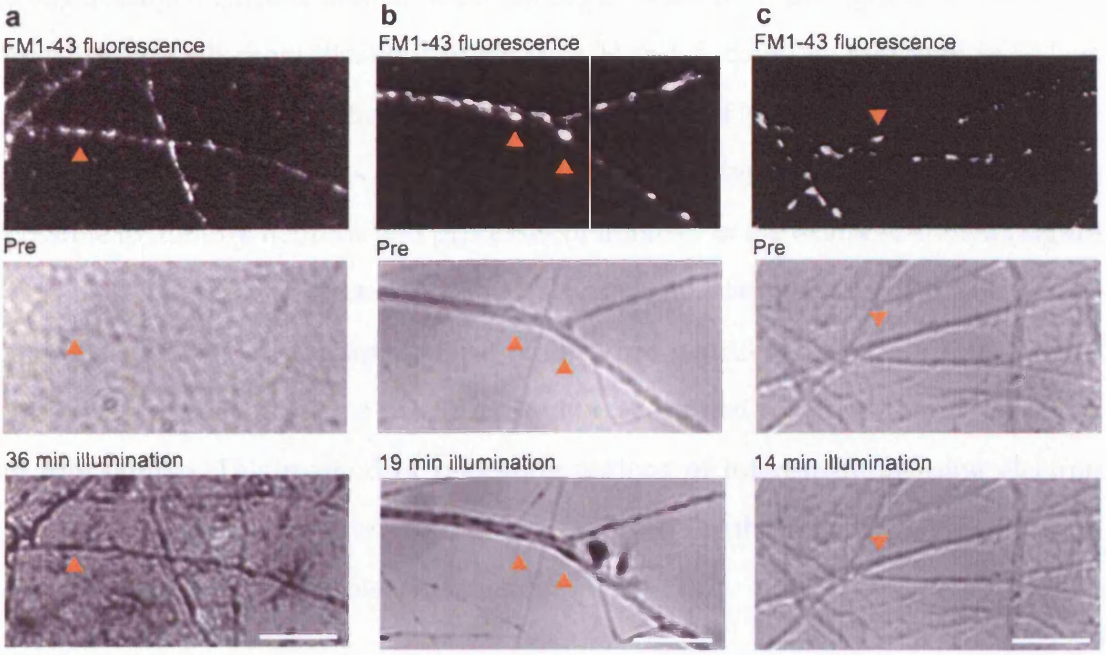

Figure 4.1 – Photoconversion of FM1-43

Fluorescence images of FM1-43 positive boutons and the corresponding brightfield DIC images before and after incubation with DAB and illumination with 475/40 nm light for varying times; (**a**) 36 min illumination (**b**) 19 min illumination and (**c**) 14 min. Orange arrowheads highlight regions in DIC images that correspond to FM1-43 positive boutons in fluorescence images. Scale bars, 10 μm

4.2.2 Correlation of light and electron microscopy

To study individual synapses identified by fluorescence microscopy in EM, a technique of correlating images acquired from both microscopes was applied (Harata et al., 2001b; Schikorski and Stevens, 2001). At the light level a montage of 4x, 10x and 60x magnification DIC and fluorescence images was prepared by overlaying and aligning successive images using the graphics software package XARA. The images were first used to identify the neurons of interest when embedded in EPON to allow their selection for serial sectioning. Figure 4.2a shows a cluster of neurons at 4x magnification, while in Figure 4.2b, the same region is shown again, but in this case after fixation, photoconversion and embedding in EPON. A selection of neurons, clearly visible in both images, are highlighted by yellow arrowheads and act as landmarks for identification purposes. The region of interest to be sectioned for EM analysis was marked out on the EPON samples

using a scalpel. Once sectioned, the same region studied at the light level, shown at both 10x and 60x magnifications in Figure 4.2c and d, could be relocated in EM, as seen in the low magnification electron micrograph in Figure 4.2e. The architecture and layout of the neurons were well preserved in the EM sections, and it was possible to identify neurons and processes of interest. In the example shown (Figure 4.2) thick neuronal processes can be clearly matched between the 60x DIC image and the electron micrograph. Many of the fine neurites are also visible in this micrograph, while all of the neurites could be accounted for in other serial sections of this sample. This method of relocating regions of interest by aligning electron micrographs and light microscope images allowed for the reliable re-identification of individual synapses by electron microscopy.

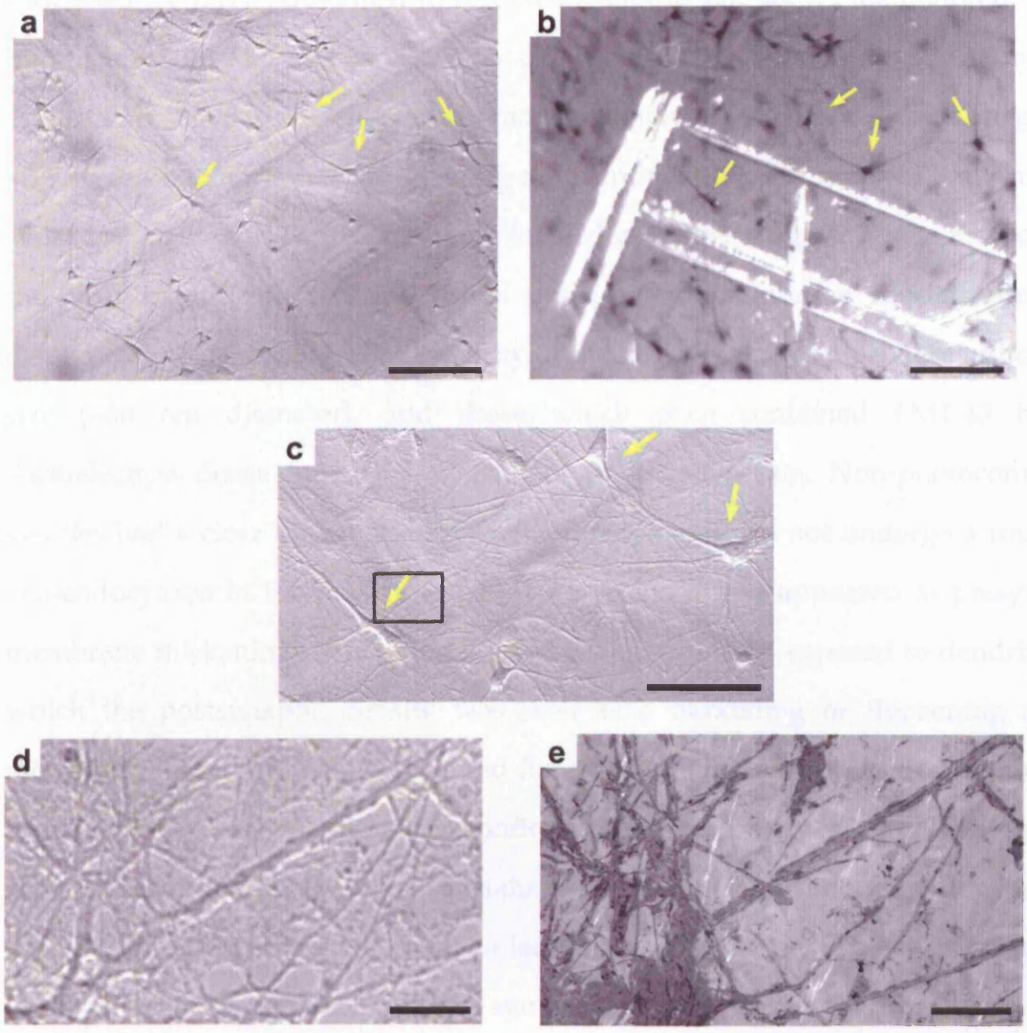

Figure 4.2– Correlation of light and EM images

(**a**) Low magnification brightfield image of live hippocampal neurons on an astrocyte feeder layer. Scale bar 200 μm. (**b**) A low magnification brightfield image of same neurons as in **a** following fixation, dehydration and embedding in EPON resin. Neurons visible in both images are marked with yellow arrows. Scale bar 200 μm. (**c**) Brightfield image showing the neurons from **a** that were selected for EM analysis. Scale bar, 100 μm. (**d**) A high magnification brightfield image of a neuronal process later re-identified in electron micrographs and shown in (**e**). Scale bars,10 μm.

4.2.3 Visualizing FM1-43 labelled vesicles by EM

The methods of photoconversion and CLEM were combined to visualize the recycling pool of vesicles at synapses initially identified by fluorescence microscopy. Figure 4.3a is a 60x magnification DIC image of a neuron and Figure 4.3b is a fluorescence image of the same area loaded with FM1-43 using a protocol to access the recycling pool. This preparation was subsequently photoconverted and

processed for EM as described in section 2.7. Figure 4.3c shows the region outlined by red boxes in Figure 4.3a and b as an overlay of DIC and fluorescence images. Figure 4.3d shows the same region again as an overlay of a fluorescence image and an electron micrograph, thus allowing the identification of functional boutons. The synapses labelled in Figure 4.3e were imaged at higher magnifications to allow for the clear identification of individual vesicles and membrane specializations as displayed in Figure 4.3f-h. The majority of the vesicles at synapses were uniform in size (~50 nm diameter), and those which once contained FM1-43 had a dark/electron dense lumen as a result of photoconversion. Non-photoconverted vesicles had a clear lumen and represented those that did not undergo a round of exo-endocytosis in the presence of FM1-43. Active zones appeared as presynaptic membrane thickenings containing docked vesicles, closely apposed to dendrites on which the postsynaptic density was seen as a darkening or thickening of the membrane. In all synapses considered for analysis, one or both of these membrane specializations was identified to confirm the mature state of the synapse. The prominence of these membrane specializations depended on the angle at which the synapse had been sectioned, so that a lack of these features was not a confirmation of an immature synapse. However, synapses lacking these indicators of maturity were not included in this study. Serial sectioning allowed the entire vesicle population of a synapse to be captured as demonstrated in Figure 4.3i.

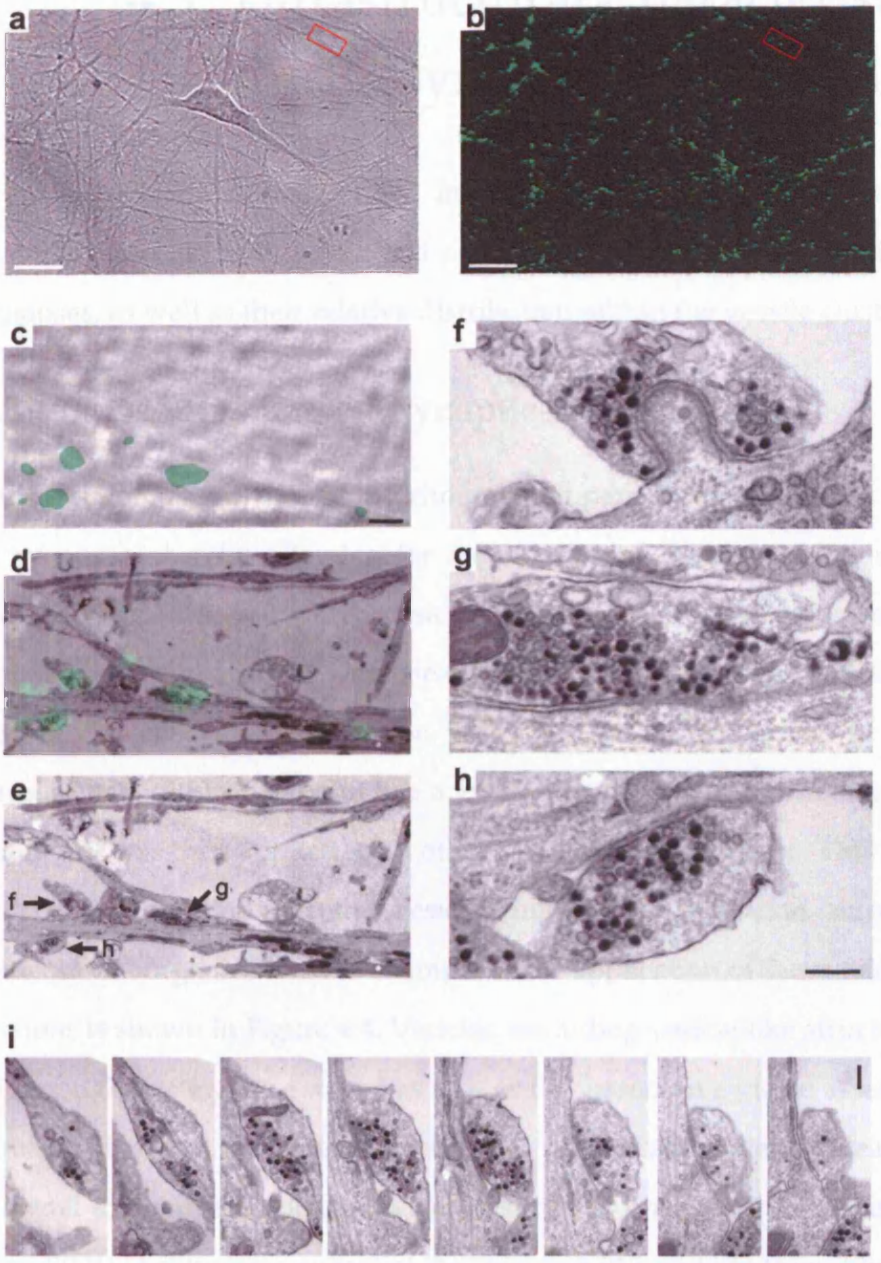

Figure 4.3 – Ultrastructural identification of FM1-43 positive vesicles.

Correlative light and electron microscopy was used to directly visualize FM1-43 labelled vesicles at the ultrastructural level. (**a**) DIC and (**b**) fluorescence views of FM1-43 labelled neurons. Scale bars, 15 μm (**c**) Brightfield and fluorescence overlay of region in red box from **a** and **b**. Scale bar,1 μm (**d**) Electron micrograph with fluorescence overlay of the region from **c**. (**e-h**) Electron micrographs show the marked synapses (**e**: arrows) in greater detail in **f-h**. FM1-43 labelled vesicles appear with a dark lumen arising from photoconversion (PC+) and are distinct from non-labelled (PC-) vesicles. Scale bars, 0.2 μm. (**i**) A complete serial section series of a representative bouton. Scale bar, 0.2 μm

4.3 Ultrastructural Characteristics of the Presynaptic Vesicle Cluster

The CLEM techniques described in the previous section could be used for the quantification of the recycling and non-recycling populations of vesicles present at synapses, as well as their relative distribution within the vesicle cluster.

4.3.1 Quantification of synaptic vesicle number

Serial sectioning is a powerful technique that permits an account of all the vesicles at synapses, thereby allowing for an estimate of the size of the recycling pool. However, in order to quantify vesicle numbers at synapses, the lateral limits of the presynaptic compartment were first defined. This was marked as the edge of the vesicle cluster in the EM section with the longest continuum of vesicles lying successively within 100 nm of one another, in a plane longitudinal to the axon. This boundary was then applied to all other sections of the synapse. This proved to be a satisfactory definition of the vesicle cluster that took into account its three-dimensional organization. An example of the application of these rules to a series of sections is shown in Figure 4.4. Vesicles, excluding vesicle-like structures exceeding 55 nm in diameter, were scored as PC+ or PC- based on a visual assessment of their lumenal densities. In vesicles where this classification was unclear, the ratio of lumenal to membrane density was measured as previously described (Rizzoli and Betz, 2004). Analysing a subset of the data (n = 913 vesicles from 3 boutons) by this vesicle scoring method revealed a bimodal distribution in density histograms with peaks at 0.9 and 1.2, corresponding to empty and full vesicles respectively (Figure 4.5a). Full vesicles were defined as those with a relative density of > 1.075. As an alternative method to discriminate between PC+ and PC- vesicles at synapses, the optical density along a line drawn through the centre of the vesicle was measured to create a line density profile. The line density profiles of vesicles in photobleached synapses were indistinguishable from those of PC- vesicles in non-photobleached

boutons, while the density profiles of both these groups were strikingly different from those of PC+ vesicles (Figure 4.5b).

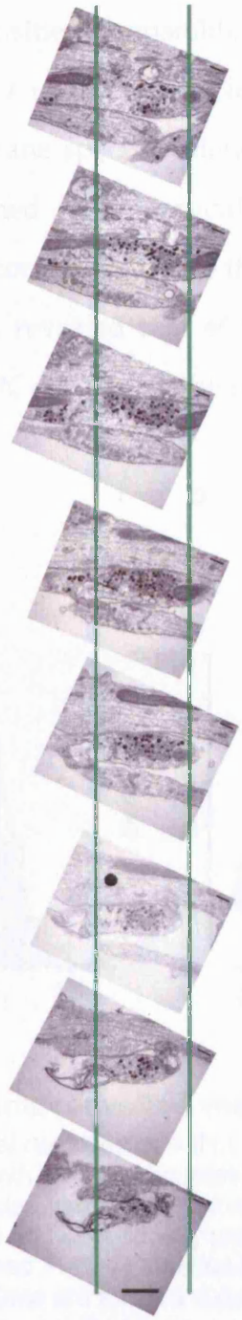

Figure 4.4– Defining the boundaries of the vesicle cluster

A complete series of serial EM sections were initially aligned on top of each other using landmarks which traversed sections as for serial reconstructions. Sections were positioned and aligned as shown, so that the boundary of the vesicle cluster could be established and applied to each section as demonstrated by the vertical green lines. Scale bar, 0.5 μm.

The number of vesicles in the recycling pool of synapses was determined by combining photoconversion and CLEM. The recycling pool of vesicles was labelled with FM1-43 using a maximal stimulation of 600 APs at 10 Hz as in Chapter 3. Synapses with fluorescence intensities comparable to each other were identified at the light level and examined at the ultrastructural level. Only those with identifiable pre- and/or postsynaptic membrane specializations were used. All the vesicles, in all of the serial sections obtained for a particular synapse, were counted and classified as either PC+ or PC-, corresponding to those in the recycling and resting pools respectively. The analysis revealed that 46.0 ± 7.4% (mean ± s.e.m.) of the vesicles in these synapses were PC+ or part of the recycling pool.

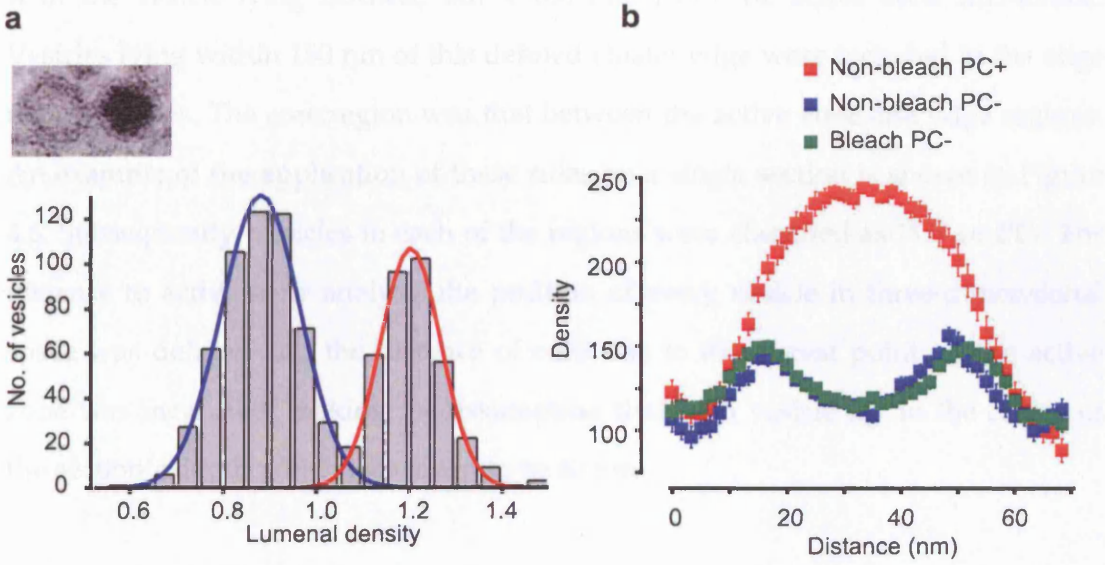

Figure 4.5– Identification of photoconverted vesicles

(**a**) Distribution plot of vesicle lumenal densities (*n* = 913 vesicles, from three FM1-43 labelled boutons). The data was fit with Gaussian curves to reveal two peaks at 0.9 and 1.2, corresponding to PC- and PC+ vesicles, respectively. Inset shows an example electron micrograph of PC- and PC+ vesicles. (**b**) Line density profiles of vesicles from photobleached and non-photobleached FM1-43 labelled boutons that were subsequently photoconverted and viewed in EM. Data are mean ± s.e.m.

4.3.2 Spatial characteristics of recycling pool

Previous studies using photoconversion of FM1-43 at hippocampal synapses have primarily addressed the readily releasable pool vesicles and their relationship with the active zone. Interestingly, the organization of the entire recycling pool of

vesicles within a synapse and their relationship to the active zone as well as other resting pool vesicles has not been characterized to date.

To study the spatial organization of vesicles, two methods, regional analysis and measurement of vesicle distance to active zone, were used. These methods of analysis were applied to the three serial sections centred around the active zone for each synapse. For regional analysis, the presynaptic vesicle cluster was split into three regions, active zone, core and edge, in each of the three serial sections. The active zone region was a compartment extending 100 nm from the active zone into the vesicle cluster. The edge region was a single continuous line of the outermost vesicles each lying within two vesicle diameters (100 nm) of one another, starting with the vesicle lying furthest, but < 100 nm, from the active zone membrane. Vesicles lying within 150 nm of this defined cluster edge were included in the edge region groups. The core region was that between the active zone and edge regions. An example of the application of these rules on a single section is shown in Figure 4.6. Subsequently, vesicles in each of the regions were classified as PC+ or PC-. For distance to active zone analysis the position of every vesicle in three-dimensional space was defined and the distance of each one to its nearest point on the active zone was measured, making the assumption that each vesicle lay in the center of the section's depth which was taken to be 60 nm.

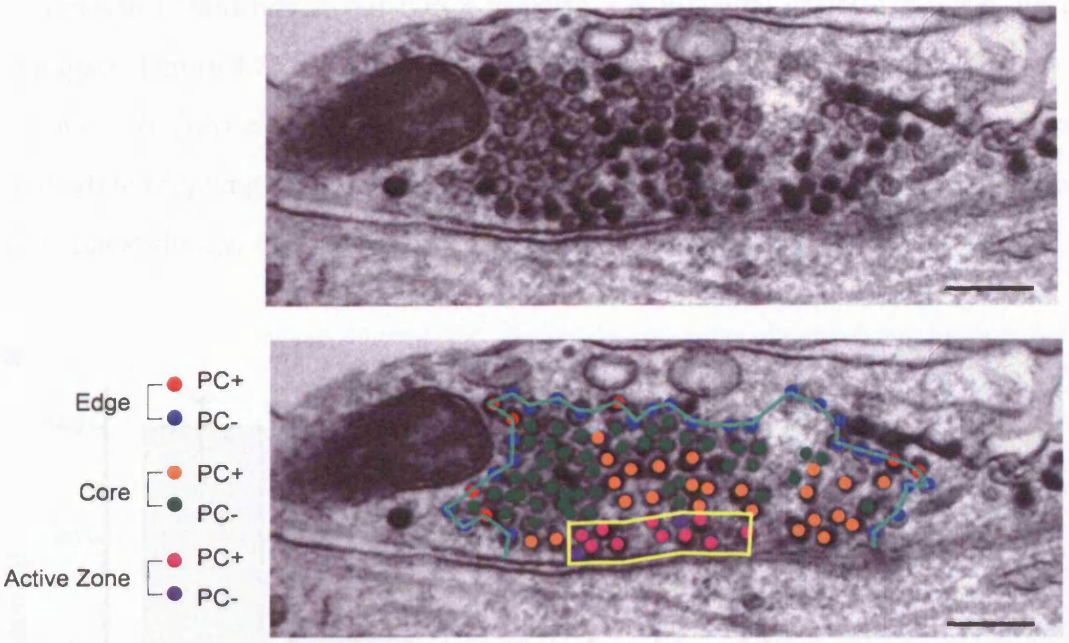

Figure 4.6– Defining regions within the vesicle cluster

(**a**) Single EM section of an FM1-43 labelled, photoconverted bouton. PC+ and PC- vesicles are organized around a single active zone containing docked vesicles of both types. (**b**) Example image detailing the categorization of vesicles into active zone, core and edge regions and the subsequent classification of vesicles as either PC+ or PC-. Scale bars, 0.2 μm.

Hippocampal cultures were stimulated with a 600AP stimulus at 10 Hz in the presence of FM1-43 to label the recycling pool of vesicles. Synapses identified by fluorescence signal were photoconverted, processed for EM, and later re-identified in electron micrographs. Vesicles were then classified as PC+ or PC-, and their spatial positioning assigned as described above. PC+ vesicles, corresponding to recycling pool vesicles, were present in all regions of the synapse, as indicated by both regional analysis and distance to active zone measurements. A comparison of the relative proportion of PC+ vesicles in the three zones used in regional analysis with that of the total vesicle population revealed no significant differences in their distributions in the active zone and core regions (paired *t*-test, active zone region: $P = 0.37$, all, 13.8 ± 1.6%, PC+, 15.9 ± 2.4%; core region: $P = 0.39$, , all, 39.1 ± 5.8%, PC+, 41.1 ± 5.1%). However, the proportion of PC+ vesicles in the edge region was significantly lower (paired *t*-test, edge region: $P = 0.05$, all, 47.2 ± 4.4%, PC+, 43.2 ± 4.3%), (Figure 4.7a). The distribution of vesicle distances to the active zone for all vesicles and PC+ vesicles only was also found to be similar between the two groups

(Kolmogorov-Smirnov, P > 0.2; PC+ vesicles, n = 367; total vesicles, n = 806, from 5 synapses, Figure 4.7b). But here again the tendency for the proportion of PC+ to be higher in regions closer to the active zone was evident. These results demonstrate that while recycling pool vesicles are not spatially restricted to any specific region of the vesicle cluster, they are not evenly distributed throughout the synapse.

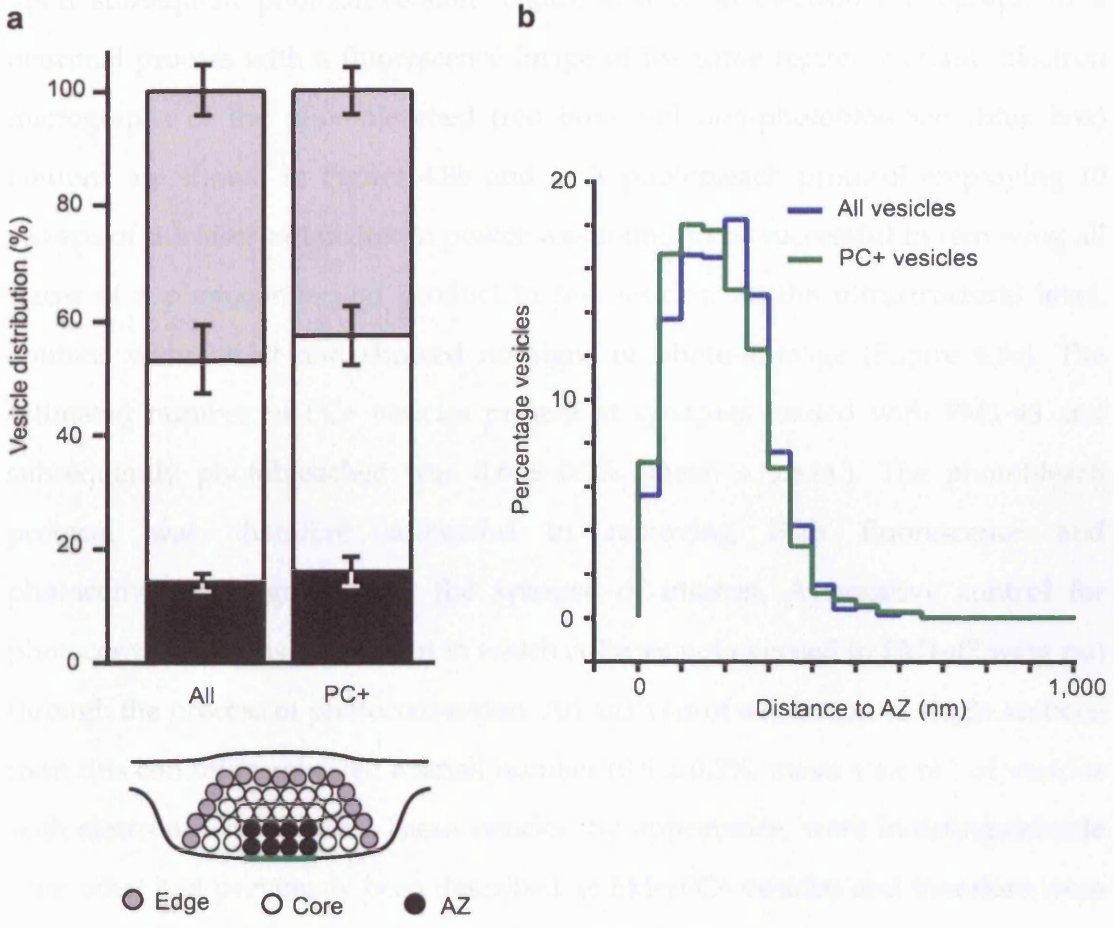

Figure 4.7– Spatial distribution of vesicle pools within boutons

(**a**) The relative distribution of vesicles in boutons, labelled with FM1-43 by a 600 AP 10 Hz stimulation, in edge, core and active zone regions. Left: all vesicles (47.2 ± 4.4%, 39.1 ± 5.8%, 13.8 ± 1.6%). Right: recycling pool vesicles only (43.2 ± 4.3%, 41.1 ± 5.1%, 15.9 ± 2.4%). Data are mean ± s.e.m. (**b**) Histograms comparing vesicle to active zone distances of recycling pool vesicles to the total vesicle pool in the same synapses.

4.3.3 Photobleaching FM1-43 and ultrastructural analysis

In order to study the transport and incorporation of FM dye fluorescence at synapses, the FRAP protocol used previously (Figure 3.5) was extended to the EM level. It was important to confirm that the photobleaching of a fluorescent signal actually rendered it incapable of producing an electron dense reaction product upon subsequent photoconversion. Figure 4.8a is an electron micrograph of a neuronal process with a fluorescence image of the same region overlaid. Electron micrographs of the photobleached (red box) and non-photobleached (blue box) boutons are shown in Figure 4.8b and c. A photobleach protocol employing 10 sweeps of the laser at maximum power was found to be successful in removing all traces of a photoconversion product in the vesicles. At the ultrastructural level, boutons were intact and showed no signs of photo-damage (Figure 4.8c). The estimated number of PC+ vesicles present at synapses loaded with FM1-43 and subsequently photobleached was 0.8 ± 0.2% (mean ± s.e.m.). The photobleach protocol was therefore successful in removing both fluorescence and photoconversion signals from the synapse of interest. A negative control for photoconversion was carried out in which cultures not exposed to FM1-43 were put through the process of photoconversion. An analysis of a selection of single sections from this condition revealed a small number (0.9 ± 0.3%, mean ± s.e.m.) of vesicles with electron dense lumen. These vesicles, by appearance, were indistinguishable from what had previously been described as FM+/PC+ vesicles and therefore were classified as PC+. These vesicles may have contained aminergic neurotransmitters which can form electron dense precipitate upon fixation. Given the small number of these vesicles, false PC+ vesicles at synapses should contribute minimally in vesicle quantification. These data are plotted in Figure 4.8d along with the proportion of PC+ vesicles representing the recycling pool

To confirm that the photobleach protocol was not having a toxic effect on the synapse, the ability of photobleached boutons to take up and release the FM dye was assessed by light microscopy. The protocol is outlined in the schematic in Figure 4.9a. Synapses were labelled with FM1-43 (600 APs at 10 Hz) and then

photobleached with 10 sweeps of the laser at maximum power. The photobleach protocol was the same as that used to prevent the formation of FM1-43-derived photoconversion products in EM. The entire preparation was then destained with 900 APs at 10 Hz and subsequently stimulated (600 APs at 10 Hz) in the presence of FM1-43. The photobleached synapses reloaded with FM1-43 and could be destained once again. Figure 4.9b shows a sample image sequence from the experiment. The ratio of dye uptake as defined by fluorescence intensity measured in the second load compared to the first load (F2/F1), is shown for both photobleached boutons and control boutons outside the bleach region in Figure 4.9c. Photobleached synapses showed the same extent of dye-uptake prior to photobleaching (F1) as they did after photobleaching (F2, t-test, $P = 0.99$, $n = 20$, mean F1 = 44.02 ± 1.95, mean F2 = 44.07 ± 5.26). Moreover, F2/F1 for photobleached and control non-photobleached synapses was not significantly different (t-test, $P = 0.57$, bleach: $n = 20$, mean ratio F2/F1 = 0.98 ± 0.09; control: $n = 21$, mean ratio F2/F1 = 1.05 ± 0.08). These results establish that the photobleach protocol was not detrimental to bouton health.

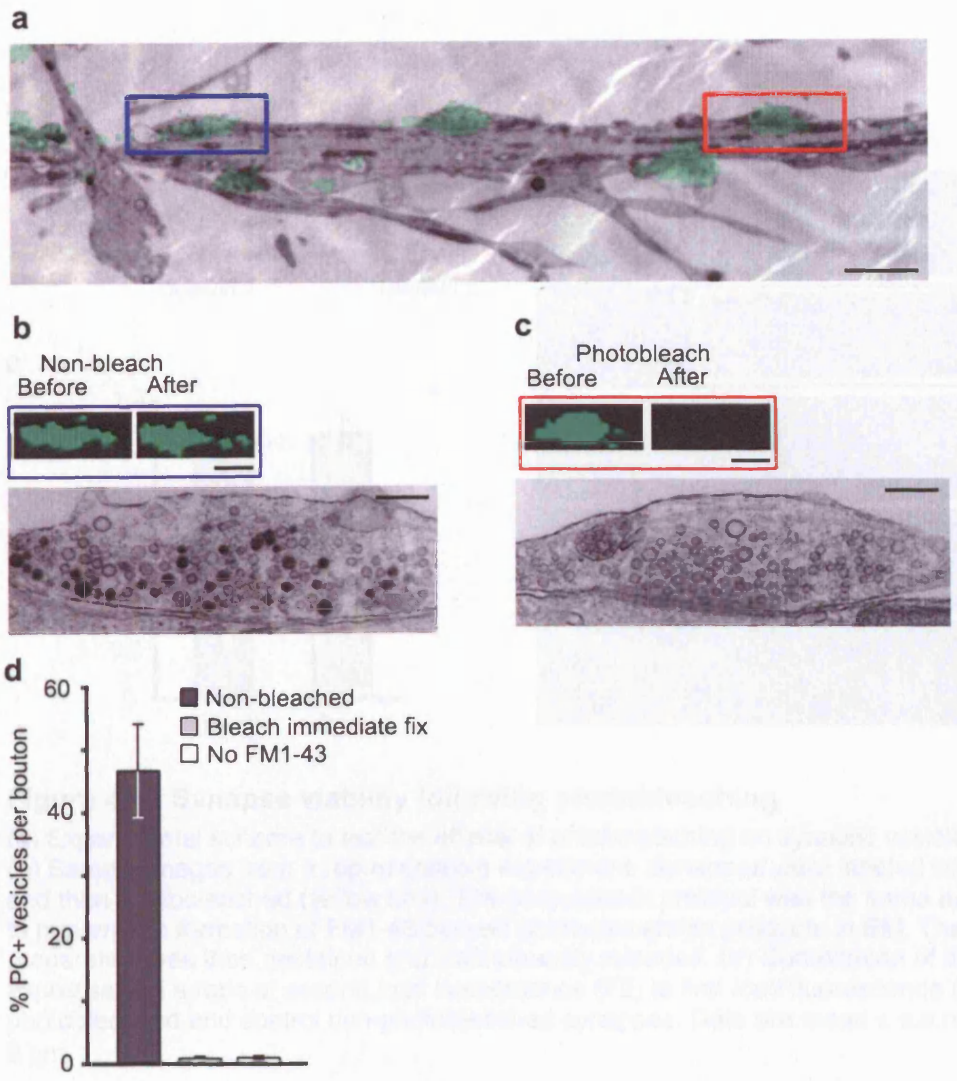

Figure 4.8– Preventing the photoconversion of FM1-43 by photobleaching.

(**a**) Electron micrograph of a neuronal process with an FM1-43 fluorescence overlay (green) of the same area identifying functional boutons. Bouton in red box (right) was photobleached immediately prior to fixation while bouton in blue box (left) was not. Scale bar, 2 μm (**b**) High magnification EM image of non-photobleached bouton (blue box) with its fluorescence image above. (**c**) High magnification EM image of photobleached bouton (red box) with fluorescence images before and after photobleaching shown above. All the vesicles are PC-, corresponding to the complete ablation of the FM1-43 fluorescence prior to photoconversion. Scale bars: fluorescence, 1 μm; EM 0.2 μm (**d**) Summary of the proportion of PC+ vesicles in non-photobleached (n = 5), photobleach-immediate fix boutons (n = 6) and photoconverted boutons not exposed to FM1-43 (n = 3). Data are mean ± s.e.m.

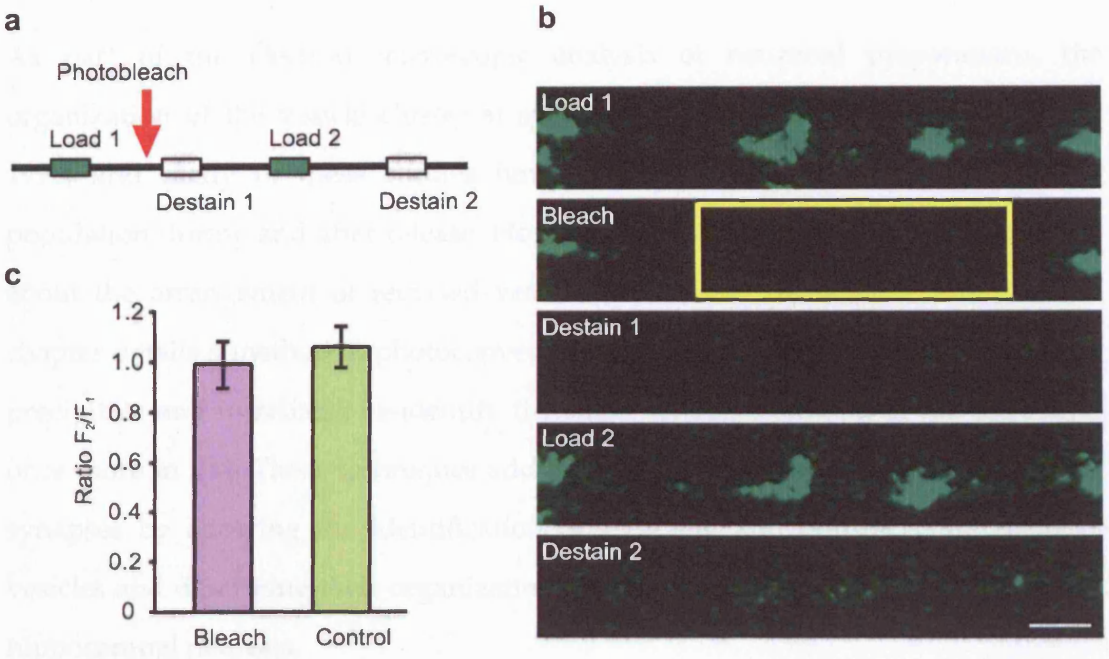

Figure 4.9– Synapse viability following photobleaching

(**a**) Experimental scheme to test the effects of photobleaching on synaptic vesicle turnover. (**b**) Sample images from a representative experiment. Synapses were labeled with FM1-43 and then photobleached (yellow box). The photobleach protocol was the same as that used to prevent the formation of FM1-43 derived photoconversion products in EM. The entire preparation was then destained and subsequently reloaded. (**c**) Comparison of dye-uptake, expressed as a ratio of second load fluorescence (F2) to first load fluorescence (F1) for photobleached and control non-photobleached synapses. Data are mean ± s.e.m. Scale bar, 2 μm.

4.4 Discussion

As part of the electron microscopic analysis of neuronal preparations, the organization of the vesicle cluster at synapses has been described (Peters et al., 1991) and many of these studies have concerned the changes to the vesicle population during and after release. However, little information has been gathered about the arrangement of recycled vesicles within the presynaptic bouton. This chapter details a method to photoconvert FM dye fluorescence to an electron dense precipitate and to reliably re-identify the same synapses studied at the light level once more in EM. These techniques add another level of resolution to the study of synapses by allowing the identification of recycling and non-recycling pools of vesicles and describing their organization within the presynaptic vesicle clusters of hippocampal neurons.

Oxidative reactions involving DAB can be used to label neurons and their proteins. The enzyme horseradish peroxidase (HRP) conjugated to antigen-specific antibodies can catalyse the oxidative reaction of hydrogen peroxide and DAB to produce a stable opaque reaction product, visible by light microscopy, that allows the immuno-localization of proteins (Janeway et al., 2001). The polymerized DAB reaction product can also be visualized by electron microscopy following treatment with osmium tetroxide. Fluid-phase markers such as solutions of HRP (Micheva and Smith, 2005) or antibodies directed against synaptic vesicle proteins conjugated to HRP (Kraszewski et al., 1995) have been used to label recycling vesicles. In this chapter the FM family of strylyl dyes were used to label endocytosed vesicles as in Chapter 3. The photolabile nature of the FM dyes makes them ideal candidates for photoconversion, and with the development of fixable forms of the dyes, their location and fluorescence can be preserved through the fixation process. These features suggested that FM dyes should be useful for the ultrastructural study of recycling pool vesicles.

The time taken to achieve sufficient photoconversion of FM dye for visualization by electron microscopy was optimized in relation to changes observed at the light level (Figure 4.1). The darkening of neurites and boutons following longer illumination times probably reflects the non-specific photoconversion of residual plasma membrane-associated fluorescence and mitochondria. In the majority of cases photoconversion was an all-or-nothing reaction and vesicles could be easily classified as PC+ or PC- as demonstrated by the distribution plot of vesicle lumenal densities from photoconverted boutons, which displayed two clear populations of vesicles (Figure 4.5). However, as suggested by the overlap between the distribution curves, there were a small number of vesicles of intermediate lumenal density. In classifying these vesicles, the opacity of the cytoplasm surrounding the vesicles was also considered, as a dark lumen may represent a staining artefact contributed by the cytoplasm. Further controls for the counting and classification of vesicles will be discussed in the next chapter.

The majority of synapses formed between hippocampal neurons in culture are *en passant*, with axons and dendrites often running parallel to one another. At the ultrastructural level these synapses are seen as clusters of vesicles, offset slightly from the center of the process and juxtaposed to a dendrite. In order to quantify vesicle number, it was necessary to devise a system of marking the boundaries of these *en passant* synapses. By aligning the EM serial sections as described in section 2.7.6 and laying them out vertically (Figure 4.4) the 3-d nature of the synapse could be appreciated without the need for a reconstruction.

In this chapter, the proportion of PC+ vesicles, representing the recycling pool at synapses was estimated to be ~46%. Given that the average total vesicle count in the boutons considered here was 338, the recycling pool was estimated to contain 155 vesicles. This was comparable to the value of 127 recycling vesicles per bouton noted previously for a 400 AP stimulus load derived from fluorescence data only (Ryan et al., 1997), but much larger than the estimate of ~30 vesicles following a 600 AP stimulus from ultrastructural analysis (Harata et al., 2001a), and of ~25 vesicles for a 600AP stimulation from fluorescence data (Murthy and Stevens, 1999). A

recent study demonstrated that the size of the recycling pool at hippocampal synapses can vary with temperature. When loaded with HRP using a 600 AP stimulus the recycling pool contained ~110 vesicles at 35°C compared to an average of 50 when loaded at 23°C (Micheva and Smith, 2005). All of the experiments in this thesis were carried out at ~35°C and the estimate of recycling pool size correlates well with that of Micheva and Smith from similar conditions (Micheva and Smith, 2005). The previous ultrastructural study of recycling pool size using FM1-43 and photoconversion considered a large heterogenous population of synapses in the analysis (Harata et al., 2001b). In some cases the proportion of PC+ vesicles at synapses was found to be as high as 85%, but the average for the whole population was ~15% (Harata et al., 2001a). In this thesis, FM1-43-positive boutons were chosen for EM analysis based on similarities in their fluorescence intensities with each other and across experiments. This methodology may have biased the selection for synapses with larger recycling pools and could explain the above differences in estimates of recycling pool size. Alternatively, if lower temperatures, as used by Harata et al, favour a greater heterogeneity in release probabilities at synapses then such differences in individual release sites might explain the large variation in PC+ vesicle numbers observed.

The organization of the vesicle cluster and the distribution of recycling pool vesicles contained within a bouton was described by two methods (Figure 4.7) applied to the three middle sections of the bouton. While all of the sections for each bouton were used to quantify vesicle numbers at synapses, the three middle sections of a bouton centered around the active zone gave a good representation of vesicle distribution. In previous studies examining the spatial organization of vesicles at synapses, single sample sections alone have been used (Schikorski and Stevens, 2001) or alternatively, to take into consideration the three dimensional nature of the vesicle cluster, three consecutive sections were collapsed into a single plane and neighbour relationships considered (Rizzoli and Betz, 2004). In the current study, the coordinate positions of vesicles and active zones were marked and the shortest distance of each vesicle to the active zone in three dimensions was recorded. The

distribution of vesicle distances to the active zone were similar for both recycling pool vesicles and the total vesicle population, as were their proportions in the active zone and core regions (Figure 4.7). Readily releasable pool vesicles at hippocampal synapses have been found to distribute unevenly throughout the vesicle cluster, with a tendency to be closer to the active zone (Schikorski and Stevens, 2001). However, a similar ultrastructural study at the frog neuromuscular junction found the readily releasable pool vesicles to be distributed throughout the vesicle cluster (Rizzoli and Betz, 2004). The results in this chapter deal solely with the total recycling pool of vesicles and indicate that while there is no preferential spatial location for these vesicles within the cluster, their distribution is skewed in a similar way to the that observed for the RRP vesicles (Schikorski and Stevens, 2001). Even though the proportion of PC+ vesicles was significantly reduced in the outer regions of the cluster and increased in regions close to the active zone, the spatial relationship of these vesicles with the release site is unlikely to be the sole determinant for their inclusion in the recycling pool. It may also be that some intrinsic properties of the vesicles determine their preferential participation in release events.

In preparation for studying the incorporation of non-native FM dye fluorescence at photobleached synapses by electron microscopy, as will be described in the next chapter, it was necessary to confirm that the photobleaching of FM1-43 fluorescence at the light level corresponded to an absence of photoconversion product in EM. It was found that a rather stringent photobleaching protocol was required to inhibit the formation of a photoconversion product. The photobleaching of FM1-43 fluorescence to levels similar to that used in fluorescence time-lapse studies (section 3.4.1) did not completely prevent the formation of photoconversion product. This presumably reflects the amplifying nature of the photo-oxidation procedure, such that a small amount of non-photobleached FM1-43 was sufficient to create an identifiable precipitate in vesicles. The photobleaching protocol devised in this chapter satisfactorily prevented the formation of a photoconversion product as shown in Figure 4.8 and summarized in Figure 4.8d. It was feared that this robust

protocol would result in severely photo-damaged synapses. However, there was no evidence of photo-damage at the EM level; the mitochondria and surrounding cytoplasmic membrane were intact and not over contrasted as seen in cases of photo-damage (personal communication; Oleg Shupliakov). The capacity of photobleached synapses to undergo multiple rounds of exocytosis provided further confirmation of the non-toxic nature of the photobleach protocol (Figure 4.9).

Chapter 5 | Ultrastructural Analysis of Synaptic Vesicle Mobility

5.1 Introduction

Time-lapse fluorescence microscopy was used in Chapter 3 to detect the movement of FM dye-labelled vesicles within axons. In combination with FRAP measurements, this gave an estimate of the extent to which mobile fluorescence signal was incorporated into synapses. However, due to the limited resolution of light microscopy, little information could be gathered about the nature of the fluorescent transport packages. Are they clusters of synaptic vesicles or pleimorphic endosomal structures as seen previously (Ahmari et al., 2000)? While imported FM dye-labelled vesicles participated in exocytosis with similar kinetics to native vesicles, it was of interest as to how this functional incorporation was represented spatially. Electron microscopy in combination with the photoconversion of FM1-43 allowed mobile fluorescent packets to be identified in axons. Also, newly imported vesicles at boutons could be visualized so as to establish whether they were restricted to the periphery of the synapse or if they had access to all areas of the presynaptic vesicle cluster. In this chapter, a selection of the techniques outlined in previous chapters was used to study inter-bouton vesicle exchange at the level of the electron microscope.

5.2 Departure of Recycling Pool Vesicles from Synapses

The synaptic connections in cultures of the age used in these experiments would be expected to be in a mature state (Verderio et al., 1995; Verderio et al., 1999b). This is further supported by general observations from pre- and postsynaptic labelling conducted in experiments described in earlier chapters. As such, the fluorescently labelled recycling pool vesicles, seen to be imported into synapses by FRAP experiments in Chapter 3, most probably originated from sites of synaptic vesicle endocytosis, rather than from the non-synaptic uptake of FM dye. In order to prove that mature resting synapses could release recycling pool vesicles for transport and reuse elsewhere, a combination of photobleaching and time-lapse imaging was used to detect the departure of small fluorescent packets from synapses. Subsequently, the photoconversion and CLEM techniques detailed in Chapter 4 were used to establish what the mobile fluorescence that departed from donor synapses represented at the ultrastructural level.

5.2.1 Exit of fluorescently labelled vesicles from synapses

The presynaptic boutons of hippocampal neurons were labelled with FM1-43fx using a 600 AP, 10 Hz loading stimulus. In order to visualize the movement of small packets of fluorescence, sections of the axonal regions surrounding a target bouton were photobleached to eliminate the fluorescence. The boutons chosen for shedding experiments were approximately similarly sized and arranged with respect to neighbouring boutons. The target regions were imaged at a rate of one frame per 10 s for a short period of time (≤ 330 s). High gain and high power settings were found to be optimal for detecting mobile packets following the photobleach protocol. As a result of this, the initial pre-bleach images were over-exposed and a flaring of fluorescence was seen in these images. The departure of fluorescent units from synapses into photobleached axons was observed as indicated by the yellow arrowheads in Figure 5.1. This appeared to be a common phenomenon, with

evidence of departing fluorescence seen in the majority of boutons examined (11 from 15 experiments). The time taken to observe these events varied from just 40 s to 270 s, reflecting the stochastic and seemingly frequent nature of the process. In the 4 out of 15 boutons that did not show any evidence of vesicle departure, there was nothing about their initial fluorescence intensity, shape or distance from neighbours that distinguished them from the other 11 boutons that underwent vesicle shedding. With more time, release events may have been recorded at these boutons. However, in general, a short time-window of observation was employed as this reduced the likelihood of fluorescence material from outerlying, non-photobleached regions entering the region of interest and confounding the detection of fluorescent packets mobilized from the target synapse.

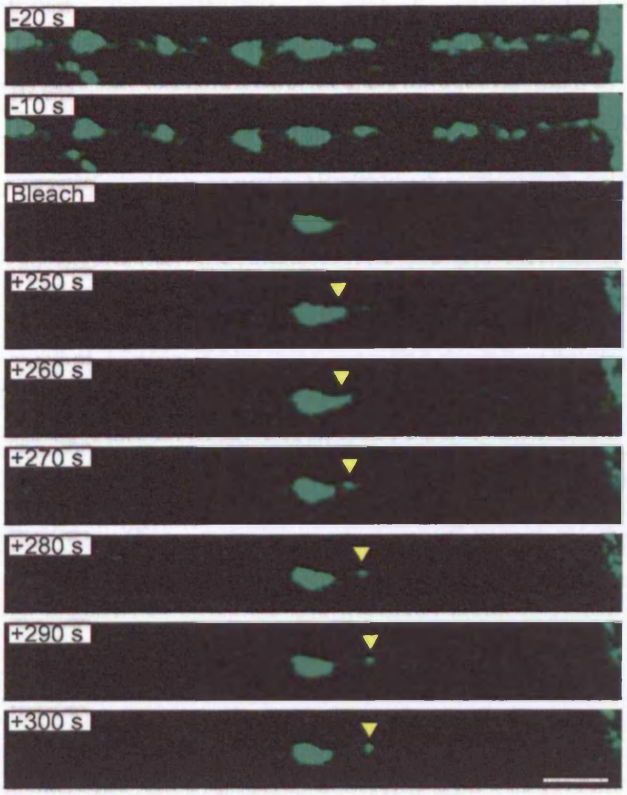

Figure 5.1– Shedding of fluorescent packets from synapses

The selective photobleaching of axonal regions surrounding a single FM1-43 labelled synapse allowed the clear identification of fluorescence movement out of the target bouton. A small package of FM1-43 fluorescence moving out of the synapse and along the axon was captured in the time-lapse sequence and is highlighted with yellow arrowheads. The maturity of synapse was later determined by CLEM. Scale bar, 5 µm.

Identification of mobile units of fluorescence in EM

From the fluorescence shedding experiments described above, a selection of the samples was fixed immediately upon observing the departure of fluorescent packets from the synapse. After photoconversion, the donor synapses and surrounding axons were identified by CLEM techniques, thus allowing the ultrastructural nature of the mobile fluorescence signal to be studied. In previous fluorescence-based experiments, mature synapses were identified by dual labelling of pre- and postsynaptic elements. However, in experiments in this chapter a post-hoc ultrastructural analysis identified pre- and postsynaptic membrane specializations of donor synapses to confirm their maturity. The sample time-lapse images used to identify a mobile fluorescent packet, similar to Figure 5.1, are shown in Figure 5.2a. In this experiment, as soon as a packet of fluorescence moved out

from the synapse at 70 s post-photobleaching, the sample was fixed, photoconverted and processed for EM. A section of the final fluorescence image, showing both the donor synapse and the fluorescent packet is displayed with a corresponding single electron micrograph and a 3-dimensional reconstruction of the same region (Figure 5.2b). The cluster of vesicles highlighted by the yellow arrowhead in both the single electron micrograph and the 3-d reconstruction of the axonal region correspond to the mobile fluorescent packet identified by time-lapse imaging. These results clearly establish that mobile FM dye fluorescence relates to vesicle clusters, and implies that the fluorescence recovery observed previously at boutons (Figure 3.5) arises from the movement of properly formed vesicles along axons rather than endosomal intermediates produced during vesicle recycling (Takei et al., 1996).

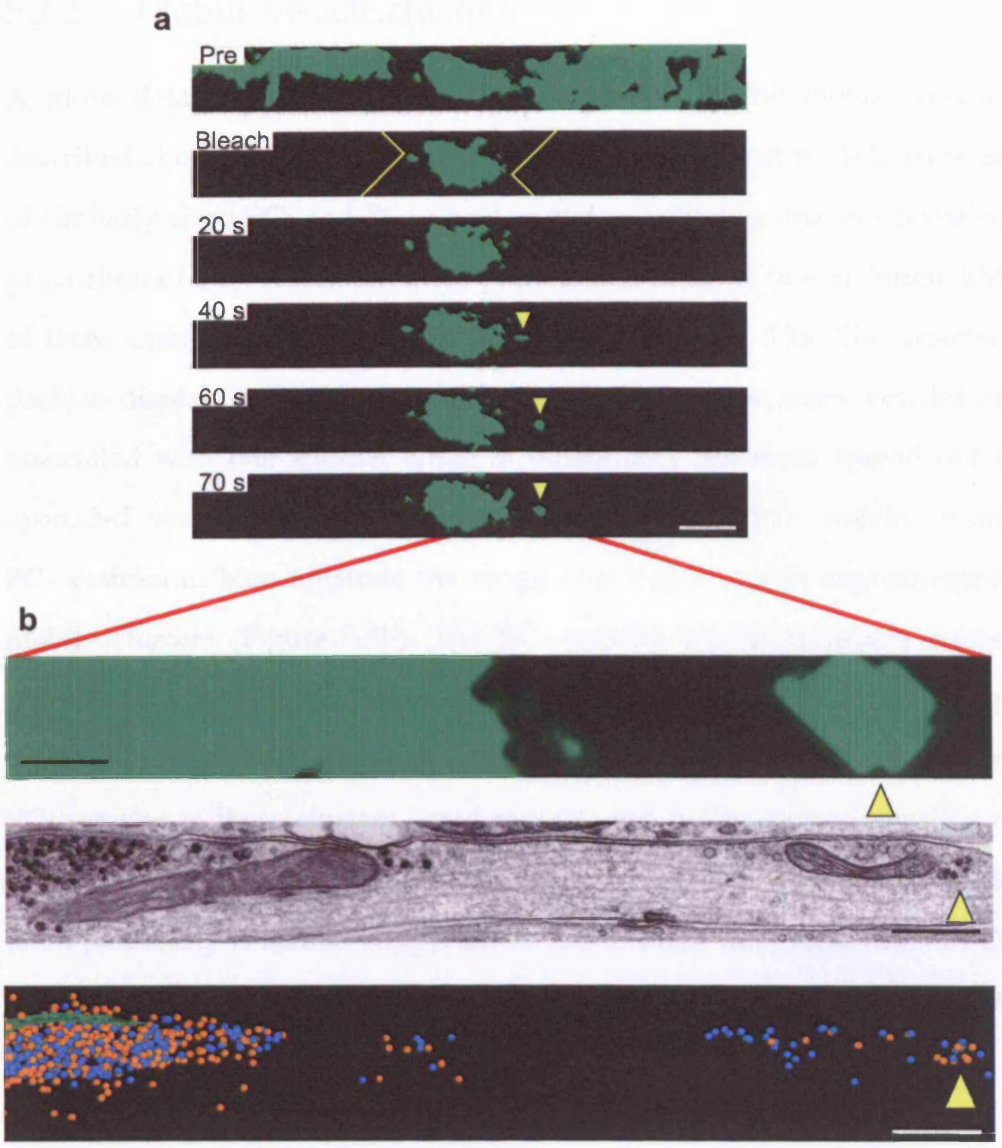

Figure 5.2– Identification of mobile packets using CLEM techniques

(**a**) Regions (yellow box) adjacent to an FM1-43 positive bouton were photobleached as in Figure 5.1. A time-lapse sequence shows the departure of a fluorescent packet from the bouton (yellow arrowhead). Note: the digital contrast was scaled differently in the pre- versus post-photobleach images to allow the clear visualization of bouton and packet. Scale bar, 5 µm. (**b**) A correlation between the final frame of the fluorescence time-lapse sequence and a single EM section of the axonal region showing both the synapse and extra-synaptic vesicle cluster (yellow arrowhead). A 3-d reconstruction of the same area shows the synapse and loose clusters of vesicles identified as PC+ (orange) and PC- (blue) and corresponding to the fluorescent packets identified in **a** (yellow arrowhead). The active zone is shown in green. Scale bar, 0.5 µm.

5.2.2 Mobile vesicle clusters

A more detailed ultrastructural characterization of the mobile vesicle clusters described above was undertaken. The identified transport packets were aggregates of similarly sized PC- and PC+ vesicles, and quantitative analysis revealed that the proportion of PC+ vesicles in these packets was 36 ± 7% (n = 5). Single EM sections of three example vesicle packets are shown in Figure 5.3a. The vesicles in these packets display multiple arrangements, where in some cases vesicles are tightly associated with one another while in others they are more spread out along the axon. 3-d reconstructions of two sample packets with PC+ vesicles in orange and PC- vesicles in blue illustrate the range of possible vesicle organizations in these mobile clusters (Figure 5.3b). The PC- vesicles in the transport packets might represent newly formed or photobleached vesicles already in transit along the axon that were joined by PC+ vesicles upon their shedding. Alternatively the presence of PC- vesicles in these clusters could indicate the ability of non-recycling or resting pool vesicles to depart from the synapse jointly with recycling pool vesicles. This latter possibility is further supported by the fact that the proportion of PC+ vesicles present in mobile clusters (36 ± 7%) is similar to that seen at synapses (46.0 ± 7.4%).

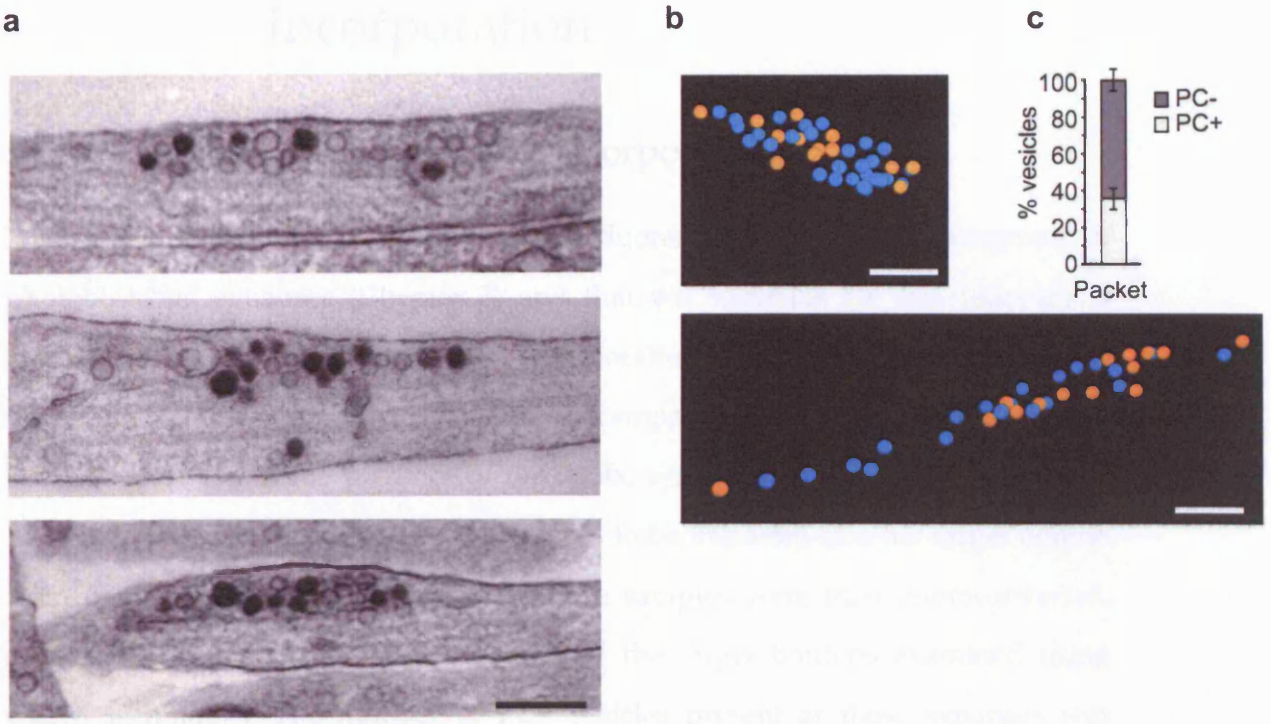

Figure 5.3– Ultrastructural detail of mobile packets

(**a**) Example electron micrographs of extra-synaptic vesicle clusters identified by time-lapse imaging and CLEM. (**b**) 3-d reconstructions of representative mobile vesicle clusters. PC+ vesicles in orange, PC- vesicles in blue. Scale bars, 0.2 µm. (**c**) Bar graph comparing the proportion of PC+ and PC- vesicles in the dentified mobile packets.

5.3 Ultrastructural Analysis of Vesicle Incorporation

5.3.1 Quantification of vesicle incorporation

Having established that non-native FM4-64 fluorescence can become integrated at photobleached synapses (Chapter 3) and that the substrate for this recovery is clusters of vesicles (this chapter), the incorporation of vesicles into synapses was next studied by electron microscopy. Hippocampal neurons were stimulated with 600 APs at 10 Hz in the presence of FM1-43fx, synapses were photobleached and fixed after ~18 min, to allow time for vesicles to be imported into the target bouton from other non-photobleached boutons. The samples were then photoconverted, serially sectioned, and the ultrastructure of the target boutons examined using CLEM techniques. The number of PC+ vesicles present at these synapses was compared to those at photobleached, time-matched controls where axonal transport had been compromized, and to non-photobleached boutons to estimate the size of the recycling pool.

As criteria for inclusion in these experiments, all boutons had intact outer membranes and were confirmed to be mature synapses by a post-hoc ultrastructural identification of pre- and post-synaptic specializations. Efforts were made at the fluorescence level to choose boutons of a similar size. All synapses included in this study contained fewer than 700 vesicles and the average number of vesicles per bouton for each experimental condition was not significantly different (Kruskal-Wallis ANOVA, $P = 0.89$, median and inter-quartile ranges (IQR), non-photobleached: median, 279, IQR, 235-445; photobleached and fixed immediately: median, 295, IQR, 254-345; jasplakinolide-treated photobleached and fixed after 18 min: median, 357, IQR, 309-384; photobleached and fixed after 18 min: median, 262, IQR, 149-488). The similarities in the boutons across each of the experimental conditions validated the subsequent comparisons made between these experimental groups.

Displayed in Figure 5.4 are sample EM sections of boutons representing each of the three conditions mentioned above. Synapses which had been photobleached and allowed to recover prior to fixation are shown in Figure 5.4a. PC+ vesicles, which based on previous time-lapse studies (section 3.4.1) have presumably moved in from neighbouring non-photobleached synapses, are present within the vesicle cluster. At these synapses an average of 8.2 ± 1.3% (n = 11, Figure 5.4d) of the total vesicles were PC+. Example electron micrographs of time-matched controls are shown in Figure 5.4b; here neurons had been pre-treated with jasplakinolide for 15 mins prior to photobleaching to inhibit axonal transport (see Figure 3.4). These boutons fixed ~18 mins after photobleaching, contained significantly fewer PC+ vesicles than the experimental condition (t-test, P = 0.013, 2.6 ± 0.6%, n = 5; Figure 5.4d). These results agree with earlier experiments in Chapter 3, where fluorescence recovery at synapses marked with EGFP-GluR2 and FM4-64 was disrupted by jasplakinolide, and supports the idea that PC+ vesicles are imported into photobleached synapses via axonal transport. While there was some variation in the extent to which individual synapses incorporated PC+ vesicles, >90% of the photobleached boutons showed more recovery than time-matched jasplakinolide controls indicating that this import process was robust.

A subset of sections from a non-photobleached, photoconverted synapse is shown in Figure 5.4c. For this condition the average number of PC+ vesicles at synapses, representing the recycling pool, was 46.0 ± 7.4%, n = 5 (Figure 5.4d and previously in Figure 4.8). Given the size of the recycling pool, the fact that ~8% of vesicles in bleached boutons were PC+ at the end of the recovery period would suggest that newly imported vesicles contribute substantially to host recycling pools.

The quantification of vesicle numbers at synapses involved the alignment of all serial sections for each bouton using multiple membrane and organelle landmarks and the classification of each vesicle (n = 7878 from 27 boutons) as either PC+ or PC- (see section 4.3.1). Given the large amount of vesicle counting involved and the subjective nature of vesicle classification, there was a fear that experimenter error might influence the results. As a control for the scoring of PC+ and PC- vesicles, a

random selection of the data (n = 2682), including samples from all experimental conditions, was analysed blind by a third party. A comparison of the results indicated that the proportion of vesicles from each vesicle class, in each experimental condition scored by the third party was not significantly different from non-blind counts. Samples that were photobleached and fixed immediately, by non-blind and blind counts contained 0.6 ± 0.4% and 0.4 ± 0.4% PC+ vesicles, respectively (mean ± s.e.m. *t*-test, $P = 0.502$). In samples that were jasplakinolide-treated, photobleached and fixed after 18 min, non-blind and blind counts yielded 2.3 ± 0.7% and 2.5 ± 1.1% PC+ vesicles, respectively (mean ± s.e.m. *t*-test, $P = 0.840$). Samples that were photobleached and fixed after 18 min, by non-blind and blind counts contained, 7.5 ± 1.6% and 9.2 ± 2.1% PC+ vesicles, respectively (mean ± s.e.m. *t*-test, $P = 0.105$). In non-photobleached samples, non-blind and blind counts yielded 44.6 ± 7.2% and 53.2 ± 9.7% PC+ vesicles, respectively (mean ± s.e.m. *t*-test, $P = 0.079$). While in some cases the difference between blind and non-blind counts was nearing significance, in each condition the non-blind counts consistently underestimated the proportion of PC+ vesicles present at synapses. This suggested that while there may be a variation in vesicle counting, the overall trends remained the same, and if anything the extent of vesicle incorporation may have been underestimated by non-blind analysis.

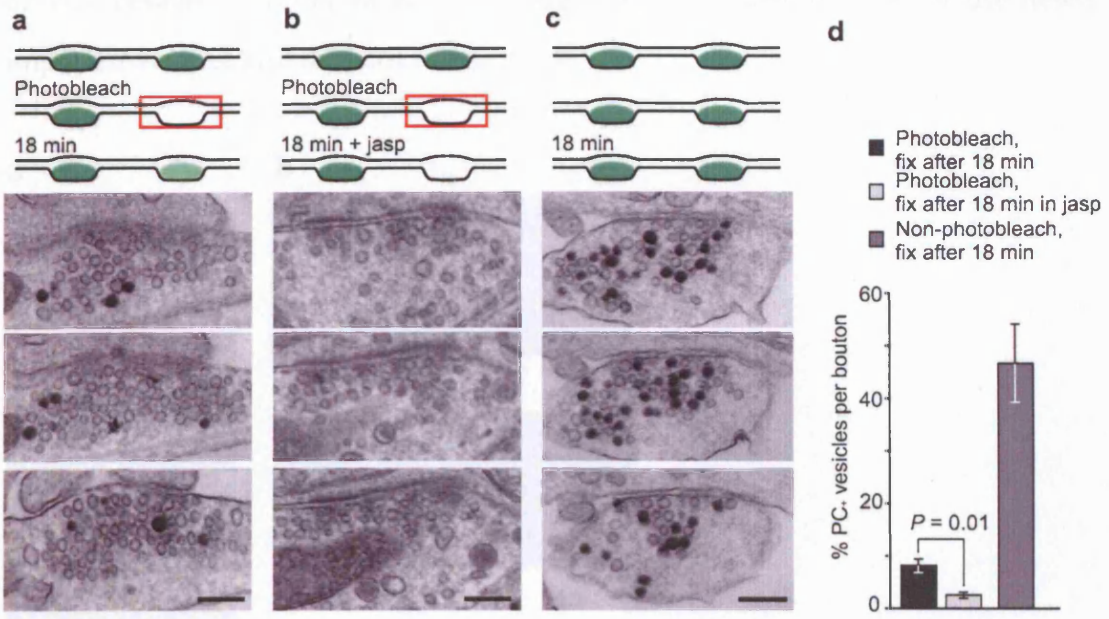

Figure 5.4– Vesicle incorporation visualized by electron microscopy

Consecutive serial sections of representative boutons from three experimental conditions: (**a**) photobleached and fixed after 18 min; (**b**) jasplakinolide-treated (1 μM), photobleached and fixed after 18 min; (**c**) non-photobleached. In the schematics (top) red boxes denote photobleaching. Scale bars, 0.2 μm. (**d**) Plot summarizes average percentage of photoconverted vesicles per bouton for each of the three conditions. Data are mean ± s.e.m.

5.3.2 Spatial distribution of newly imported vesicles

As a first step to establishing the spatial arrangement of imported vesicles within non-native synapses, 3-d reconstructions were used to give an overview of the vesicle cluster and the position of vesicles with respect to the active zone. A complete series of serial sections from a synapse that had been photobleached and allowed to recover for 18 min is shown in Figure 5.5a. These sections were then used to make a 3-d reconstruction of the synapse. Non-photoconverted vesicles representing the native vesicle cluster are shown in blue, and newly incorporated photoconverted vesicles are in orange, with the active zone shown in green (Figure 5.5b). The newly imported vesicles were distributed throughout the native vesicle pool, from near the active zone out to the cluster edge. There was little evidence of the clustering of PC+ vesicles in this reconstruction or in any of the other synapses examined. The same 3-d reconstruction is shown in Figure 5.5c without the native

or PC- vesicles in order to better illustrate the relationship between the newly imported vesicles and the active zone.

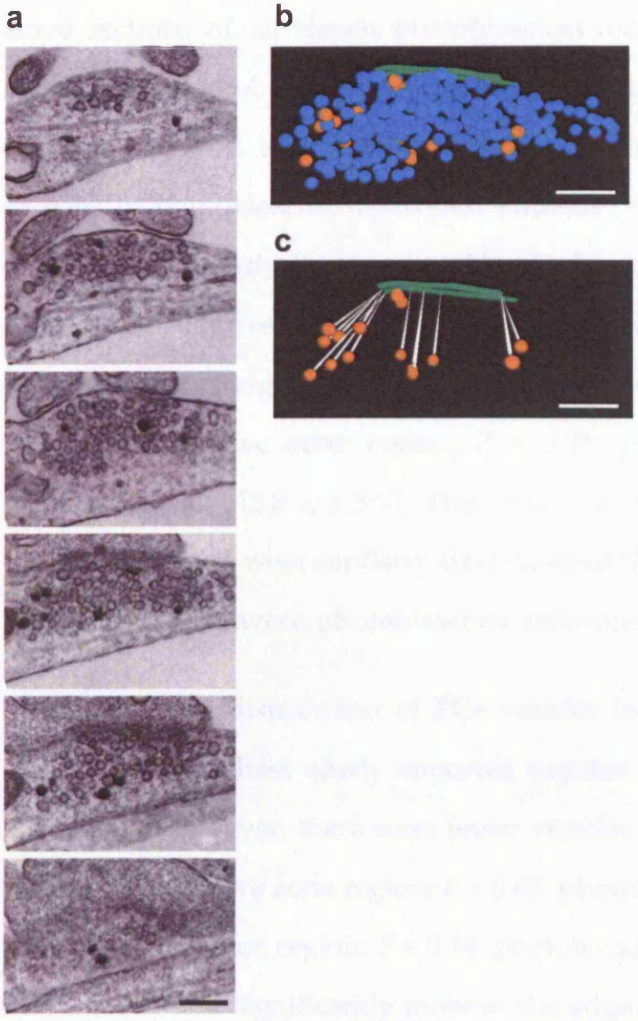

Figure 5.5– 3-dimensional reconstruction of FRAP bouton

(**a**) A complete set of serial sections of a photobleached-recovered bouton. (**b**) 3-d reconstruction of photobleached-recovered bouton from **a**, showing newly imported (PC+) vesicles (orange) distributed throughout the native (PC-) vesicle cluster (blue). (**c**) The same reconstruction as **b** but without the native vesicles, illustrating the distance from the active zone of the newly imported vesicle. The active zones in both reconstructions are shown in green. Scale bars, 0.2 µm.

Having obtained an overall impression of vesicle incorporation from 3-d reconstructions, the spatial integration of non-native vesicles was quantified by the two methods described in section 4.3.2. These methods were applied to the middle three sections of all eleven photobleached-recovered boutons from Figure 5.4d. Firstly, the region-based analysis, where vesicles were sorted into active zone, core and edge regions, indicated that the distribution of all vesicles across these three regions in photobleached-recovered boutons was not significantly different from that seen previously in non-photobleached boutons (Figure 4.7a and Figure 5.6a, paired *t*-test, edge region: $P = 0.54$, photobleach all, 50.1 ± 2.5%, non-photobleach all, 47.1 ± 4.3%; core region: $P = 0.33$, photobleach all, 32.2 ± 3.8%, non-photobleach all, 39.1 ± 5.8%; active zone region: $P = 0.38$, photobleach all, 17.8 ± 2.8%, non-photobleach all, 13.8 ± 1.6%). This result, in combination with the fact that all boutons analysed were similarly sized justifies the comparison of the ultrastructural characteristics between photobleached and non-photobleached boutons.

Next, when the distribution of PC+ vesicles in photobleached-recovered boutons was considered, these newly imported vesicles were present in all three regions of the cluster. However, there were fewer vesicles in the active zone and core regions (paired *t*-test, active zone region: $P = 0.05$, photobleach PC+, 7.9 ± 6.2%, photobleach all, 17.8 ± 2.8%; core region: $P = 0.14$, photobleach PC+, 21.7 ± 6.1%, photobleach all, 32.2 ± 3.8%) and significantly more at the edge of the vesicle cluster (paired *t*-test, edge region: $P = 0.02$, photobleach PC+, 70.5 ± 6.4%, photobleach all, 50.1 ± 2.5%) (Figure 5.6a). When analysing the distribution of vesicle distances to the active zone, newly imported vesicles were seen to have a similar overall distribution to that of the entire population of vesicles (Figure 5.6b). However, there were fewer PC+ vesicles closer to the active zone and none within 50 nm of it. This correlates with the reduced number of PC+ vesicles seen in active zone and core regions of photobleached boutons by the regional analysis above. In contrast, there were a higher proportion of PC+ vesicles towards the edge of the cluster. This finding, in combination with the results from the region based analysis would suggest that the cluster edge acts as the entry point for these newly imported vesicles.

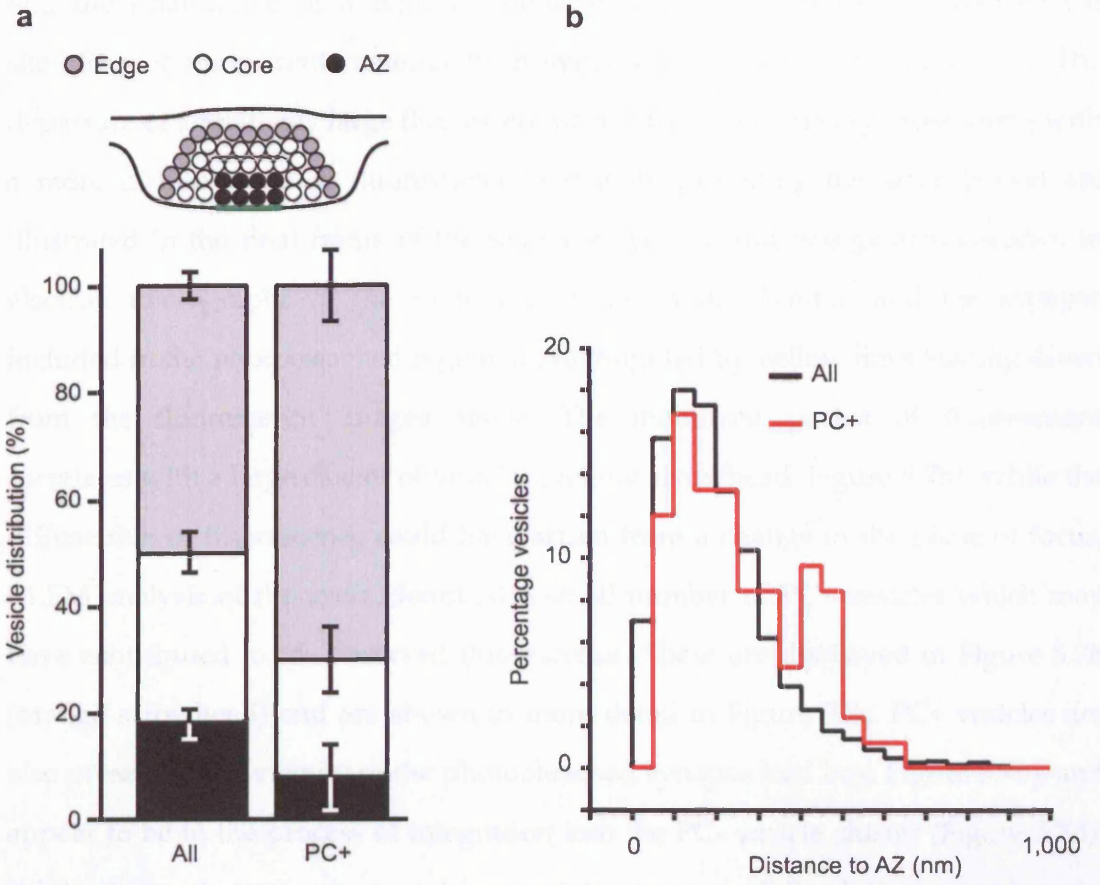

Figure 5.6– Analysis of the spatial distribution of newly incorporated vesicles within boutons

(**a**) The relative distribution of vesicles in photobleached-recovered boutons in edge, core and active zone regions. Left: all vesicles (50.1 ± 2.5%, 32.2 ± 3.8%, 17.8 ± 2.8%). Right: incorporated vesicles only (70.5 ± 6.4%, 21.7 ± 6.1%, 7.9 ± 6.2%). (**b**) Histograms comparing the distribution vesicle to active zone distances for incorporated vesicles and the total vesicle population in photobleached-recovered synapses.

5.3.3 Shedding and incorporation viewed simultaneously by electron microscopy

In some experiments designed to examine the departure of vesicles from synapses, the region of axon around the target bouton included FM labelled synapses which were also photobleached. While this made the study of mobile vesicle packets difficult due to a direct source of both photobleached and PC- vesicles in the region, it was possible to observe the apparent incorporation of non-native PC+ vesicles arising from the target non-photobleached bouton into these synapses in electron micrographs. The images acquired immediately before and after photobleaching,

and the final frame of a typical time-lapse sequence designed to observe the shedding of fluorescent material from synapses are shown in Figure 5.7a. The departure of a relatively large fluorescent packet from the target synapse along with a more diffuse wave of fluorescence seemingly preceding the large packet are illustrated in the final frame of the sequence (yellow and orange arrowheads). In electron micrographs of the same region, the donor bouton and the synapse included in the photobleached region are highlighted by yellow lines leading down from the fluorescence images above. The mobilized packet of fluorescence correlates with a large cluster of vesicles (yellow arrowhead, Figure 5.7b). While the diffuse flux of fluorescence could have arisen from a change in the plane of focus, CLEM analysis of the axon identified a small number of PC+ vesicles which may have contributed to the observed fluorescence. These are displayed in Figure 5.7b (orange arrowhead) and are shown in more detail in Figure 5.7c. PC+ vesicles are also present in the vicinity of the photobleached synapse (red box, Figure 5.7b), and appear to be in the process of integration into the PC- vesicle cluster (Figure 5.7d). While these electron micrographs are static images of fixed tissue, taking the fluorescence time-lapse sequence into account, these micrographs, showing a donor bouton, mobile recycling pool vesicles and their integration into a non-native synapse, encapsulate the whole process of inter-bouton vesicle sharing.

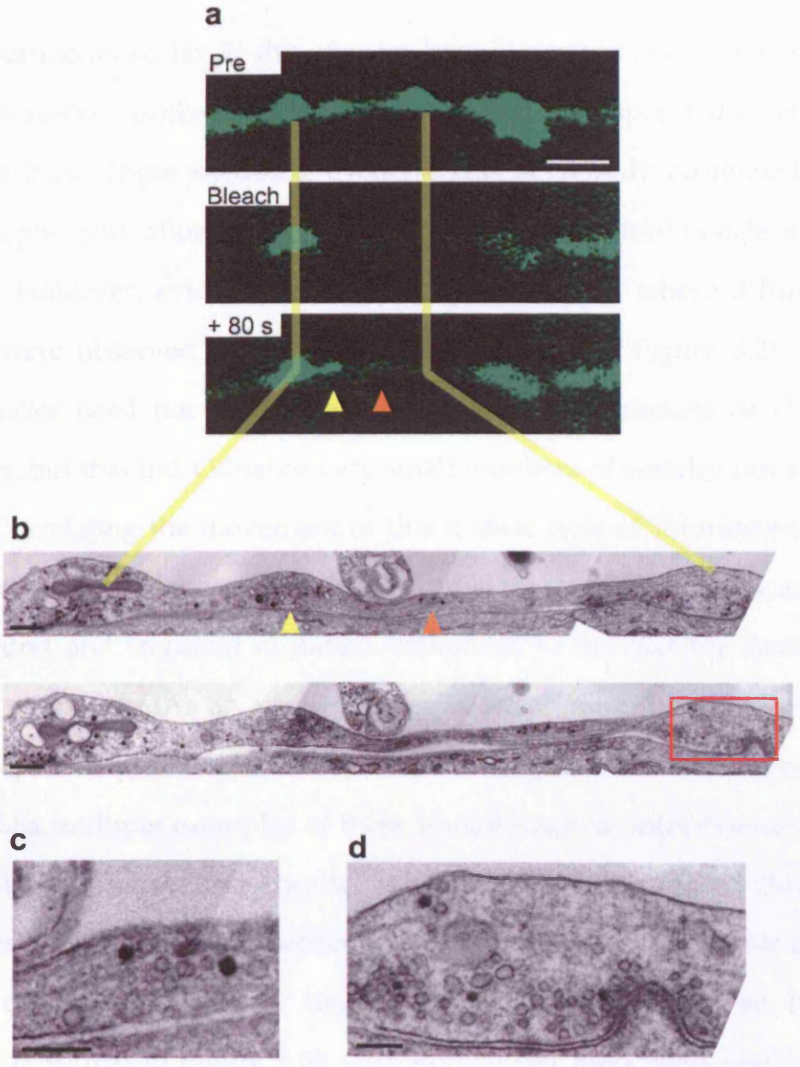

Figure 5.7– Vesicle shedding and incorporation at the ultrastructural level

(**a**) Fluorescence images acquired immediately before, immediatley after photobleaching the regions of axon around a single FM1-43 positive bouton, and 80 s after photobleaching. In the final frame a yellow arrowhead indicates the departure of a large fluorescent packet preceeded by a more diffuse spread of fluorescence (orange arrowhead). Vertical yellow lines indicate the donor synapse and a synapse within the photobleach region which contained some of the mobilized fluorescence at the time of fixation. Scale bars, 5 µm. (**b**) Two EM sections of the area corresponding to that denoted by the two vertical yellow lines in **a**. A yellow arrowhead marks a cluster of vesicles corresponding to the large fluorescent packet seen in **a**, while an orange arrowhead highlights PC+ vesicles corresponding to the diffuse fluorescence. Scale bars, 0.5 µm. (**c**) A more detailed image of a vesicle cluster corresponding to the diffuse fluorescence seen in **a** and denoted by orange arrowheads in **b**. Scale bar, 0.2 µm. (**d**) High magnification electron micrograph of the photobleached synapse from **a** and denoted by the red box in **b**. PC+ vesicles are present close to and within the cluster of PC- vesicles around an active zone. Scale bars, 0.2 µm.

5.3.4 Non-cluster based vesicle movement

The experiments so far in this chapter have described the departure of relatively large fluorescent packets from synapses, which corresponded to clusters of 10 or more vesicles. These shedding events could be readily correlated with electron micrographs and allowed the substrate of inter-bouton vesicle exchange to be studied. However, evidence from time-lapse imaging, where diffuse fluorescence signals were observed arising between synapses (see Figure 3.2), would suggest that vesicles need not travel exclusively as discrete packets or clusters between synapses, but that individual or very small numbers of vesicles can also move along axons. Correlating the movement of this diffuse type of fluorescence with vesicles in electron micrographs was difficult, given that the signal was barely above background and transient in nature compared to the discrete fluorescent packets studied previously. As an alternative approach to describing this process, electron micrographs of photobleached inter-bouton regions of axons were examined. In Figure 5.8a multiple examples of these photobleached, inter-bouton axonal regions are displayed. Orange arrowheads highlight individual or small clusters of vesicles along the axon whose fluorescence was not sufficient to rise above the background during confocal imaging. A single electron micrograph of an FM1-43-labelled synapse is shown in Figure 5.8b with non-cluster associated vesicles indicated by yellow arrowheads. Taken together, this data would suggest that the source of imported vesicles at synapses need not exclusively be discrete packets of vesicles but that individual vesicles can both leave and join the vesicle cluster at synapses.

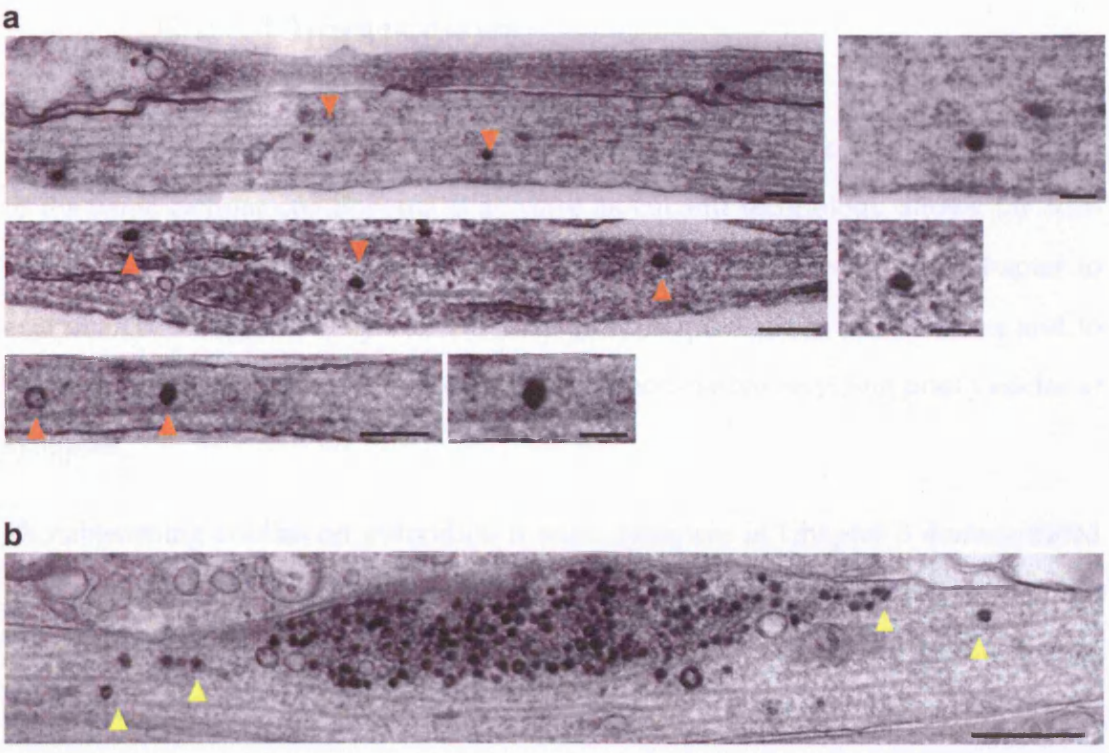

Figure 5.8– Non-clustered movement of vesicles

(**a**) An example of an FM1-43 positive bouton in EM. Yellow arrowheads indicate single vesicles away from the edge of the cluster which may have been in the process of leaving the synapse. (**b**) Sample electron micrographs of inter-bouton axonal regions. Orange arrowheads highlight individual vesicles. Scale bars, 0.2 μm. A selection of these un-associated vesicles is shown in greater detail on the right. Scale bars, 0.1 μm.

5.4 Discussion

The correlation of live fluorescence imaging with post-fixation electron micrographs of the same cellular components is as close as current technology allows for real-time electron microscopy. These techniques have been employed in this chapter to examine the mechanisms by which individual synapses share their vesicles and to probe the ultrastructure of the incorporation of non-native recycling pool vesicles at synapses.

Photobleaching studies on individual mature synapses in Chapter 3 demonstrated that mobile synaptic vesicles in axons can become functionally integrated into synapses (Figure 3.9). However, in order to regulate vesicle cluster size, synapses should be capable of releasing vesicles as well as gaining them. To test this idea, a photobleach method was used to observe the departure of FM dye-labelled vesicles from synapses (Figure 5.1) whose maturity was confirmed by post-hoc ultrastructural analysis (Figure 5.2). This result confirms that mature synapses can act as the vesicular source of fluorescence recovery recorded in previous chapters (Figure 3.5).

In other studies, concerned particularly with the early stages of neuronal development, mobile vesicular material appeared as pleimorphic membrane structures (Ahmari et al., 2000) or the nature of the observed mobile fluorescence was left unprobed (Hopf et al., 2002; Krueger et al., 2003). In this chapter, the mobile FM dye-related fluorescence, previously shown to contribute to the functional recycling pool of synapses (Figure 3.9), was identified as discrete clusters of synaptic vesicles (Figure 5.3). These vesicular transport packages are unlike tubulovesicular transport packages seen in developing systems (Nakata et al., 1998) and further illustrate that synaptic vesicle movements between mature synapses are distinct from the axonal movement of synaptic vesicle components observed in developing neurons associated with synapse formation (Matteoli et al., 2004). However, in some cases mobile vesicle-related fluorescence, identified in immature

processes of developing hippocampal neurons, has been shown to relate to individual or small groups of vesicles by electron microscopy (Kraszewski et al., 1995). While the mobile vesicles seen in this chapter may make use of transport mechanisms similar to developing systems, they are found in mature axonal processes between established synapses. An ultrastructural study of CA3-CA1 connectivity in adult rat hippocampal slices by Shepherd and Harris revealed small, loose clusters of vesicles along axons between mature synapses following 3-d reconstructions of axonal processes (Shepherd and Harris, 1998). The arrangement of these vesicles was strikingly similar to that shown in this chapter, and such a similarity raises the possibility that an analagous exchange of vesicles may occur in the adult CNS.

The vesicle-transport packages identified in this chapter by CLEM were made up of both PC+ and PC- vesicles of varying arrangements. If the PC- vesicles arose from the resting pool of donor synapses, this would agree with observations from synaptophysin-EGFP experiments where a comparison of the extents of fluorescence recovery between FM dye and SypI-EGFP labelled vesicles suggested that vesicles other than those of the recycling pool contributed to the SypI-EGFP FRAP signal (Figure 3.10). Taken together, these results would indicate that all vesicles at synapses and not just those of the recycling pool participate in the process of inter-bouton vesicle sharing. However, given that it was only possible to reliably mark recycling pool vesicles for fluorescence imaging and electron microscopy via photoconversion, a quantitative examination of the full extent of vesicle sharing between synapses was not possible.

The recovery of fluorescence at photobleached boutons described in Chapter 3 was shown to correlate with the appearance of photoconverted synaptic vesicles at target mature synapses in a transport-dependent manner (Figure 5.4). This accumulation of non-native recycling pool vesicles, taken together with the shedding of small clusters of vesicles from mature synapses (Figure 5.2), provides evidence for the sharing of functional vesicles between synapses in established neuronal networks. The mechanism of sharing is mediated by the movement of

synaptic vesicles and is unlikely to involve endosomal intermediaries. Previously in Chapter 4, the photobleach protocol was shown to prevent the appearance of PC+ vesicles in synapses (Figure 4.8). While the number of PC+ vesicles at photobleached synapses in time-matched controls that had been treated with jasplakinolide to inhibit axonal transport, was significantly less than that seen in the experimental group (Figure 5.4), there were more PC+ vesicles present than in photobleach controls (Figure 4.8). The most likely explanation for the appearance of these vesicles is that the jasplakinolide block of axonal transport was not 100% effective. Given that the recycling pool was estimated to make up about 46% of the total vesicle cluster at synapses (Figure 5.4d), the extent of photoconverted vesicle recovery observed in this chapter would indicate that imported vesicles over an 18 min period constitute 18% of the recycling pool. Vesicle sharing, as described here is an apparently constitutive process, and the above calculations imply that a substantial proportion of the vesicle population at given synapse could arise from the vesicle cycle at another synapse.

Qualitative 3-d reconstructions of photobleached-recovered synapses and quantitative positional analysis were used to describe the incorporation of imported vesicles in synapses. While imported or PC+ vesicles were present in all areas of the vesicle cluster as classified by regional analysis, imported vesicles were never found docked at the active zone of host synapses. Given that docked vesicles have been reported to detach from the active zone over time (Murthy and Stevens, 1999), it is probable that a larger sample size may have revealed imported vesicles docked at the active zone. The spatial integration of imported vesicles, as described here, agrees well with previous experiments in Chapter 3 where newly imported vesicles could undergo exocytosis as effectively as the native vesicles.

The extent of non-native vesicle integration at host synapses indicates that, upon entering a new synapse, imported vesicles appear to be mobile within the cluster. Previous studies estimating the movement of vesicles within synapses by spot photobleaching reported little movement prior to the onset of stimulation (Kraszewski et al., 1996). However, more recent studies making use of FCS

detection methodologies (Jordan et al., 2005; Lemke and Klingauf, 2005; Shtrahman et al., 2005) have reported the movement of individual vesicles within synapses. In particular, the model for vesicle movement proposed by Shtrahman et al (Shtrahman et al., 2005) predicts that a substantial proportion (~27%) of vesicles in synapses is freely diffusible for a significant fraction of the time (~30%). It seems possible, therefore, that the level of intra-bouton vesicle movement observed in these FCS studies could account for the mixing of newly incorporated vesicles at synapses reported here.

This chapter confirmed that the basis for the observed fluorescence recovery at synapses described in earlier chapters is made up of two related but distinct components. In the first, discrete transport packages, easily observed at both the light and EM level, consisting of numerous vesicles, can contribute to the vesicle clusters of non-native synapses as exemplified in Figure 5.7. While these movements are the most obvious, it may be misleading to regard them as the sole or even the predominant means by which vesicles are exchanged between synapses. Another mode of vesicle movement, distinct from transport packages, could also contribute to the vesicle clusters of synapses. At the light level, the diffuse flux of fluorescence material between synapses was observed (Figure 3.2). Such diffuse signal could represent the individual PC+ vesicles that were present along axons, presumably in the process of moving between boutons (Figure 5.8a). These individual vesicles highlight another less obvious type of vesicle movement which may also be a part of the vesicle sharing mechanism in neurons.

The various modes by which vesicles are moved along axons suggest possible mechanisms by which vesicles are released from synapses. Discrete packet-like movement indicates that clusters of both recycling and non-recycling vesicles can shed from the synapse *en masse*, while evidence of individual vesicles in axonal regions would suggest that single vesicles are also released from vesicle clusters (Figure 5.8b). This may mean that the links between vesicles vary in strength and number, such that at times a group of tightly associated vesicles may be attached to

the rest of the cluster by relatively weak links and would therefore be prone to detaching from the cluster as a group.

Chapter 6 | Concluding Remarks

The classical view of synapses as self-sustaining, autonomous units was established by the ultrastructural studies of frog neuromuscular junctions (Ceccarelli et al., 1973; Heuser and Reese, 1973). The research in this thesis applies multiple vesicle labelling and imaging techniques to highlight a non-classical aspect of synaptic activity by describing the dynamic nature of presynaptic vesicle clusters at mature synapses in established small neuronal networks. The results demonstrate the role of presynaptic vesicle clusters in the inter-synaptic movement of vesicles in hippocampal neurons at both the light and electron microscopy level. Mobile recycling pool vesicles appear to be actively transported bi-directionally along axons and can become both functionally and spatially integrated into non-native synaptic vesicle clusters.

Time-lapse imaging of FM4-64 labelled neuronal cultures revealed the movement of fluorescence material along axons (Figure 3.2). However, as fluorescent packets regularly encountered stable, fluorescently labelled synapses it was difficult to reliably track their movement against this background of similar fluorescence. It was not clear if, when a fluorescent packet encountered a labelled synaptic cluster whether a certain proportion of the packet remained at the synapse or if some of the fluorescently labelled vesicles already there became mobilized and joined the moving packet. A novel approach to differentiate individual or subsets of boutons within cultures was needed to help determine the effects of vesicle mobility on synaptic vesicle clusters. At first, the local loading of a small group of synapses was attempted, so as the egress of fluorescence from this region into unlabelled areas might be recorded. In these experiments FM dyes were applied locally from a puff pipette onto individual processes while the cultures were stimulated by either field potentials or a hyperkalemic solution contained in the puff pipette, as described previously ((Liu and Tsien, 1995). While boutons could be labelled in this way, it was not possible to establish clear boundaries between the labelled and unlabelled areas, as the FM dye had a tendency to diffuse away from the pipette tip and along

the membrane to weakly label boutons other than those targeted. As an alternative way of producing clear boundaries between labelled and unlabelled areas a photobleach method was used. In this way all of the synapses within the culture were labelled and individual boutons photobleached so as the movement of fluorescence into the target bouton could be recorded. This method, in combination with postsynaptic labelling protocols, proved to be a satisfactory way to establish that mobile recycling pool vesicles could become integrated into mature synapses (Figure 3.5). Photobleaching has been used previously to increase the signal-to-noise ratio in fluorescence experiments, such as in the case of synaptopHluorin, where it permitted individual release events to be monitored (Gandhi and Stevens, 2003). Similarly, in this current study, photobleaching was used to track the movement of small fluorescent packets out of and between boutons. Kymograph plots of photobleached inter-bouton regions revealed how individual packets, seen as continuous diagonal lines through the plot, moved along axons at different rates, which correlated with the slope of these lines (Figure 3.7). The ability of styryl dyes to change their fluorescence as they rapidly and reversibly associate with membranes has been used extensively to examine synaptic vesicle exocytosis (Cochilla et al., 1999; Kavalali, 2006). In this thesis, these properties were used to label the recycling pool of synapses and to study the functionality of mobile vesicles within neurons. The FRAP signal at target boutons destained upon stimulation at a similar rate to surrounding non-photobleached boutons (Figure 3.9). This result demonstrates that mobilized recycling pool vesicles retain their functional capacity to undergo exocytosis and as such contribute to the recycling pool of non-native synapses (Figure 3.9).

Previously the axonal transport of synaptic vesicle clusters has been considered with respect to mechanisms of presynaptic assembly in developing and mature neurons. The recruitment of tubulovesicular transport packets to presynaptic sites of axo-dendritic contact has been observed in what are thought to be the early stages of synaptogenesis in hippocampal neurons (Ahmari et al., 2000). Vesicle recycling and synaptic vesicles themselves have been identified in immature

neuronal processes (Matteoli et al., 1992; Sun and Poo, 1987). While neurotransmitter release is believed to play a role in axon guidance (Zheng et al., 1994), these sometimes mobile vesicles are also thought to function in synapse formation (Kraszewski et al., 1995; Matteoli et al., 2004). In more mature neurons the movement of synaptic vesicles has been linked to the rapid formation of new synapses (Krueger et al., 2003). The findings described in this thesis demonstrate that aside from the potential use of mobile synaptic vesicle clusters in nascent synapse formation, a significant proportion of functional vesicles are exchanged between mature synapses.

The constitutive sharing of the recycling pool between boutons would extend the functional range of the synaptic vesicle cycle beyond individual synapses and could provide a mechanism whereby synaptic properties are shared amongst neighbouring synapses. The movements of synaptic components described here, may be involved in the modification of synaptic strengths seen in response to concurrent pre- and postsynaptic activation, such as during LTP or LTD. Whereas changes are thought to be largely restricted to synapses directly involved in the correlated activity (Gustafsson et al., 1987; Kandel and O'Dell, 1992; Stent, 1973), evidence suggests that neighbouring synapses, inactive during the conditioning stimulus could also be affected by the activity (Murthy, 1997). The presynaptic spread of LTP has been reported in cultured hippocampal slices (Bonhoeffer et al., 1989). While a more recent report indicates that LTP in hippocampal slices is generated and expressed postsynaptically (Engert and Bonhoeffer, 1997), the postsynaptic generation of diffusible messengers, may act either pre- or postsynaptically to facilitate the spread of LTP (Schuman and Madison, 1994). If the mobile vesicles and their associated proteins retained their functional identity by the preservation of the protein composition of vesicles, such as the existing protein-protein interactions or phosphorylation states. This could in turn affect the synapse into which they become incorporated, and as such, facilitate the presynaptic spread of functional changes during synaptic plasticity.

While the mobilization of vesicles between release sites may mediate some aspect of the spreading of synaptic strength, these movements could also provide a basis for the observed similarity in the release probabilities of neighbouring release sites in hippocampal neurons under basal conditions (Murthy et al., 1997). The mechanism of vesicle sharing described here could enable neurons to redistribute synaptic weights across multiple release sites, by a mechanism similar to that discussed above, so as to allow the coordinated regulation of neighbouring recycling pools.

The fluorescence flux observed at individual boutons (Figure 3.2c) would imply that a given bouton can approximately maintain the size of its vesicle pool over time, presumably because departing vesicles are replaced in a non-correlated way by newly arriving ones. A number of studies have demonstrated the relationship between presynaptic function and synaptic vesicle pools. The size of the recycling pool at synapses can be homeostatically regulated in response to overall levels of excitability (Murthy et al., 2001). A compensatory rise in the size of the recycling pool of synapses was seen in hippocampal cultures following a chronic treatment with tetrodotoxin which decreased the over all excitability of the system (Murthy et al., 2001). The size of the readily releasable pool has been correlated with release probability in hippocampal neurons, with larger RRPs corresponding to increased release probability (Murthy et al., 1997). Furthermore, modulation in the size of the RRP by phorbol esters has suggested that this may be a possible target for the expression of changes related to long-term synaptic plasticity (Stevens and Sullivan, 1998). At individual hippocampal synapses, a change in the relationship between the incorporation or release of vesicles could be a means by which neurons rapidly change the size of synaptic vesicle pools. This would suggest another possible role for the vesicle sharing phenomenon in synaptic plasticity, distinct from the distribution of synaptic properties discussed above. An increase in the size of the presynaptic vesicle pools, following the local generation of retrograde signals during the postsynaptic induction of long-term potentiation, could result in the selective augmentation of synaptic efficacy. The source of these newly recruited vesicles is of interest. If potentiated synapses were to acquire vesicles locally, then

this could have an adverse effect on the signalling strength of the neighbouring synapses and result in a negative correlation between neighbouring release probabilities, counter to the similarities seen previously in basal state neurons (Murthy et al., 1997). However, this effect would be lessened if the vesicles were available from synapses outside of the immediate vicinity. In conditions that induced long-lasting depression vesicle, shedding might be favoured over incorporation and as a result reduce the vesicle cluster size. Support for this idea comes from a study in developing neurons where a depressive stimulus lead to an NMDA-dependent reduction in synaptic efficacy that was matched by the dismantling of FM1-43 positive boutons (Hopf et al., 2002).

The bi-directional transport of synaptic components in axons is most probably mediated by the actions of multiple motor proteins. The kinesin motor protein KIF1a has been implicated in the movement of synaptic vesicle precursor organelles in developing systems (Okada et al., 1995; Yonekawa et al., 1998). In hippocampal neurons, a fluorescently tagged version of the protein exhibited both anterograde and retrograde movement along axons (Lee et al., 2003) and is a likely candidate for mediating the observed anterograde movement of vesicles in the current study. The bi-directional nature of the movement is thought to arise from the antagonistic actions of plus and minus-end directed motors simultaneously associated with the cargo. The reported association between KIF1a and cytoplasmic dynein in a yeast-two-hybrid screen lends further support to this idea of cooperative switching between co-localized motors to achieve bi-directional axonal transport (Ligon et al., 2004).

The ability to study the same synapses by both light and electron microscopy, combined with the photoconversion of FM-fluorescence signals to a stable electron dense material allowed vesicles that had been through a round of exo-endocytosis to be identified at the EM level (Figure 4.3). Previously these techniques have been used to examine the size of the recycling pool of hippocampal neurons (Harata et al., 2001b) or the localization of the readily releasable pool (Schikorski and Stevens, 2001). In this current study, the spatial arrangement of the entire recycling pool

within presynaptic terminals was considered for the first time. The proportion of recycling and non-recycling vesicles was measured in different regions of the vesicle cluster in a manner similar to that used previously at the frog NMJ (Rizzoli and Betz, 2004). In addition, the distance of all vesicles to the active zone was measured, so as to compare the distribution of recycling and non-recycling vesicles within synapses. Both methods of analysis revealed similar results, with the recycling pool of vesicles found to distribute throughout the vesicle cluster with a small tendency to be located closer to the active zone. A comparable skew in the distribution of the RRP at hippocampal synapses has been noted previously (Schikorski and Stevens, 2001). In a study of frog NMJ, the RRP exhibited no preference for any location within the synapse (Rizzoli and Betz, 2004), while at the *Drosophila* NMJ, a reluctantly releasable portion of the recycling pool termed the reserve pool was localized to the core of the synapse (Kuromi and Kidokoro, 1998). The correlation between the spatial location of vesicles and their functionality is apparently dependent on the synapse and the particular pool studied. At hippocampal synapses the recycling pool does not display a strong preference for any location within the cluster. It is therefore possible that vesicles belong to a particular functional pool because of differences in their mobility within the cluster, which in turn, define their participation in release events. A heterogeneity in the molecular composition of the vesicles within synapses might underlie these differences and could explain the lack of spatial definition of the recycling pool at hippocampal synapses.

Describing the departure of vesicles from mature synapses was an important test of the vesicle sharing hypothesis. By combining the techniques of FM dye labelling with the photobleaching of axonal regions and electron microscopy, the source of the fluorescence recovery observed previously (see Figure 3.5) was studied. In developing neurons synaptic vesicle-precursor organelles travel along axons (Nakata et al., 1998) and in some cases may only mature at synapses (Hannah et al., 1999). It was possible that mobilized endosomal organelles produced during vesicle cycling, may have constituted the observed fluorescence recovery. However, the

fluorescent transport packages observed moving between synapses (Figure 3.2) were confirmed to be clusters of vesicles originating from both the recycling and resting pool of synapses (Figure 5.3).

The re-identification of photobleached boutons, fixed after a period of recovery, by electron microscopy allowed the ultrastructural examination of vesicle incorporation. The recovery monitored in electron microscopy correlated to that observed by fluorescence imaging. By allowing for the differences in the recovery period used for both experiments (560 s for fluorescence versus 1080 s for EM) and the non-specific axonal recovery of fluorescence measurements (~10%), the estimate from EM studies that imported vesicles constitute ~18% of the recycling pool at synapses would agree with the ~20% recovery in FM4-64 fluorescence. However, the fluorescence recovery at boutons could be influenced by both non-localized axonal recovery as well as the effect of imaging-related photobleaching, making an accurate assessment of the extent of vesicle incorporation difficult. To avoid such issues, ultrastructural analysis was the preferred method for quantifying the number of vesicles incorporated over time (Figure 5.4).

The non-static nature of resting vesicle clusters was highlighted by the ability of incorporated vesicles to mix with native vesicles. However, the arrival of large packets of vesicles, made up of both PC+ and PC- vesicles, at the host synapse could give the impression of mixing without the actual assimilation of non-native vesicles into the host vesicle cluster. The assumption that imported vesicles can move within synapses is supported by the following observations: the presence of non-native vesicles in most regions of the vesicle cluster, including close to the active zone (Figure 5.6), the occurrence of non-packet based movement (Figure 5.8) and recent reports of vesicle movements within synapses (Jordan et al., 2005; Shtrahman et al., 2005). Taken together these findings would suggest that imported vesicles can move within synapses.

The results in this thesis define the inter-bouton movement of synaptic vesicles between mature synapses in cultured hippocampal neurons. These findings suggest

that the vesicle cycle is not restricted to individual synapses as previously believed, but is in fact spread across many synapses, with recycling pool vesicles being transported between, and used by, multiple release sites. While vesicle movement was observed in organotypic hippocampal slices, it was not possible to study this phenomenon in acute slices due to an inability to remove FM dye from the extracellular membrane. The expression of fluorescently labelled synaptic vesicle proteins by the use of viral vectors, biolistic gene transfer or transgenic mice, might allow the study of inter-bouton vesicle movements in acute slice preparations or *in vivo* by multi-photon imaging. The range over which vesicles are distributed between synapses by the sharing mechanism described here was not investigated. While the local loading of FM dyes might allow vesicle movements out of labelled regions to be followed over longer distances, the problems of dye diffusion discussed previously makes this technique less promising. Labelling synaptic vesicle proteins with a photoswitchable fluorophore, such a Kaede, whose emission changes from green to red following illumination with light in the UV range (Ando et al., 2002), provides a potential alternative means for studying vesicle movement. In this way, the vesicles at individual boutons could be photoswitched and the movement of their red fluorescence along axons and into other synapses, identified by the green fluorescence, could be tracked. This technique should allow the extent and range to which vesicles from one synapse are distributed amongst other boutons to be assessed. Finally, as discussed above, the mobility of vesicles in neurons highlights a potential mechanism by which activated synapses could rapidly recruit or donate recycling pool vesicles so as to dynamically modulate presynaptic release properties. Selective potentiation or de-potentiation of individual synapses, possibly by the local uncaging of glutamate (Matsuzaki et al., 2004), should permit testing of these hypotheses in future experiments.

Bibliography

Ahmari, S.E., J. Buchanan, and S.J. Smith. 2000. Assembly of presynaptic active zones from cytoplasmic transport packets. *Nat Neurosci.* 3:445-51.

Ahnert-Hilger, G., M. Holtje, I. Pahner, S. Winter, and I. Brunk. 2003. Regulation of vesicular neurotransmitter transporters. *Rev Physiol Biochem Pharmacol.* 150:140-60.

Alberts, B. 2002. Molecular biology of the cell. Garland Science, New York. xxxiv, 1463, [86] pp.

Altrock, W.D., S. tom Dieck, M. Sokolov, A.C. Meyer, A. Sigler, C. Brakebusch, R. Fassler, K. Richter, T.M. Boeckers, H. Potschka, C. Brandt, W. Loscher, D. Grimberg, T. Dresbach, A. Hempelmann, H. Hassan, D. Balschun, J.U. Frey, J.H. Brandstatter, C.C. Garner, C. Rosenmund, and E.D. Gundelfinger. 2003. Functional inactivation of a fraction of excitatory synapses in mice deficient for the active zone protein bassoon. *Neuron.* 37:787-800.

Amaral, D.G., and J.A. Dent. 1981. Development of the mossy fibers of the dentate gyrus: I. A light and electron microscopic study of the mossy fibers and their expansions. *J Comp Neurol.* 195:51-86.

Ando, R., H. Hama, M. Yamamoto-Hino, H. Mizuno, and A. Miyawaki. 2002. An optical marker based on the UV-induced green-to-red photoconversion of a fluorescent protein. *Proc Natl Acad Sci U S A.* 99:12651-6.

Aravanis, A.M., J.L. Pyle, and R.W. Tsien. 2003. Single synaptic vesicles fusing transiently and successively without loss of identity. *Nature.* 423:643-7.

Augustin, I., A. Betz, C. Herrmann, T. Jo, and N. Brose. 1999a. Differential expression of two novel Munc13 proteins in rat brain. *Biochem J.* 337 :363-71.

Augustin, I., C. Rosenmund, T.C. Sudhof, and N. Brose. 1999b. Munc13-1 is essential for fusion competence of glutamatergic synaptic vesicles. *Nature.* 400:457-61.

Baas, P.W., and D.W. Buster. 2004. Slow axonal transport and the genesis of neuronal morphology. *J Neurobiol.* 58:3-17.

Baas, P.W., J.S. Deitch, M.M. Black, and G.A. Banker. 1988. Polarity orientation of microtubules in hippocampal neurons: uniformity in the axon and nonuniformity in the dendrite. *Proc Natl Acad Sci U S A.* 85:8335-9.

Bamji, S.X., K. Shimazu, N. Kimes, J. Huelsken, W. Birchmeier, B. Lu, and L.F. Reichardt. 2003. Role of beta-catenin in synaptic vesicle localization and presynaptic assembly. *Neuron.* 40:719-31.

Bearer, E.L., and T.S. Reese. 1999. Association of actin filaments with axonal microtubule tracts. *J Neurocytol.* 28:85-98.

Becherer, U., C. Guatimosim, and W. Betz. 2001. Effects of staurosporine on exocytosis and endocytosis at frog motor nerve terminals. *J Neurosci.* 21:782-7.

Bellen, H.J. 1999. Neurotransmitter release. Oxford University Press, Oxford; New York. xviii, 437 p., [2] p. of plates pp.

Bennett, M.K., and R.H. Scheller. 1993. The molecular machinery for secretion is conserved from yeast to neurons. *Proc Natl Acad Sci U S A.* 90:2559-63.

Betz, A., U. Ashery, M. Rickmann, I. Augustin, E. Neher, T.C. Sudhof, J. Rettig, and N. Brose. 1998. Munc13-1 is a presynaptic phorbol ester receptor that enhances neurotransmitter release. *Neuron.* 21:123-36.

Betz, A., P. Thakur, H.J. Junge, U. Ashery, J.S. Rhee, V. Scheuss, C. Rosenmund, J. Rettig, and N. Brose. 2001. Functional interaction of the active zone proteins Munc13-1 and RIM1 in synaptic vesicle priming. *Neuron.* 30:183-96.

Betz, W.J., and A.W. Henkel. 1994. Okadaic acid disrupts clusters of synaptic vesicles in frog motor nerve terminals. *J Cell Biol.* 124:843-54.

Biederer, T., Y. Sara, M. Mozhayeva, D. Atasoy, X. Liu, E.T. Kavalali, and T.C. Sudhof. 2002. SynCAM, a synaptic adhesion molecule that drives synapse assembly. *Science.* 297:1525-31.

Biederer, T., and T.C. Sudhof. 2000. Mints as Adaptors. DIRECT BINDING TO NEUREXINS AND RECRUITMENT OF Munc18. *J. Biol. Chem.* 275:39803-39806.

Biederer, T., and T.C. Sudhof. 2001. CASK and Protein 4.1 Support F-actin Nucleation on Neurexins. *J. Biol. Chem.* 276:47869-47876.

Bloom, O., E. Evergren, N. Tomilin, O. Kjaerulff, P. Low, L. Brodin, V.A. Pieribone, P. Greengard, and O. Shupliakov. 2003. Colocalization of synapsin and actin during synaptic vesicle recycling. *J. Cell Biol.* 161:737-747.

Bodian, D. 1966. Electron microscopy: two major synaptic types on spinal motoneurons. *Science.* 151:1093-4.

Bonhoeffer, T., V. Staiger, and A. Aertsen. 1989. Synaptic plasticity in rat hippocampal slice cultures: local "Hebbian" conjunction of pre- and postsynaptic stimulation leads to distributed synaptic enhancement. *Proc Natl Acad Sci U S A.* 86:8113-7.

Bradke, F., and C.G. Dotti. 2000. Establishment of neuronal polarity: lessons from cultured hippocampal neurons. *Curr Opin Neurobiol.* 10:574-81.

Brady, S.T., R.J. Lasek, R.D. Allen, H.L. Yin, and T.P. Stossel. 1984. Gelsolin inhibition of fast axonal transport indicates a requirement for actin microfilaments. *Nature.* 310:56-8.

Bresler, T., M. Shapira, T. Boeckers, T. Dresbach, M. Futter, C.C. Garner, K. Rosenblum, E.D. Gundelfinger, and N.E. Ziv. 2004. Postsynaptic density assembly is fundamentally different from presynaptic active zone assembly. *J Neurosci.* 24:1507-20.

Bridgman, P.C. 2004. Myosin-dependent transport in neurons. *J Neurobiol.* 58:164-74.

Brodsky, F.M., C.Y. Chen, C. Knuehl, M.C. Towler, and D.E. Wakeham. 2001. Biological basket weaving: formation and function of clathrin-coated vesicles. *Annu Rev Cell Dev Biol.* 17:517-68.

Brose, N., C. Rosenmund, and J. Rettig. 2000. Regulation of transmitter release by Unc-13 and its homologues. *Curr Opin Neurobiol.* 10:303-11.

Brown, A. 2000. Slow axonal transport: stop and go traffic in the axon. *Nat Rev Mol Cell Biol.* 1:153-6.

Brown, A. 2003. Axonal transport of membranous and nonmembranous cargoes: a unified perspective. *J Cell Biol.* 160:817-21.

Brown, S.S. 1999. Cooperation between microtubule- and actin-based motor proteins. *Annu Rev Cell Dev Biol.* 15:63-80.

Brumback, A.C., J.L. Lieber, J.K. Angleson, and W.J. Betz. 2004. Using FM1-43 to study neuropeptide granule dynamics and exocytosis. *Methods*. 33:287-94.

Butz, S., M. Okamoto, and T.C. Sudhof. 1998. A tripartite protein complex with the potential to couple synaptic vesicle exocytosis to cell adhesion in brain. *Cell*. 94:773-82.

Calakos, N., and R.H. Scheller. 1994. Vesicle-associated membrane protein and synaptophysin are associated on the synaptic vesicle. *J Biol Chem*. 269:24534-7.

Castillo, P.E., R. Janz, T.C. Sudhof, T. Tzounopoulos, R.C. Malenka, and R.A. Nicoll. 1997. Rab3A is essential for mossy fibre long-term potentiation in the hippocampus. *Nature*. 388:590-3.

Catterall, W.A. 2000. Structure and regulation of voltage-gated Ca2+ channels. *Annu Rev Cell Dev Biol*. 16:521-55.

Ceccarelli, B., W.P. Hurlbut, and A. Mauro. 1973. Turnover of transmitter and synaptic vesicles at the frog neuromuscular junction. *J Cell Biol*. 57:499-524.

Chan, C.-S., E.J. Weeber, S. Kurup, J.D. Sweatt, and R.L. Davis. 2003. Integrin Requirement for Hippocampal Synaptic Plasticity and Spatial Memory. *J. Neurosci.* 23:7107-7116.

Chan, C.-S., E.J. Weeber, L. Zong, E. Fuchs, J.D. Sweatt, and R.L. Davis. 2006. {beta}1-Integrins Are Required for Hippocampal AMPA Receptor-Dependent Synaptic Transmission, Synaptic Plasticity, and Working Memory. *J. Neurosc* 26:223-232.

Chapman, E.R., P.I. Hanson, S. An, and R. Jahn. 1995. Ca2+ regulates the interaction between synaptotagmin and syntaxin 1. *J Biol Chem*. 270:23667-71.

Chavis, P., and G. Westbrook. 2001. Integrins mediate functional pre- and postsynaptic maturation at a hippocampal synapse. *Nature*. 411:317-21.

Chi, P., P. Greengard, and T.A. Ryan. 2001. Synapsin dispersion and reclustering during synaptic activity. *Nat Neurosci*. 4:1187-93.

Chi, P., P. Greengard, and T.A. Ryan. 2003. Synaptic vesicle mobilization is regulated by distinct synapsin I phosphorylation pathways at different frequencies. *Neuron*. 38:69-78.

Chung, S.H., G. Joberty, E.A. Gelino, I.G. Macara, and R.W. Holz. 1999. Comparison of the effects on secretion in chromaffin and PC12 cells of Rab3 family members and mutants. Evidence that inhibitory effects are independent of direct interaction with Rabphilin3. *J Biol Chem.* 274:18113-20.

Cline, H. 2005. Synaptogenesis: a balancing act between excitation and inhibition. *Curr Biol.* 15:R203-5.

Cochilla, A.J., J.K. Angleson, and W.J. Betz. 1999. Monitoring secretory membrane with FM1-43 fluorescence. *Annu Rev Neurosci.* 22:1-10.

Colicos, M.A., B.E. Collins, M.J. Sailor, and Y. Goda. 2001. Remodeling of synaptic actin induced by photoconductive stimulation. *Cell.* 107:605-16.

Cowan, W.M., T.C. S©*dhof, C.F. Stevens, and Howard Hughes Medical Institute. 2001. Synapses. Johns Hopkins University Press, Baltimore. xiii, 767 pp.

Craig, A.M., and G. Banker. 1994. Neuronal polarity. *Annu Rev Neurosci.* 17:267-310.

Cremona, O., G. Di Paolo, M.R. Wenk, A. Luthi, W.T. Kim, K. Takei, L. Daniell, Y. Nemoto, S.B. Shears, R.A. Flavell, D.A. McCormick, and P. De Camilli. 1999. Essential role of phosphoinositide metabolism in synaptic vesicle recycling. *Cell.* 99:179-88.

Custer, K.L., N.S. Austin, J.M. Sullivan, and S.M. Bajjalieh. 2006. Synaptic vesicle protein 2 enhances release probability at quiescent synapses. *J Neurosci.* 26:1303-13.

Dai, Z., and H.B. Peng. 1996. Dynamics of synaptic vesicles in cultured spinal cord neurons in relationship to synaptogenesis. *Mol Cell Neurosci.* 7:443-52.

Darchen, F., and B. Goud. 2000. Multiple aspects of Rab protein action in the secretory pathway: focus on Rab3 and Rab6. *Biochimie.* 82:375-84.

De-Miguel, F.F., and C. Trueta. 2005. Synaptic and extrasynaptic secretion of serotonin. *Cell Mol Neurobiol.* 25:297-312.

De Camilli, P., and K. Takei. 1996. Molecular mechanisms in synaptic vesicle endocytosis and recycling. *Neuron.* 16:481-6.

De Paola, V., S. Arber, and P. Caroni. 2003. AMPA receptors regulate dynamic equilibrium of presynaptic terminals in mature hippocampal networks. *Nat Neurosci.* 6:491-500.

De Robertis, E.D., and H.S. Bennett. 1955. Some features of the submicroscopic morphology of synapses in frog and earthworm. *J Biophys Biochem Cytol.* 1:47-58.

Deacon, S.W., A.S. Serpinskaya, P.S. Vaughan, M. Lopez Fanarraga, I. Vernos, K.T. Vaughan, and V.I. Gelfand. 2003. Dynactin is required for bidirectional organelle transport. *J Cell Biol.* 160:297-301.

Desai, A., and T.J. Mitchison. 1997. Microtubule polymerization dynamics. *Annu Rev Cell Dev Biol.* 13:83-117.

Dickman, D.K., J.A. Horne, I.A. Meinertzhagen, and T.L. Schwarz. 2005. A slowed classical pathway rather than kiss-and-run mediates endocytosis at synapses lacking synaptojanin and endophilin. *Cell.* 123:521-33.

Dillon, C., and Y. Goda. 2005. The actin cytoskeleton: integrating form and function at the synapse. *Annu Rev Neurosci.* 28:25-55.

dos Remedios, C.G., D. Chhabra, M. Kekic, I.V. Dedova, M. Tsubakihara, D.A. Berry, and N.J. Nosworthy. 2003. Actin binding proteins: regulation of cytoskeletal microfilaments. *Physiol Rev.* 83:433-73.

Dotti, C.G., C.A. Sullivan, and G.A. Banker. 1988. The establishment of polarity by hippocampal neurons in culture. *J Neurosci.* 8:1454-68.

Dresbach, T., A. Hempelmann, C. Spilker, S. tom Dieck, W.D. Altrock, W. Zuschratter, C.C. Garner, and E.D. Gundelfinger. 2003. Functional regions of the presynaptic cytomatrix protein bassoon: significance for synaptic targeting and cytomatrix anchoring. *Mol Cell Neurosci.* 23:279-91.

Dresbach, T., B. Qualmann, M.M. Kessels, C.C. Garner, and E.D. Gundelfinger. 2001. The presynaptic cytomatrix of brain synapses. *Cell Mol Life Sci.* 58:94-116.

Dunaevsky, A., and E.A. Connor. 2000. F-actin is concentrated in nonrelease domains at frog neuromuscular junctions. *J Neurosci.* 20:6007-12.

Eccles, J.C. 1982. The synapse: from electrical to chemical transmission. *Annu Rev Neurosci.* 5:325-39.

Edelmann, L., P.I. Hanson, E.R. Chapman, and R. Jahn. 1995. Synaptobrevin binding to synaptophysin: a potential mechanism for controlling the exocytotic fusion machine. *Embo J.* 14:224-31.

Elmqvist, D., and D.M. Quastel. 1965. A quantitative study of end-plate potentials in isolated human muscle. *J Physiol.* 178:505-29.

Engert, F., and T. Bonhoeffer. 1997. Synapse specificity of long-term potentiation breaks down at short distances. *Nature.* 388:279-84.

Fenster, S.D., W.J. Chung, R. Zhai, C. Cases-Langhoff, B. Voss, A.M. Garner, U. Kaempf, S. Kindler, E.D. Gundelfinger, and C.C. Garner. 2000. Piccolo, a presynaptic zinc finger protein structurally related to bassoon. *Neuron.* 25:203-14.

Fernandez-Alfonso, T., and T.A. Ryan. 2004. The kinetics of synaptic vesicle pool depletion at CNS synaptic terminals. *Neuron.* 41:943-53.

Fesce, R., F. Grohovaz, F. Valtorta, and J. Meldolesi. 1994. Neurotransmitter release: fusion or 'kiss-and-run'? *Trends Cell Biol.* 4:1-4.

Fischer von Mollard, G., T.C. Sudhof, and R. Jahn. 1991. A small GTP-binding protein dissociates from synaptic vesicles during exocytosis. *Nature.* 349:79-81.

Flanagan, J.G., and P. Vanderhaeghen. 1998. The ephrins and Eph receptors in neural development. *Annu Rev Neurosci.* 21:309-45.

Friedman, H.V., T. Bresler, C.C. Garner, and N.E. Ziv. 2000. Assembly of new individual excitatory synapses: time course and temporal order of synaptic molecule recruitment. *Neuron.* 27:57-69.

Gahwiler, B.H., M. Capogna, D. Debanne, R.A. McKinney, and S.M. Thompson. 1997. Organotypic slice cultures: a technique has come of age. *Trends Neurosci.* 20:471-7.

Galli, T., P.S. McPherson, and P. De Camilli. 1996. The V0 sector of the V-ATPase, synaptobrevin, and synaptophysin are associated on synaptic vesicles in a Triton X-100-resistant, freeze-thawing sensitive, complex. *J Biol Chem.* 271:2193-8.

Gandhi, S.P., and C.F. Stevens. 2003. Three modes of synaptic vesicular recycling revealed by single-vesicle imaging. *Nature.* 423:607-13.

Garner, C.C., R.G. Zhai, E.D. Gundelfinger, and N.E. Ziv. 2002. Molecular mechanisms of CNS synaptogenesis. *Trends Neurosci.* 25:243-51.

Geppert, M., Y. Goda, R.E. Hammer, C. Li, T.W. Rosahl, C.F. Stevens, and T.C. Sudhof. 1994. Synaptotagmin I: a major Ca2+ sensor for transmitter release at a central synapse. *Cell.* 79:717-27.

Gerrow, K., S. Romorini, S.M. Nabi, M.A. Colicos, C. Sala, and A. El-Husseini. 2006. A preformed complex of postsynaptic proteins is involved in excitatory synapse development. *Neuron*. 49:547-62.

Ginsberg, M.H., A. Partridge, and S.J. Shattil. 2005. Integrin regulation. *Curr Opin Cell Biol*. 17:509-16.

Gitler, D., Y. Takagishi, J. Feng, Y. Ren, R.M. Rodriguiz, W.C. Wetsel, P. Greengard, and G.J. Augustine. 2004. Different presynaptic roles of synapsins at excitatory and inhibitory synapses. *J Neurosci*. 24:11368-80.

Glickstein, M. 2006. Golgi and Cajal: The neuron doctrine and the 100th anniversary of the 1906 Nobel Prize. *Curr Biol*. 16:R147-51.

Goda, Y., and G.W. Davis. 2003. Mechanisms of synapse assembly and disassembly. *Neuron*. 40:243-64.

Goldberg, D.J., D.A. Harris, B.W. Lubit, and J.H. Schwartz. 1980. Analysis of the mechanism of fast axonal transport by intracellular injection of potentially inhibitory macromolecules: evidence for a possible role of actin filaments. *Proc Natl Acad Sci U S A*. 77:7448-52.

Goldstein, L.S., and Z. Yang. 2000. Microtubule-based transport systems in neurons: the roles of kinesins and dyneins. *Annu Rev Neurosci*. 23:39-71.

Goode, B.L., D.G. Drubin, and G. Barnes. 2000. Functional cooperation between the microtubule and actin cytoskeletons. *Curr Opin Cell Biol*. 12:63-71.

Greengard, P., F. Valtorta, A.J. Czernik, and F. Benfenati. 1993. Synaptic vesicle phosphoproteins and regulation of synaptic function. *Science*. 259:780-5.

Grindstaff, K.K., C. Yeaman, N. Anandasabapathy, S.C. Hsu, E. Rodriguez-Boulan, R.H. Scheller, and W.J. Nelson. 1998. Sec6/8 complex is recruited to cell-cell contacts and specifies transport vesicle delivery to the basal-lateral membrane in epithelial cells. *Cell*. 93:731-40.

Gundelfinger, E.D., W. Altrock, and A. Fejtove. 2006. Encyclopedia of Neuroscience. Springer Verlag, Heidelberg.

Gustafsson, B., H. Wigstrom, W.C. Abraham, and Y.Y. Huang. 1987. Long-term potentiation in the hippocampus using depolarizing current pulses as the conditioning stimulus to single volley synaptic potentials. *J Neurosci*. 7:774-80.

Hamada, S., and T. Yagi. 2001. The cadherin-related neuronal receptor family: a novel diversified cadherin family at the synapse. *Neurosci Res.* 41:207-15.

Hannah, M.J., A.A. Schmidt, and W.B. Huttner. 1999. Synaptic vesicle biogenesis. *Annu Rev Cell Dev Biol.* 15:733-98.

Hanson, P.I., J.E. Heuser, and R. Jahn. 1997. Neurotransmitter release - four years of SNARE complexes. *Curr Opin Neurobiol.* 7:310-5.

Harata, N., J.L. Pyle, A.M. Aravanis, M. Mozhayeva, E.T. Kavalali, and R.W. Tsien. 2001a. Limited numbers of recycling vesicles in small CNS nerve terminals: implications for neural signaling and vesicular cycling. *Trends Neurosci.* 24:637-43.

Harata, N., T.A. Ryan, S.J. Smith, J. Buchanan, and R.W. Tsien. 2001b. Visualizing recycling synaptic vesicles in hippocampal neurons by FM 1-43 photoconversion. *Proc Natl Acad Sci U S A.* 98:12748-53.

Harata, N.C., S. Choi, J.L. Pyle, A.M. Aravanis, and R.W. Tsien. 2006. Frequency-dependent kinetics and prevalence of kiss-and-run and reuse at hippocampal synapses studied with novel quenching methods. *Neuron.* 49:243-56.

Harlow, M.L., D. Ress, A. Stoschek, R.M. Marshall, and U.J. McMahan. 2001. The architecture of active zone material at the frog's neuromuscular junction. *Nature.* 409:479-84.

Harris, K.M., and P. Sultan. 1995. Variation in the number, location and size of synaptic vesicles provides an anatomical basis for the nonuniform probability of release at hippocampal CA1 synapses. *Neuropharmacology.* 34:1387-95.

Hata, Y., S. Butz, and T.C. Sudhof. 1996. CASK: a novel dlg/PSD95 homolog with an N-terminal calmodulin-dependent protein kinase domain identified by interaction with neurexins. *J. Neurosci.* 16:2488-2494.

Hata, Y., C.A. Slaughter, and T.C. Sudhof. 1993. Synaptic vesicle fusion complex contains unc-18 homologue bound to syntaxin. *Nature.* 366:347-51.

Haucke, V., and P. De Camilli. 1999. AP-2 recruitment to synaptotagmin stimulated by tyrosine-based endocytic motifs. *Science.* 285:1268-71.

Henkel, A.W., J. Lubke, and W.J. Betz. 1996a. FM1-43 dye ultrastructural localization in and release from frog motor nerve terminals. *Proc Natl Acad Sci U S A.* 93:1918-23.

Henkel, A.W., L.L. Simpson, R.M. Ridge, and W.J. Betz. 1996b. Synaptic vesicle movements monitored by fluorescence recovery after photobleaching in nerve terminals stained with FM1-43. *J Neurosci.* 16:3960-7.

Henze, D.A., N.N. Urban, and G. Barrionuevo. 2000. The multifarious hippocampal mossy fiber pathway: a review. *Neuroscience.* 98:407-27.

Heuser, J.E., and T.S. Reese. 1973. Evidence for recycling of synaptic vesicle membrane during transmitter release at the frog neuromuscular junction. *J Cell Biol.* 57:315-44.

Hiesinger, P.R., A. Fayyazuddin, S.Q. Mehta, T. Rosenmund, K.L. Schulze, R.G. Zhai, P. Verstreken, Y. Cao, Y. Zhou, J. Kunz, and H.J. Bellen. 2005. The v-ATPase V0 subunit a1 is required for a late step in synaptic vesicle exocytosis in Drosophila. *Cell.* 121:607-20.

Hirokawa, N., K. Sobue, K. Kanda, A. Harada, and H. Yorifuji. 1989. The cytoskeletal architecture of the presynaptic terminal and molecular structure of synapsin 1. *J Cell Biol.* 108:111-26.

Hirokawa, N., and R. Takemura. 2004. Molecular motors in neuronal development, intracellular transport and diseases. *Curr Opin Neurobiol.* 14:564-73.

Hirokawa, N., and R. Takemura. 2005. Molecular motors and mechanisms of directional transport in neurons. *Nat Rev Neurosci.* 6:201-14.

Hiruma, H., T. Katakura, S. Takahashi, T. Ichikawa, and T. Kawakami. 2003. Glutamate and amyloid beta-protein rapidly inhibit fast axonal transport in cultured rat hippocampal neurons by different mechanisms. *J Neurosci.* 23:8967-77.

Hokfelt, T., O. Johansson, and M. Goldstein. 1984. Chemical anatomy of the brain. *Science.* 225:1326-34.

Hopf, F.W., J. Waters, S. Mehta, and S.J. Smith. 2002. Stability and plasticity of developing synapses in hippocampal neuronal cultures. *J Neurosci.* 22:775-81.

Huang, J.D., S.T. Brady, B.W. Richards, D. Stenolen, J.H. Resau, N.G. Copeland, and N.A. Jenkins. 1999. Direct interaction of microtubule- and actin-based transport motors. *Nature.* 397:267-70.

Hui, E., J. Bai, P. Wang, M. Sugimori, R.R. Llinas, and E.R. Chapman. 2005. Three distinct kinetic groupings of the synaptotagmin family: candidate sensors for rapid and delayed exocytosis. *Proc Natl Acad Sci U S A.* 102:5210-4.

Huttner, W.B., W. Schiebler, P. Greengard, and P. De Camilli. 1983. Synapsin I (protein I), a nerve terminal-specific phosphoprotein. III. Its association with synaptic vesicles studied in a highly purified synaptic vesicle preparation. *J Cell Biol.* 96:1374-88.

Jahn, R., T. Lang, and T.C. Sudhof. 2003. Membrane fusion. *Cell.* 112:519-33.

Jahn, R., and T.C. Sudhof. 1994. Synaptic vesicles and exocytosis. *Annu Rev Neurosci.* 17:219-46.

Janeway, C., P. Travers, M. Walport, and M. Shlomchik. 2001. Immunobiology 5: the immune system in health and disease. Garland Pub., New York. xviii, 732 pp.

Janz, R., Y. Goda, M. Geppert, M. Missler, and T.C. Sudhof. 1999. SV2A and SV2B function as redundant Ca2+ regulators in neurotransmitter release. *Neuron.* 24:1003-16.

Jockusch, W.J., G.J. Praefcke, H.T. McMahon, and L. Lagnado. 2005. Clathrin-dependent and clathrin-independent retrieval of synaptic vesicles in retinal bipolar cells. *Neuron.* 46:869-78.

Jones, L.S. 1996. Integrins: possible functions in the adult CNS. *Trends Neurosci.* 19:68-72.

Jordan, R., E.A. Lemke, and J. Klingauf. 2005. Visualization of synaptic vesicle movement in intact synaptic boutons using fluorescence fluctuation spectroscopy. *Biophys J.* 89:2091-102.

Kandel, E.R., and T.J. O'Dell. 1992. Are adult learning mechanisms also used for development? *Science.* 258:243-5.

Katz, B. 1969. The Release of Neural Transmitter Substances. Liverpool University Press, Liverpool.

Kavalali, E.T. 2006. Synaptic vesicle reuse and its implications. *Neuroscientist.* 12:57-66.

King, S.M. 2000. The dynein microtubule motor. *Biochim Biophys Acta.* 1496:60-75.

Klingauf, J., E.T. Kavalali, and R.W. Tsien. 1998. Kinetics and regulation of fast endocytosis at hippocampal synapses. *Nature*. 394:581-5.

Koenig, J.H., and K. Ikeda. 1989. Disappearance and reformation of synaptic vesicle membrane upon transmitter release observed under reversible blockage of membrane retrieval. *J Neurosci*. 9:3844-60.

Koenig, J.H., and K. Ikeda. 1996. Synaptic vesicles have two distinct recycling pathways. *J Cell Biol*. 135:797-808.

Kohmura, N., K. Senzaki, S. Hamada, N. Kai, R. Yasuda, M. Watanabe, H. Ishii, M. Yasuda, M. Mishina, and T. Yagi. 1998. Diversity revealed by a novel family of cadherins expressed in neurons at a synaptic complex. *Neuron*. 20:1137-51.

Koushika, S.P., J.E. Richmond, G. Hadwiger, R.M. Weimer, E.M. Jorgensen, and M.L. Nonet. 2001. A post-docking role for active zone protein Rim. *Nat Neurosci*. 4:997-1005.

Kramar, E.A., J.A. Bernard, C.M. Gall, and G. Lynch. 2003. Integrins Modulate Fast Excitatory Transmission at Hippocampal Synapses. *J. Biol. Chem.* 278:10722-10730.

Kraszewski, K., L. Daniell, O. Mundigl, and P. De Camilli. 1996. Mobility of synaptic vesicles in nerve endings monitored by recovery from photobleaching of synaptic vesicle-associated fluorescence. *J Neurosci*. 16:5905-13.

Kraszewski, K., O. Mundigl, L. Daniell, C. Verderio, M. Matteoli, and P. De Camilli. 1995. Synaptic vesicle dynamics in living cultured hippocampal neurons visualized with CY3-conjugated antibodies directed against the lumenal domain of synaptotagmin. *J Neurosci*. 15:4328-42.

Krueger, S.R., A. Kolar, and R.M. Fitzsimonds. 2003. The presynaptic release apparatus is functional in the absence of dendritic contact and highly mobile within isolated axons. *Neuron*. 40:945-57.

Kuromi, H., and Y. Kidokoro. 1998. Two distinct pools of synaptic vesicles in single presynaptic boutons in a temperature-sensitive Drosophila mutant, shibire. *Neuron*. 20:917-25.

Kuznetsov, S.A., G.M. Langford, and D.G. Weiss. 1992. Actin-dependent organelle movement in squid axoplasm. *Nature*. 356:722-5.

Lalli, G., S. Gschmeissner, and G. Schiavo. 2003. Myosin Va and microtubule-based motors are required for fast axonal retrograde transport of tetanus toxin in motor neurons. *J Cell Sci.* 116:4639-50.

Landis, D.M., A.K. Hall, L.A. Weinstein, and T.S. Reese. 1988. The organization of cytoplasm at the presynaptic active zone of a central nervous system synapse. *Neuron.* 1:201-9.

Langford, G.M. 2002. Myosin-V, a versatile motor for short-range vesicle transport. *Traffic.* 3:859-65.

Lasek, R.J., J.A. Garner, and S.T. Brady. 1984. Axonal transport of the cytoplasmic matrix. *J Cell Biol.* 99:212s-221s.

Lee, J.R., H. Shin, J. Ko, J. Choi, H. Lee, and E. Kim. 2003. Characterization of the movement of the kinesin motor KIF1A in living cultured neurons. *J Biol Chem.* 278:2624-9.

Lemke, E.A., and J. Klingauf. 2005. Single synaptic vesicle tracking in individual hippocampal boutons at rest and during synaptic activity. *J Neurosci.* 25:11034-44.

Li, C., B. Ullrich, J.Z. Zhang, R.G. Anderson, N. Brose, and T.C. Sudhof. 1995. Ca(2+)-dependent and -independent activities of neural and non-neural synaptotagmins. *Nature.* 375:594-9.

Li, Z., J. Burrone, W.J. Tyler, K.N. Hartman, D.F. Albeanu, and V.N. Murthy. 2005. Synaptic vesicle recycling studied in transgenic mice expressing synaptopHluorin. *Proc Natl Acad Sci U S A.* 102:6131-6.

Li, Z., and V.N. Murthy. 2001. Visualizing postendocytic traffic of synaptic vesicles at hippocampal synapses. *Neuron.* 31:593-605.

Ligon, L.A., M. Tokito, J.M. Finklestein, F.E. Grossman, and E.L. Holzbaur. 2004. A direct interaction between cytoplasmic dynein and kinesin I may coordinate motor activity. *J Biol Chem.* 279:19201-8.

Lim, S.S., K.J. Edson, P.C. Letourneau, and G.G. Borisy. 1990. A test of microtubule translocation during neurite elongation. *J. Cell Biol.* 111:123-130.

Lim, S.S., P.J. Sammak, and G.G. Borisy. 1989. Progressive and spatially differentiated stability of microtubules in developing neuronal cells. *J. Cell Biol.* 109:253-263.

Lin, R.C., and R.H. Scheller. 2000. Mechanisms of synaptic vesicle exocytosis. *Annu Rev Cell Dev Biol.* 16:19-49.

Lippman, J., and A. Dunaevsky. 2005. Dendritic spine morphogenesis and plasticity. *J Neurobiol.* 64:47-57.

Liu, G., and R.W. Tsien. 1995. Properties of synaptic transmission at single hippocampal synaptic boutons. *Nature.* 375:404-8.

Lou, X., V. Scheuss, and R. Schneggenburger. 2005. Allosteric modulation of the presynaptic Ca2+ sensor for vesicle fusion. *Nature.* 435:497-501.

Madison, J.M., S. Nurrish, and J.M. Kaplan. 2005. UNC-13 interaction with syntaxin is required for synaptic transmission. *Curr Biol.* 15:2236-42.

Malenka, R.C., D.V. Madison, and R.A. Nicoll. 1986. Potentiation of synaptic transmission in the hippocampus by phorbol esters. *Nature.* 321:175-7.

Malgaroli, A., A.E. Ting, B. Wendland, A. Bergamaschi, A. Villa, R.W. Tsien, and R.H. Scheller. 1995. Presynaptic component of long-term potentiation visualized at individual hippocampal synapses. *Science.* 268:1624-8.

Maranto, A.R. 1982. Neuronal mapping: a photooxidation reaction makes Lucifer yellow useful for electron microscopy. *Science.* 217:953-5.

Martin, T.F. 2002. Prime movers of synaptic vesicle exocytosis. *Neuron.* 34:9-12.

Maruyama, I.N., and S. Brenner. 1991. A phorbol ester/diacylglycerol-binding protein encoded by the unc-13 gene of Caenorhabditis elegans. *Proc Natl Acad Sci U S A.* 88:5729-33.

Marz, K.E., and P.I. Hanson. 2002. Sealed with a twist: complexin and the synaptic SNARE complex. *Trends Neurosci.* 25:381-3.

Matsuzaki, M., N. Honkura, G.C. Ellis-Davies, and H. Kasai. 2004. Structural basis of long-term potentiation in single dendritic spines. *Nature.* 429:761-6.

Matteoli, M., S. Coco, U. Schenk, and C. Verderio. 2004. Vesicle turnover in developing neurons: how to build a presynaptic terminal. *Trends Cell Biol.* 14:133-40.

Matteoli, M., K. Takei, M.S. Perin, T.C. Sudhof, and P. De Camilli. 1992. Exo-endocytotic recycling of synaptic vesicles in developing processes of cultured hippocampal neurons. *J Cell Biol.* 117:849-61.

Matthew, W.D., L. Tsavaler, and L.F. Reichardt. 1981. Identification of a synaptic vesicle-specific membrane protein with a wide distribution in neuronal and neurosecretory tissue. *J. Cell Biol. 257.* 91:257-269.

Maximov, A., and I. Bezprozvanny. 2002. Synaptic Targeting of N-Type Calcium Channels in Hippocampal Neurons. *J. Neurosci.* 22:6939-6952.

McCleskey, E.W., A.P. Fox, D.H. Feldman, L.J. Cruz, B.M. Olivera, R.W. Tsien, and D. Yoshikami. 1987. Omega-conotoxin: direct and persistent blockade of specific types of calcium channels in neurons but not muscle. *Proc Natl Acad Sci U S A.* 84:4327-31.

Megias, M., Z. Emri, T.F. Freund, and A.I. Gulyas. 2001. Total number and distribution of inhibitory and excitatory synapses on hippocampal CA1 pyramidal cells. *Neuroscience.* 102:527-40.

Micheva, K.D., and S.J. Smith. 2005. Strong effects of subphysiological temperature on the function and plasticity of mammalian presynaptic terminals. *J Neurosci.* 25:7481-8.

Miesenbock, G., D.A. De Angelis, and J.E. Rothman. 1998. Visualizing secretion and synaptic transmission with pH-sensitive green fluorescent proteins. *Nature.* 394:192-5.

Mintz, I.M., V.J. Venema, K.M. Swiderek, T.D. Lee, B.P. Bean, and M.E. Adams. 1992. P-type calcium channels blocked by the spider toxin omega-Aga-IVA. *Nature.* 355:827-9.

Morales, M., M.A. Colicos, and Y. Goda. 2000. Actin-dependent regulation of neurotransmitter release at central synapses. *Neuron.* 27:539-50.

Morel, N. 2003. Neurotransmitter release: the dark side of the vacuolar-H+ATPase. *Biol Cell.* 95:453-7.

Moulder, K.L., and S. Mennerick. 2006. Synaptic vesicles: turning reluctance into action. *Neuroscientist.* 12:11-5.

Mozhayeva, M.G., Y. Sara, X. Liu, and E.T. Kavalali. 2002. Development of vesicle pools during maturation of hippocampal synapses. *J Neurosci.* 22:654-65.

Murai, K.K., and E.B. Pasquale. 2004. Eph receptors, ephrins, and synaptic function. *Neuroscientist.* 10:304-14.

Murase, S., and E.M. Schuman. 1999. The role of cell adhesion molecules in synaptic plasticity and memory. *Curr Opin Cell Biol.* 11:549-53.

Murthy, M., D. Garza, R.H. Scheller, and T.L. Schwarz. 2003. Mutations in the exocyst component Sec5 disrupt neuronal membrane traffic, but neurotransmitter release persists. *Neuron.* 37:433-47.

Murthy, V.N. 1997. Synaptic plasticity: neighborhood influences. *Curr Biol.* 7:R512-5.

Murthy, V.N., and P. De Camilli. 2003. Cell biology of the presynaptic terminal. *Annu Rev Neurosci.* 26:701-28.

Murthy, V.N., T. Schikorski, C.F. Stevens, and Y. Zhu. 2001. Inactivity produces increases in neurotransmitter release and synapse size. *Neuron.* 32:673-82.

Murthy, V.N., T.J. Sejnowski, and C.F. Stevens. 1997. Heterogeneous release properties of visualized individual hippocampal synapses. *Neuron.* 18:599-612.

Murthy, V.N., and C.F. Stevens. 1998. Synaptic vesicles retain their identity through the endocytic cycle. *Nature.* 392:497-501.

Murthy, V.N., and C.F. Stevens. 1999. Reversal of synaptic vesicle docking at central synapses. *Nat Neurosci.* 2:503-7.

Nagafuchi, A., S. Ishihara, and S. Tsukita. 1994. The roles of catenins in the cadherin-mediated cell adhesion: functional analysis of E-cadherin-alpha catenin fusion molecules. *J Cell Biol.* 127:235-45.

Nagy, G., K. Reim, U. Matti, N. Brose, T. Binz, J. Rettig, E. Neher, and J.B. Sorensen. 2004. Regulation of releasable vesicle pool sizes by protein kinase A-dependent phosphorylation of SNAP-25. *Neuron.* 41:417-29.

Nakata, T., and N. Hirokawa. 2003. Microtubules provide directional cues for polarized axonal transport through interaction with kinesin motor head. *J. Cell Biol.* 162:1045-1055.

Nakata, T., S. Terada, and N. Hirokawa. 1998. Visualization of the dynamics of synaptic vesicle and plasma membrane proteins in living axons. *J Cell Biol.* 140:659-74.

Nascimento, A.A., J.T. Roland, and V.I. Gelfand. 2003. Pigment cells: a model for the study of organelle transport. *Annu Rev Cell Dev Biol.* 19:469-91.

Neher, E., and A. Marty. 1982. Discrete changes of cell membrane capacitance observed under conditions of enhanced secretion in bovine adrenal chromaffin cells. *Proc Natl Acad Sci U S A.* 79:6712-6.

Neves, G., and L. Lagnado. 1999. The kinetics of exocytosis and endocytosis in the synaptic terminal of goldfish retinal bipolar cells. *J Physiol.* 515 (Pt 1):181-202.

Nusbaum, M.P., D.M. Blitz, A.M. Swensen, D. Wood, and E. Marder. 2001. The roles of co-transmission in neural network modulation. *Trends Neurosci.* 24:146-54.

Okabe, S., and N. Hirokawa. 1992. Differential behavior of photoactivated microtubules in growing axons of mouse and frog neurons. *J. Cell Biol.* 117:105-120.

Okada, Y., H. Yamazaki, Y. Sekine-Aizawa, and N. Hirokawa. 1995. The neuron-specific kinesin superfamily protein KIF1A is a unique monomeric motor for anterograde axonal transport of synaptic vesicle precursors. *Cell.* 81:769-80.

Olsen, O., K.A. Moore, M. Fukata, T. Kazuta, J.C. Trinidad, F.W. Kauer, M. Streuli, H. Misawa, A.L. Burlingame, R.A. Nicoll, and D.S. Bredt. 2005. Neurotransmitter release regulated by a MALS-liprin-{alpha} presynaptic complex. *J. Cell Biol.* 170:1127-1134.

Ozawa, M., M. Ringwald, and R. Kemler. 1990. Uvomorulin-catenin complex formation is regulated by a specific domain in the cytoplasmic region of the cell adhesion molecule. *Proc Natl Acad Sci U S A.* 87:4246-50.

Palay, S.L. 1956. Synapses in the central nervous system. *J Biophys Biochem Cytol.* 2:193-202.

Palay, S.L., and G.E. Palade. 1955. The fine structure of neurons. *J Biophys Biochem Cytol.* 1:69-88.

Pennuto, M., D. Dunlap, A. Contestabile, F. Benfenati, and F. Valtorta. 2002. Fluorescence resonance energy transfer detection of synaptophysin I and vesicle-associated membrane protein 2 interactions during exocytosis from single live synapses. *Mol Biol Cell.* 13:2706-17.

Perin, M.S., V.A. Fried, G.A. Mignery, R. Jahn, and T.C. Sudhof. 1990. Phospholipid binding by a synaptic vesicle protein homologous to the regulatory region of protein kinase C. *Nature.* 345:260-3.

Peters, A., S.L. Palay, and H.d. Webster. 1991. The fine structure of the nervous system: neurons and their supporting cells. Oxford University Press, New York. xviii, 494 pp.

Pfenninger, K., K. Akert, H. Moor, and C. Sandri. 1972. The fine structure of freeze-fractured presynaptic membranes. *J Neurocytol.* 1:129-49.

Phillips, G.R., J.K. Huang, Y. Wang, H. Tanaka, L. Shapiro, W. Zhang, W.S. Shan, K. Arndt, M. Frank, R.E. Gordon, M.A. Gawinowicz, Y. Zhao, and D.R. Colman. 2001. The presynaptic particle web: ultrastructure, composition, dissolution, and reconstitution. *Neuron.* 32:63-77.

Pielage, J., R.D. Fetter, and G.W. Davis. 2005. Presynaptic spectrin is essential for synapse stabilization. *Curr Biol.* 15:918-28.

Pieribone, V.A., O. Shupliakov, L. Brodin, S. Hilfiker-Rothenfluh, A.J. Czernik, and P. Greengard. 1995. Distinct pools of synaptic vesicles in neurotransmitter release. *Nature.* 375:493-7.

Pyle, J.L., E.T. Kavalali, S. Choi, and R.W. Tsien. 1999. Visualization of synaptic activity in hippocampal slices with FM1-43 enabled by fluorescence quenching. *Neuron.* 24:803-8.

Pyle, J.L., E.T. Kavalali, E.S. Piedras-Renteria, and R.W. Tsien. 2000. Rapid reuse of readily releasable pool vesicles at hippocampal synapses. *Neuron.* 28:221-31.

Rao-Mirotznik, R., A.B. Harkins, G. Buchsbaum, and P. Sterling. 1995. Mammalian rod terminal: architecture of a binary synapse. *Neuron.* 14:561-9.

Rapisardi, S.C., and L. Lipsenthal. 1984. Asymmetric and symmetric synaptic junctions in the dorsal lateral geniculate nucleus of cat and monkey. *J Comp Neurol.* 224:415-24.

Reid, C.A., J.M. Bekkers, and J.D. Clements. 2003. Presynaptic Ca2+ channels: a functional patchwork. *Trends Neurosci.* 26:683-7.

Reim, K., M. Mansour, F. Varoqueaux, H.T. McMahon, T.C. Sudhof, N. Brose, and C. Rosenmund. 2001. Complexins regulate a late step in Ca2+-dependent neurotransmitter release. *Cell.* 104:71-81.

Reinsch, S.S., T.J. Mitchison, and M. Kirschner. 1991. Microtubule polymer assembly and transport during axonal elongation. *J. Cell Biol.* 115:365-379.

Renger, J.J., C. Egles, and G. Liu. 2001. A developmental switch in neurotransmitter flux enhances synaptic efficacy by affecting AMPA receptor activation. *Neuron*. 29:469-84.

Rhee, J.S., A. Betz, S. Pyott, K. Reim, F. Varoqueaux, I. Augustin, D. Hesse, T.C. Sudhof, M. Takahashi, C. Rosenmund, and N. Brose. 2002. Beta phorbol ester- and diacylglycerol-induced augmentation of transmitter release is mediated by Munc13s and not by PKCs. *Cell*. 108:121-33.

Richards, D.A., C. Guatimosim, and W.J. Betz. 2000. Two endocytic recycling routes selectively fill two vesicle pools in frog motor nerve terminals. *Neuron*. 27:551-9.

Richmond, J.E., W.S. Davis, and E.M. Jorgensen. 1999. UNC-13 is required for synaptic vesicle fusion in C. elegans. *Nat Neurosci*. 2:959-64.

Rizzoli, S.O., and W.J. Betz. 2004. The structural organization of the readily releasable pool of synaptic vesicles. *Science*. 303:2037-9.

Rizzoli, S.O., and W.J. Betz. 2005. Synaptic vesicle pools. *Nat Rev Neurosci*. 6:57-69.

Roos, J., T. Hummel, N. Ng, C. Klambt, and G.W. Davis. 2000. Drosophila Futsch regulates synaptic microtubule organization and is necessary for synaptic growth. *Neuron*. 26:371-82.

Rosenmund, C., J. Rettig, and N. Brose. 2003. Molecular mechanisms of active zone function. *Curr Opin Neurobiol*. 13:509-19.

Rosenmund, C., A. Sigler, I. Augustin, K. Reim, N. Brose, and J.S. Rhee. 2002. Differential control of vesicle priming and short-term plasticity by Munc13 isoforms. *Neuron*. 33:411-24.

Rosenmund, C., and C.F. Stevens. 1996. Definition of the readily releasable pool of vesicles at hippocampal synapses. *Neuron*. 16:1197-207.

Rothman, J.E., and L. Orci. 1992. Molecular dissection of the secretory pathway. *Nature*. 355:409-15.

Rougon, G., and O. Hobert. 2003. New insights into the diversity and function of neuronal immunoglobulin superfamily molecules. *Annu Rev Neurosci*. 26:207-38.

Royle, S.J., and L. Lagnado. 2003. Endocytosis at the synaptic terminal. *J Physiol.* 553:345-55.

Rutishauser, U., and L. Landmesser. 1996. Polysialic acid in the vertebrate nervous system: a promoter of plasticity in cell-cell interactions. *Trends Neurosci.* 19:422-7.

Ryan, T.A. 2001. Presynaptic imaging techniques. *Curr Opin Neurobiol.* 11:544-9.

Ryan, T.A., H. Reuter, and S.J. Smith. 1997. Optical detection of a quantal presynaptic membrane turnover. *Nature.* 388:478-82.

Ryan, T.A., and S.J. Smith. 1995. Vesicle pool mobilization during action potential firing at hippocampal synapses. *Neuron.* 14:983-9.

Ryan, T.A., N.E. Ziv, and S.J. Smith. 1996. Potentiation of evoked vesicle turnover at individually resolved synaptic boutons. *Neuron.* 17:125-34.

Sabatini, B.L., and W.G. Regehr. 1999. Timing of synaptic transmission. *Annu Rev Physiol.* 61:521-42.

Sabo, S.L., and A.K. McAllister. 2003. Mobility and cycling of synaptic protein-containing vesicles in axonal growth cone filopodia. *Nat Neurosci.* 6:1264-9.

Sampo, B., S. Kaech, S. Kunz, and G. Banker. 2003. Two distinct mechanisms target membrane proteins to the axonal surface. *Neuron.* 37:611-24.

Sankaranarayanan, S., P.P. Atluri, and T.A. Ryan. 2003. Actin has a molecular scaffolding, not propulsive, role in presynaptic function. *Nat Neurosci.* 6:127-35.

Sankaranarayanan, S., and T.A. Ryan. 2000. Real-time measurements of vesicle-SNARE recycling in synapses of the central nervous system. *Nat Cell Biol.* 2:197-204.

Sara, Y., M.G. Mozhayeva, X. Liu, and E.T. Kavalali. 2002. Fast Vesicle Recycling Supports Neurotransmission during Sustained Stimulation at Hippocampal Synapses. *J. Neurosci.* 22:1608-1617.

Scheiffele, P. 2003. Cell-cell signaling during synapse formation in the CNS. *Annu Rev Neurosci.* 26:485-508.

Scheiffele, P., J. Fan, J. Choih, R. Fetter, and T. Serafini. 2000. Neuroligin expressed in nonneuronal cells triggers presynaptic development in contacting axons. *Cell.* 101:657-69.

Schikorski, T., and C.F. Stevens. 1997. Quantitative ultrastructural analysis of hippocampal excitatory synapses. *J Neurosci.* 17:5858-67.

Schikorski, T., and C.F. Stevens. 2001. Morphological correlates of functionally defined synaptic vesicle populations. *Nat Neurosci.* 4:391-5.

Schluter, O.M., F. Schmitz, R. Jahn, C. Rosenmund, and T.C. Sudhof. 2004. A complete genetic analysis of neuronal Rab3 function. *J Neurosci.* 24:6629-37.

Schluter, O.M., E. Schnell, M. Verhage, T. Tzonopoulos, R.A. Nicoll, R. Janz, R.C. Malenka, M. Geppert, and T.C. Sudhof. 1999. Rabphilin knock-out mice reveal that rabphilin is not required for rab3 function in regulating neurotransmitter release. *J Neurosci.* 19:5834-46.

Schmid, S.L. 1997. Clathrin-coated vesicle formation and protein sorting: an integrated process. *Annu Rev Biochem.* 66:511-48.

Schoch, S., P.E. Castillo, T. Jo, K. Mukherjee, M. Geppert, Y. Wang, F. Schmitz, R.C. Malenka, and T.C. Sudhof. 2002. RIM1alpha forms a protein scaffold for regulating neurotransmitter release at the active zone. *Nature.* 415:321-6.

Schoch, S., F. Deak, A. Konigstorfer, M. Mozhayeva, Y. Sara, T.C. Sudhof, and E.T. Kavalali. 2001. SNARE function analyzed in synaptobrevin/VAMP knockout mice. *Science.* 294:1117-22.

Schuman, E.M., and D.V. Madison. 1994. Locally distributed synaptic potentiation in the hippocampus. *Science.* 263:532-6.

Schwartz, M.A. 2001. Integrin signaling revisited. *Trends Cell Biol.* 11:466-70.

Seiler, S., J. Kirchner, C. Horn, A. Kallipolitou, G. Woehlke, and M. Schliwa. 2000. Cargo binding and regulatory sites in the tail of fungal conventional kinesin. *Nat Cell Biol.* 2:333-8.

Setou, M., D.H. Seog, Y. Tanaka, Y. Kanai, Y. Takei, M. Kawagishi, and N. Hirokawa. 2002. Glutamate-receptor-interacting protein GRIP1 directly steers kinesin to dendrites. *Nature.* 417:83-7.

Shapira, M., R.G. Zhai, T. Dresbach, T. Bresler, V.I. Torres, E.D. Gundelfinger, N.E. Ziv, and C.C. Garner. 2003. Unitary assembly of presynaptic active zones from Piccolo-Bassoon transport vesicles. *Neuron.* 38:237-52.

Shapiro, L., and D.R. Colman. 1999. The diversity of cadherins and implications for a synaptic adhesive code in the CNS. *Neuron*. 23:427-30.

Shapiro, L., A.M. Fannon, P.D. Kwong, A. Thompson, M.S. Lehmann, G. Grubel, J.F. Legrand, J. Als-Nielsen, D.R. Colman, and W.A. Hendrickson. 1995. Structural basis of cell-cell adhesion by cadherins. *Nature*. 374:327-37.

Shepherd, G.M. 1994. Neurobiology. Oxford University Press, New York. xiv, 760 pp.

Shepherd, G.M., and K.M. Harris. 1998. Three-dimensional structure and composition of CA3-->CA1 axons in rat hippocampal slices: implications for presynaptic connectivity and compartmentalization. *J Neurosci*. 18:8300-10.

Shi, S., Y. Hayashi, J.A. Esteban, and R. Malinow. 2001. Subunit-specific rules governing AMPA receptor trafficking to synapses in hippocampal pyramidal neurons. *Cell*. 105:331-43.

Shi, S.H., Y. Hayashi, R.S. Petralia, S.H. Zaman, R.J. Wenthold, K. Svoboda, and R. Malinow. 1999. Rapid spine delivery and redistribution of AMPA receptors after synaptic NMDA receptor activation. *Science*. 284:1811-6.

Shtrahman, M., C. Yeung, D.W. Nauen, G.Q. Bi, and X.L. Wu. 2005. Probing vesicle dynamics in single hippocampal synapses. *Biophys J*. 89:3615-27.

Shupliakov, O., O. Bloom, J.S. Gustafsson, O. Kjaerulff, P. Low, N. Tomilin, V.A. Pieribone, P. Greengard, and L. Brodin. 2002. Impaired recycling of synaptic vesicles after acute perturbation of the presynaptic actin cytoskeleton. *Proc Natl Acad Sci U S A*. 99:14476-81.

Sollner, T., M.K. Bennett, S.W. Whiteheart, R.H. Scheller, and J.E. Rothman. 1993. A protein assembly-disassembly pathway in vitro that may correspond to sequential steps of synaptic vesicle docking, activation, and fusion. *Cell*. 75:409-18.

Squire, L.R. 2003. Fundamental neuroscience. Academic, San Diego, Calif. xix, 1426 pp.

Stent, G.S. 1973. A physiological mechanism for Hebb's postulate of learning. *Proc Natl Acad Sci U S A*. 70:997-1001.

Sterling, P., and G. Matthews. 2005. Structure and function of ribbon synapses. *Trends Neurosci*. 28:20-9.

Stevens, C.F., and J.M. Sullivan. 1998. Regulation of the readily releasable vesicle pool by protein kinase C. *Neuron.* 21:885-93.

Stevens, C.F., and T. Tsujimoto. 1995. Estimates for the pool size of releasable quanta at a single central synapse and for the time required to refill the pool. *Proc Natl Acad Sci U S A.* 92:846-9.

Sudhof, T.C. 2000. The synaptic vesicle cycle revisited. *Neuron.* 28:317-20.

Sudhof, T.C. 2004. The synaptic vesicle cycle. *Annu Rev Neurosci.* 27:509-47.

Sun, Y.A., and M.M. Poo. 1987. Evoked release of acetylcholine from the growing embryonic neuron. *Proc Natl Acad Sci U S A.* 84:2540-4.

Sytnyk, V., I. Leshchyns'ka, M. Delling, G. Dityateva, A. Dityatev, and M. Schachner. 2002. Neural cell adhesion molecule promotes accumulation of TGN organelles at sites of neuron-to-neuron contacts. *J. Cell Biol.* 159:649-661.

Tadokoro, S., S.J. Shattil, K. Eto, V. Tai, R.C. Liddington, J.M. de Pereda, M.H. Ginsberg, and D.A. Calderwood. 2003. Talin binding to integrin beta tails: a final common step in integrin activation. *Science.* 302:103-6.

Takao-Rikitsu, E., S. Mochida, E. Inoue, M. Deguchi-Tawarada, M. Inoue, T. Ohtsuka, and Y. Takai. 2004. Physical and functional interaction of the active zone proteins, CAST, RIM1, and Bassoon, in neurotransmitter release. *J Cell Biol.* 164:301-11.

Takei, K., P.S. McPherson, S.L. Schmid, and P. De Camilli. 1995. Tubular membrane invaginations coated by dynamin rings are induced by GTP-gamma S in nerve terminals. *Nature.* 374:186-90.

Takei, K., O. Mundigl, L. Daniell, and P. De Camilli. 1996. The synaptic vesicle cycle: a single vesicle budding step involving clathrin and dynamin. *J Cell Biol.* 133:1237-50.

Takeichi, M., and K. Abe. 2005. Synaptic contact dynamics controlled by cadherin and catenins. *Trends Cell Biol.* 15:216-21.

Togashi, H., K. Abe, A. Mizoguchi, K. Takaoka, O. Chisaka, and M. Takeichi. 2002. Cadherin regulates dendritic spine morphogenesis. *Neuron.* 35:77-89.

Torres, R., B.L. Firestein, H. Dong, J. Staudinger, E.N. Olson, R.L. Huganir, D.S. Bredt, N.W. Gale, and G.D. Yancopoulos. 1998. PDZ proteins bind, cluster, and

synaptically colocalize with Eph receptors and their ephrin ligands. *Neuron.* 21:1453-63.

Townes-Anderson, E., P.R. MacLeish, and E. Raviola. 1985. Rod cells dissociated from mature salamander retina: ultrastructure and uptake of horseradish peroxidase. *J Cell Biol.* 100:175-88.

Travis, E.R., and R.M. Wightman. 1998. Spatio-temporal resolution of exocytosis from individual cells. *Annu Rev Biophys Biomol Struct.* 27:77-103.

Tsukita, S., and H. Ishikawa. 1980. The movement of membranous organelles in axons. Electron microscopic identification of anterogradely and retrogradely transported organelles. *J. Cell Biol.* 84:513-530.

Uchida, N., Y. Honjo, K.R. Johnson, M.J. Wheelock, and M. Takeichi. 1996. The catenin/cadherin adhesion system is localized in synaptic junctions bordering transmitter release zones. *J. Cell Biol.* 135:767-779.

Ullrich, B., Y.A. Ushkaryov, and T.C. Sudhof. 1995. Cartography of neurexins: more than 1000 isoforms generated by alternative splicing and expressed in distinct subsets of neurons. *Neuron.* 14:497-507.

Vale, R.D. 2003. The molecular motor toolbox for intracellular transport. *Cell.* 112:467-80.

Valtorta, F., F. Benfenati, and P. Greengard. 1992. Structure and function of the synapsins. *J Biol Chem.* 267:7195-8.

van den Pol, A.N., K. Obrietan, A.B. Belousov, Y. Yang, and H.C. Heller. 1998. Early synaptogenesis in vitro: role of axon target distance. *J Comp Neurol.* 399:541-60.

Vaughn, D.E., and P.J. Bjorkman. 1996. The (Greek) key to structures of neural adhesion molecules. *Neuron.* 16:261-73.

Verderio, C., S. Coco, A. Bacci, O. Rossetto, P. De Camilli, C. Montecucco, and M. Matteoli. 1999a. Tetanus toxin blocks the exocytosis of synaptic vesicles clustered at synapses but not of synaptic vesicles in isolated axons. *J Neurosci.* 19:6723-32.

Verderio, C., S. Coco, G. Fumagalli, and M. Matteoli. 1995. Calcium-dependent glutamate release during neuronal development and synaptogenesis: different involvement of omega-agatoxin IVA- and omega-conotoxin GVIA-sensitive channels. *Proc Natl Acad Sci U S A.* 92:6449-53.

Verderio, C., S. Coco, E. Pravettoni, A. Bacci, and M. Matteoli. 1999b. Synaptogenesis in hippocampal cultures. *Cell Mol Life Sci.* 55:1448-62.

Verhage, M., A.S. Maia, J.J. Plomp, A.B. Brussaard, J.H. Heeroma, H. Vermeer, R.F. Toonen, R.E. Hammer, T.K. van den Berg, M. Missler, H.J. Geuze, and T.C. Sudhof. 2000. Synaptic assembly of the brain in the absence of neurotransmitter secretion. *Science.* 287:864-9.

Verhey, K.J., and T.A. Rapoport. 2001. Kinesin carries the signal. *Trends Biochem Sci.* 26:545-50.

Verstreken, P., O. Kjaerulff, T.E. Lloyd, R. Atkinson, Y. Zhou, I.A. Meinertzhagen, and H.J. Bellen. 2002. Endophilin mutations block clathrin-mediated endocytosis but not neurotransmitter release. *Cell.* 109:101-12.

Verstreken, P., T.W. Koh, K.L. Schulze, R.G. Zhai, P.R. Hiesinger, Y. Zhou, S.Q. Mehta, Y. Cao, J. Roos, and H.J. Bellen. 2003. Synaptojanin is recruited by endophilin to promote synaptic vesicle uncoating. *Neuron.* 40:733-48.

Waites, C.L., A.M. Craig, and C.C. Garner. 2005. Mechanisms of vertebrate synaptogenesis. *Annu Rev Neurosci.* 28:251-74.

Wang, C., and R.S. Zucker. 1998. Regulation of synaptic vesicle recycling by calcium and serotonin. *Neuron.* 21:155-67.

Wang, L., and A. Brown. 2002. Rapid movement of microtubules in axons. *Curr Biol.* 12:1496-1501.

Wang, L., C.L. Ho, D. Sun, R.K. Liem, and A. Brown. 2000. Rapid movement of axonal neurofilaments interrupted by prolonged pauses. *Nat Cell Biol.* 2:137-41.

Wang, X., M. Kibschull, M.M. Laue, B. Lichte, E. Petrasch-Parwez, and M.W. Kilimann. 1999. Aczonin, a 550-kD Putative Scaffolding Protein of Presynaptic Active Zones, Shares Homology Regions with Rim and Bassoon and Binds Profilin. *J. Cell Biol.* 147:151-162.

Washbourne, P., J.E. Bennett, and A.K. McAllister. 2002a. Rapid recruitment of NMDA receptor transport packets to nascent synapses. *Nat Neurosci.* 5:751-9.

Washbourne, P., P.M. Thompson, M. Carta, E.T. Costa, J.R. Mathews, G. Lopez-Bendito, Z. Molnar, M.W. Becher, C.F. Valenzuela, L.D. Partridge, and M.C. Wilson.

2002b. Genetic ablation of the t-SNARE SNAP-25 distinguishes mechanisms of neuroexocytosis. *Nat Neurosci.* 5:19-26.

Waterman-Storer, C.M., S.B. Karki, S.A. Kuznetsov, J.S. Tabb, D.G. Weiss, G.M. Langford, and E.L. Holzbaur. 1997. The interaction between cytoplasmic dynein and dynactin is required for fast axonal transport. *Proc Natl Acad Sci U S A.* 94:12180-5.

Waters, J., and S.J. Smith. 2002. Vesicle pool partitioning influences presynaptic diversity and weighting in rat hippocampal synapses. *J Physiol.* 541:811-23.

Welte, M.A. 2004. Bidirectional transport along microtubules. *Curr Biol.* 14:R525-37.

West, A.E., R.L. Neve, and K.M. Buckley. 1997. Targeting of the synaptic vesicle protein synaptobrevin in the axon of cultured hippocampal neurons: evidence for two distinct sorting steps. *J Cell Biol.* 139:917-27.

Whittaker, V.P., W.B. Essman, and G.H. Dowe. 1972. The isolation of pure cholinergic synaptic vesicles from the electric organs of elasmobranch fish of the family Torpedinidae. *Biochem J.* 128:833-45.

Whittaker, V.P., I.A. Michaelson, and R.J. Kirkland. 1964. The separation of synaptic vesicles from nerve-ending particles ('synaptosomes'). *Biochem J.* 90:293-303.

Winckler, B. 2004. Scientiae forum / models and speculations pathways for axonal targeting of membrane proteins. *Biol Cell.* 96:669-74.

Xia, Z., H. Dudek, C.K. Miranti, and M.E. Greenberg. 1996. Calcium influx via the NMDA receptor induces immediate early gene transcription by a MAP kinase/ERK-dependent mechanism. *J Neurosci.* 16:5425-36.

Xu, T., and S.M. Bajjalieh. 2001. SV2 modulates the size of the readily releasable pool of secretory vesicles. *Nat Cell Biol.* 3:691-8.

Yamagata, M., J.R. Sanes, and J.A. Weiner. 2003. Synaptic adhesion molecules. *Curr Opin Cell Biol.* 15:621-32.

Yonekawa, Y., A. Harada, Y. Okada, T. Funakoshi, Y. Kanai, Y. Takei, S. Terada, T. Noda, and N. Hirokawa. 1998. Defect in Synaptic Vesicle Precursor Transport and Neuronal Cell Death in KIF1A Motor Protein-deficient Mice. *J. Cell Biol..* 141:431-441.

Yoshihara, M., B. Adolfsen, and J.T. Littleton. 2003. Is synaptotagmin the calcium sensor? *Curr Opin Neurobiol.* 13:315-23.

Young, S.H., and M.M. Poo. 1983. Spontaneous release of transmitter from growth cones of embryonic neurones. *Nature.* 305:634-7.

Zakharenko, S., S. Chang, M. O'Donoghue, and S.V. Popov. 1999. Neurotransmitter secretion along growing nerve processes: comparison with synaptic vesicle exocytosis. *J Cell Biol.* 144:507-18.

Zakharenko, S.S., L. Zablow, and S.A. Siegelbaum. 2001. Visualization of changes in presynaptic function during long-term synaptic plasticity. *Nat Neurosci.* 4:711-7.

Zhai, R., G. Olias, W.J. Chung, R.A. Lester, S. tom Dieck, K. Langnaese, M.R. Kreutz, S. Kindler, E.D. Gundelfinger, and C.C. Garner. 2000. Temporal appearance of the presynaptic cytomatrix protein bassoon during synaptogenesis. *Mol Cell Neurosci.* 15:417-28.

Zhai, R.G., H. Vardinon-Friedman, C. Cases-Langhoff, B. Becker, E.D. Gundelfinger, N.E. Ziv, and C.C. Garner. 2001. Assembling the presynaptic active zone: a characterization of an active one precursor vesicle. *Neuron.* 29:131-43.

Zhang, J.Z., B.A. Davletov, T.C. Sudhof, and R.G. Anderson. 1994. Synaptotagmin I is a high affinity receptor for clathrin AP-2: implications for membrane recycling. *Cell.* 78:751-60.

Zhang, W., and D.L. Benson. 2001. Stages of synapse development defined by dependence on F-actin. *J Neurosci.* 21:5169-81.

Zhen, M., and Y. Jin. 2004. Presynaptic terminal differentiation: transport and assembly. *Curr Opin Neurobiol.* 14:280-7.

Zheng, J.Q., M. Felder, J.A. Connor, and M.M. Poo. 1994. Turning of nerve growth cones induced by neurotransmitters. *Nature.* 368:140-4.

Ziv, N.E., and C.C. Garner. 2004. Cellular and molecular mechanisms of presynaptic assembly. *Nat Rev Neurosci.* 5:385-99.